Improving bio-based succinate production with *Basfia succiniciproducens* through evolutionary engineering

Dissertation

zur Erlangung des Grades

des Doktors der Ingenieurwissenschaften

der Naturwissenschaftlich-Technischen Fakultät III

Chemie, Pharmazie, Bio- und Werkstoffwissenschaften

der Universität des Saarlandes

von

René Stellmacher

Saarbrücken

05. Juni 2014

Tag des Kolloquiums:	26. September 2014
Dekan:	Prof. Dr. Volkhard Helms
Berichterstatter:	Prof. Dr. Christoph Wittmann
	Prof. Dr. Gert-Wieland Kohring
Vorsitz:	Prof. Dr. Elmar Heinzle
Akad. Mitarbeiter:	Dr. Björn Becker

Publications

Partial results of this work have been published in advance under the authorization of the Department of Mechanical Engineering of the Technischen Universität Braunschweig, Institute of Biochemical Engineering, represented by Prof. Dr. C. Wittmann.

Peer-reviewed Journals

Becker, J., Reinefeld, J., **Stellmacher, R.**, Schäfer, R., Lange, A., Meyer, H., Lalk, M., Zelder, O., von Abendroth, G., Schröder, H., Haefner, S., Wittmann, C. (2013): Systems-wide analysis and engineering of metabolic pathway fluxes in bio-succinate producing *Basfia succiniciproducens*. Biotechnol. Bioeng. 110(11): 3013-23

Stellmacher, R., Hangebrauk, J., von Abendroth, G., Scholten, E., Wittmann, C. (2010). Fermentative Herstellung von Bernsteinsäure mit *Basfia succiniciproducens* DD1 in Serumflaschen. *Chem.-Ing.-Tech.* 82(8): 1223-29.

Conference contributions

Becker, J., Kind, S., **Stellmacher, R.**, Wittmann, C.: Towards superior bio-processes – shaken bioreactors in systems biotechnology. 1st European Congress of Applied Biotechnology, September 25-29, 2011, Berlin, Germany.

Stellmacher, R., Hangebrauk, J., von Abendroth, G., Wittmann, C.: Bio-based production of succinic acid by *Basfia succiniciproducens* DD1. Biotransformations 2011, August 22-25, 2011, Bad Herrenalb, Germany.

Stellmacher, R., Hangebrauk, J., Schäfer, R., von Abendroth, G., Wittmann, C.: Bio-based production of succinic acid by *Basfia succiniciproducens* DD1 – Systems metabolic engineering and bioprocess development. Annual conference of the Association for General and Applied Microbiology, April 3-6, Karlsruhe, Germany.

Hangebrauk, J.; **Stellmacher, R.**, Fürch, T., von Abendroth, G., Schröder, H., Haefner, S., Wittmann, C.: Biotechnological production of succinic acid. ProcessNet Conference, January 20-21, 2010, Frankfurt on the Main, Germany.

Danke

„Was wir wissen, ist ein Tropfen; was wir nicht wissen, ein Ozean.“ – Isaac Newton

Besonders bedanken möchte ich mich bei Herrn Prof. Dr. Christoph Wittmann, der es mir ermöglichte, diese Arbeit unter seiner Betreuung anzufertigen. Viele spannende fachliche Gespräche und Diskussionen sowie nützliche Ratschläge haben meine wissenschaftliche Weiterentwicklung gefördert und maßgeblich zur erfolgreichen Bearbeitung des Projektes beigetragen.

Herrn Prof. Dr. Elmar Heinzle und Herrn Prof. Dr. Gert-Wieland Kohring danke ich für das Interesse an meiner Arbeit und für die Bereitschaft zur Übernahme des Prüfungsvorsitzes und der Zweitbegutachtung.

„Nur mittels der Wissenschaften vom Leben kann die Beschaffenheit des Lebens von Grund auf verändert werden.“ – Aldous Huxley

Dem Bundesministerium für Bildung und Forschung danke ich für die Förderung des Projektes im Rahmen der Bioindustrie2021 – „Herstellung von Polyestern auf Basis fermentativ hergestellter Bernsteinsäure bzw. 1,4-Butandiol“ (Nr. 0315238) in Kooperation mit der BASF SE. Der BASF SE möchte ich zudem für die Fortführung der Zusammenarbeit im Rahmen einer Industriekooperation danken. Mein Dank geht dabei an Dr. Gregory von Abendroth, Dr. Hartwig Schröder, Dr. Stefan Häfner, Dr. Joanna-Martyna Krawczyk, Dr. Esther Dantas Costa, Dr. Marvin Schulz, Dr. Holger Hartmann und Dr. Oskar Zelder für die vielen faszinierenden Gespräche und konstruktiven Diskussionen während der Meetings in Braunschweig und Ludwigshafen. Bei Dr. Krawczyk möchte ich mich insbesondere für die Bereitstellung von Stämmen und Plasmiden bedanken. Bei Dr. Schulz und Dr. Hartmann bedanke ich mich für die Zusammenarbeit und vor allem für die Bearbeitung der Genomdaten. Dr. von Abendroth und Dr. Dantas Costa danke ich für die Möglichkeit der kurzweiligen, hochinteressanten Forschungsaufenthalte bei der BASF SE. In diesem Zusammenhang bedanke ich mich auch bei Klaus, Oliver, Torsten, Julia und Samy für die freundliche und kooperative Zusammenarbeit im Labor.

„Die Wissenschaft kennt kein Mitleid.“ – Romain Rolland

In diesem Sinne geht ein ganz besonders großer Dank an mein Ingenieurbüro – Gena und Jan, für die Unterstützung, die Hilfsbereitschaft und das stets offene Ohr während unserer gemeinsamen Zeit im Büro. Es hat mir immer viel Freude bereitet, mit euch Probleme und Themen, auch mal nicht wissenschaftlicher Natur, zu diskutieren oder über die täglichen Herausforderungen des Labor- und Versuchsalltags zu fachsimpeln – natürlich auch die erfolgreichen Momente mit euch zu teilen oder einfach nur ein „paar“ Gummibärchen zu verdrücken.

„Inmitten der Schwierigkeiten liegt die Möglichkeit.“ – Albert Einstein

Riesigen Dank auch an Jasper, Rudolf und den Rest des Basfia-Teams, für die vielen Ideen, die gemeinsamen schweren und guten Zeiten und die „Basfia Challenge Meetings“. Genauso möchte ich mich bei allen Spielmännern und Gaußsträßlern bedanken, für die phantastische Arbeitsatmosphäre im Labor und die erfolgreiche Zeit, die wir zusammen hatten. Ein großes Dankeschön geht auch an alle ehemaligen ibvt’ler, die mir zu guten Freunden geworden sind: Becky, Claudi, Franzi, CBo, Micha, Tille, ….

„Alles Große in unserer Welt geschieht nur, weil jemand mehr tut, als er muss.“ – Hermann Gmeiner

Ich bedanke mich bei Dr. Rebekka Biedendieck vom Institut für Mikrobiologie für die großartige Hilfe bei der Durchführung und Auswertung der Microarrays. Nelli Bill und Maike Sest vom Institut für Biochemie, Biotechnologie und Bioinformatik danke ich für die Hilfe bei der Durchführung der Biolog-Versuche.

„Studieren macht Vergnügen, bildet den Geist und erhöht die Fähigkeiten.“ – Sir Francis Bacon

Ich möchte allen meinen Studenten danken, die mich während meiner Arbeit mit unermüdlichem Fleiß tatkräftig unterstützt haben: Sarah, Marco, Jörn, Felix, Mareike, Anja und Teresa.

„Der beste Weg, einen Freund zu haben, ist der, selbst einer zu sein.“ – Ralph Waldo Emerson

Vielen Dank auch an meine langjährigen Freunde und Kommilitonen Robert, Hobbit, Jojo und Stefan; für die vielen extensiven Lernsessions während des Studiums, die Bond-Abende, die WG-Zeit und die Super Bowl Nächte.

„Allein ist der Mensch ein unvollkommenes Ding; er muss einen zweiten finden, um glücklich zu sein.“ – Blaise Pascal

[fillmoːls mɐr'siː] Steffi, du bist mir Inspiration, Antrieb und Rückhalt. Ohne dich würde diese Arbeit nicht das sein, was sie ist. Ich danke dir für die phantastische Zeit während und neben der Arbeit, und dafür, dass du immer für mich da bist.

„Reichen die Wurzeln tief, gedeihen die Zweige gut.“ (chinesisches Sprichwort)

Abschließend möchte ich den größten Dank meinen Eltern und Großeltern aussprechen. Ihr habt mich bei allem unterstützt und habt immer viel Geduld bewiesen.

Table of contents

Summary

The contemporary public and economic awareness for sustainable and ecological technologies drive the industrial development of superior biotechnological processes for bulk and fine chemicals. Regarding top-value compounds within this context, production of bio-based succinate is a highly anticipated industrial process due to its wide industrial applicability. In this work, naturally succinate producing *Basfia succiniciproducens* was systematically evolved towards improved production and tolerance properties. Small scale CO_2-enriched sequential batch cultivations enabled for successful adaptation, evaluated by cell growth and production performance. Evolved phenotypes exhibited improved abilities to cope with the applied stress such as growing at 42 °C, at a pH of 5.2 and with 25 g L^{-1} succinate – conditions not feasible for the wild-type strain. In addition, they outperformed the parent strain at standard conditions in respect to growth and succinate production reaching a maximum productivity of 2.9 g L^{-1} h^{-1}. Systems biology approaches were then applied to identify the underlying genotype-phenotype correlations. Most promising targets thereof were selectively introduced into defined production hosts and demonstrated clear improvements regarding temperature tolerance, productivity and cell separation. Taken together, this work is an important contribution to the breeding of superior cell factories of *B. succiniciproducens* for bio-based succinate production.

Zusammenfassung

Das öffentliche und wirtschaftliche Interesse an nachhaltigen, ökologischen Technologien ist Antrieb für die Entwicklung innovativer biotechnologischer Prozesse für Bulk- und Feinchemikalien. Ein Schwerpunkt liegt hier auf der biobasierten Herstellung von Succinat, einem Produkt mit vielfältigen Anwendungsbereichen. In dieser Arbeit wurde *Basfia succiniciproducens*, ein natürlicher Succinat-Produzent, zur Verbesserung der Produktions- und Toleranzeigenschaften systematisch adaptiert. Ein sequentielles Kultivierungsverfahren unter CO_2-Atmosphäre ermöglichte die erfolgreiche Adaption, mit Zellwachstum und Produktivität als Indikatoren. Die generierten Phänotypen zeichneten sich durch verbesserte Stresseigenschaften gegenüber erhöhter Temperatur und Produktkonzentration sowie niedrigerem pH-Wert aus (42 °C, 25 g L^{-1} Succinat, pH 5.2) – Bedingungen, unter denen der Wildtyp kein Wachstum aufweist. Zudem übertrafen Wachstums- und Produktionseigenschaften unter Standardbedingungen die des Ausgangsstamms (P_{max} = 2.9 g L^{-1} h^{-1}). Zur Identifizierung der zugrundeliegenden Genotyp-Phänotyp Beziehungen wurden systembiologische Methoden herangezogen. Erfolgsversprechende Targets wurden in definierte Produktionsstämme eingebracht und führten zu signifikanter Verbesserung von Temperaturtoleranz, Produktivität und Zellseparation. Diese Arbeit stellt somit einen wichtigen Schritt auf dem Weg zur Etablierung von *B. succiniciproducens* als Zellfabrik für die biobasierte Succinatproduktion dar.

1 Introduction

Nowadays, the global chemical industry is continuously challenged by decreasing oil reserves and increasing public demand for green chemicals and additional products. These emerging ecological and undeniably economic aspects triggered the concept of bioeconomy that comprises the development of new and innovative biotechnological processes. The processes will then provide attractive alternatives to common industrial routes by conversion of renewable resources to e.g. platform chemicals. Among several petrochemically produced building blocks, succinate is described as a top value-added chemical (Werpy and Peterson 2004) and attracted growing attention by various global players of the chemical market in the last few years (Beauprez et al. 2010). It is projected that the succinate market reaches about 250.000 tons by the year 2018 with a potential market value of $ 840 Mio. (MarketsandMarkets 2012; Transparency Market Research 2013). These numbers can be easily explained by the myriad of applications of succinate. Sustainably produced commodity chemicals like 1,4-butandiol or tetrahydrofuran or various specialty and fine chemicals promote this high demand in the chemical industry sector. A combination of succinate with biotechnologically produced diamines can be applied to synthesize commercially profitable bio-based polymers (Kind and Wittmann 2011). Further application fields comprise the pharmaceutical, neutraceutical and agrochemical industry sector (McKinlay et al. 2007). From a metabolic viewpoint, succinate is a ubiquitous intermediate in almost all organisms. In this line, genetic engineering of well-known platform organisms seemed encouraging. However, naturally succinate producing microorganisms were isolated throughout the last two decades (Guettler et al. 1999; Lee et al. 2002; Scholten and Dägele 2008) and currently represent the most auspicious production hosts. Among them, *Basfia succiniciproducens* shows promising features in terms of a future bioprocess application (Scholten and Dägele 2008; Scholten et al. 2009; Stellmacher et al. 2010).

Establishing a competitive bioprocess for succinate production is obviously linked to key challenges regarding a successful implementation into the industrial landscape. The most challenging features comprise the overall productivity of a production host, its ability to convert supplemented carbon sources to the desired product with high titers and the specific yield in doing so (Werpy and Peterson 2004; Patel et al. 2006) as well as its robustness concerning the bioprocess. Most of these goals can be achieved using widely applied metabolic engineering strategies. However, an integral process consideration also recommends the contemplation of further microbial physiology associated characteristics. The applied fermentation plants are mostly running semi-sterile, which increases the contamination risk. High substrate and product titers demand for strong tolerances. Some up- or downstream processes require presettings to enable economic feasibility. In this line, evolutionary adaptation represents a promising approach regarding tolerance and performance improvements.

2 Objectives

The present work aimed for the generation of *B. succiniciproducens* phenotypes, featuring optimized characteristics regarding their tolerance against fermentation associated perturbance, i.e. high temperature, high succinate levels and low pH and their overall production performance. For this purpose, evolutionary adaptation should be used to gain evolved phenotypes. In this line, strain specific physiologic limitations served as starting points. Initially, the double mutant *B. succiniciproducens* DD3 was chosen as starting strain. It harbors deletions of the genes *ldh* and *pflD*, i.e. the pathways for lactate and formate production, respectively. This yields a minimized degree of freedom on which the strain could adapt evolutionary. State-of-the-art systems biology tools, combined with sophisticated cultivation experiments should be applied to shed some light into the metabolic response regarding the adaptation approaches. Obtained phenotype profiles, consisting of fluxomics, transcriptomics and genomics should help to identify promising targets for rational strain improvement. The final objective was the implementation of identified targets into production strains and to validate their contribution to observed tolerance and performance improvements of the adapted strains. Additionally, this work should provide a promising starting point, based on the establishment of evolutionary adaptation as valid tool in industrial strain development and encourage further approaches to achieve sustainable and competitive bioprocesses in context with the bioeconomy.

3 Theoretical Background

3.1 From amber to bio-succinic acid

Succinic acid, a well-known chemical that was already described in the 16th century when it was obtained from amber (Agricola 1955), is a four carbon dicarboxylic acid, systematically denoted as butanedioic acid. Throughout the past centuries, the compound was extensively used in medical treatment for joint pain, arthritic symptoms or teething (Amber Artisans 2013; Markman 2009). Nowadays it is known to represent a ubiquitous substance in the metabolism of almost all living organisms, where it serves as intermediate in cellular processes or as metabolic end-product of fermentative growth. Beyond its widespread biochemical occurrence, succinic acid has received increasing interest during the last decades by ranking it as "Top 12 Candidate" for high value added chemicals from biomass (Werpy and Peterson 2004). So far it was preferably used for food and pharmaceutical applications (Hayes et al. 2006; USDA 2009; Transparency Market Research 2013). For these purposes, petrochemical based processes provided 15.000 tons of succinic acid per year (Lee et al. 2005). The primary production route involves catalytic hydrogenation of maleic acid, a derivate of maleic anhydride, which is obtained during the oxidation of butane, a cracking product of fossil oil (Patel et al. 2006; Bechthold et al. 2008). However, this dependency on ultimate fossil resources shortens the succinic acid production volume by directly coupling it to increasing oil prices thus limiting the opportunities for further industrial application. Alternatively, succinic acid can be produced by microbial fermentation employing renewable feedstocks while fixing external carbon dioxide. This meets the growing demand for ecological substitutes of chemicals or building blocks and the development of a clean and efficient industry regarding the progressing climate change. Lately, these ecologic and undoubtedly economic concerns have raised global companies interest in a competitive succinic acid bioprocess based on stable feedstock costs and optimal availability, efficient succinic acid recovery and purification and process optimized microorganisms (Bastidon 2012). The accomplishment of these key challenges will boost the economic viability of bio-succinic acid as a mainstay of the biorefinery concept and points out the major driving force for upvaluing the introduction of a sustainable bio-succinic acid market. In this line, bio-succinic acid's rising popularity has tremendously increased the potential of its market position accompanied by an excellent and innovative portfolio of renewable and sustainable products (Tweel 2010).

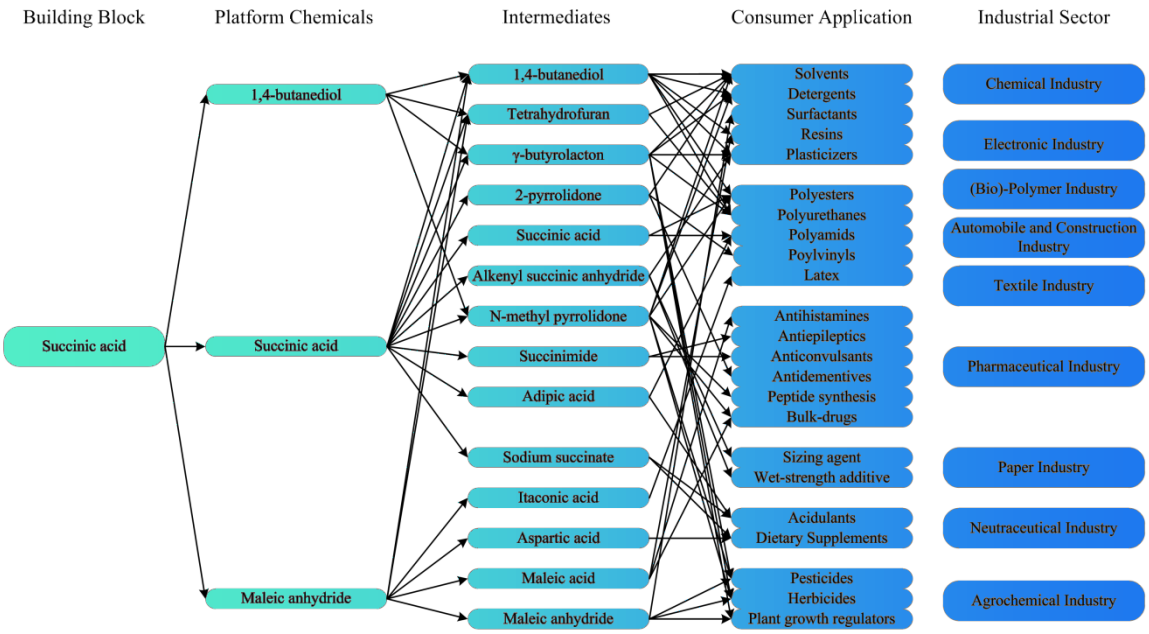

Figure 3.1 Application routes for bio-based succinic acid and its respective derivatives in various industrial sectors.

Current reports predict a market value of about $ 840 Mio by 2018, linked to a strong growth rate of 19 % reaching an annual market volume of 250,000 tons per year until 2018 (MarketsandMarkets 2012; Transparency Market Research 2013). This is particularly driven by the various possible applications of succinic acid in the chemical sector. Obviously, the compound displays a versatile C4 building block with outstanding industrial potential (Figure 3.1) due to its molecular character as a dicarboxylic acid. It might partly replace maleic anhydride with a total market share of 210,000 tons per year (Sauer et al. 2008) or maleic acid which is constantly increasing in both, demand and price (Cukalovic and Stevens 2008). In this line, succinic acid can serve as precursor for different commodity and specialty chemicals. Among them, 1,4-butanediol and its derivatives tetrahydrofuran or γ-butyrolacton cover a cumulated market volume of about 500,000 tons. Their application fields include the production of polyurethane, polyesters, adhesives, or coating resins (Paster et al. 2004; Müller 2005). They are further used as raw materials for pharmaceuticals and as components of herbicides and rubber additives (Cukalovic and Stevens 2008). Synthesis of the derivative N-methyl-2-pyrrolidone could further extend possible applications of succinic acid towards chemical synthesis and process solvents, with additional application in the pharmaceutical industry. Adipic acid, synthesized with succinic acid as ligand in combination with hydrogen peroxide or from 1,4-butanediol by carbonylation could facilitate the access to a polymer market for e.g. PA 6.6 (nylon) with a production volume of about 900,000 tons (Paster et al. 2004). Furthermore, succinic acid is an alternative monomer for the bio-polymer chemistry, e.g. for bio-based polyamides like PA 5.4 (Kind and Wittmann 2011) that involve an annual production volume of 3.5 Mio tons (Becker et al. 2012) or

for polyesters like polyethylene succinate (PES) or polybutylene succinate (PBS) (Fujimaki 1998; Oishi et al. 2006). Regarding these refining products, succinic acid's economic feasibility additionally depends on optimization and innovation of chemical engineering approaches to competitively synthesize the above mentioned compounds from fermentation derived succinic acid. However, its acid residue anion succinate, which represents the physiologically occurring variant and will thus be used as term instead of succinic acid throughout the following chapters, can also be applied as salt and contribute to the application in the fields of pharmacology, toxicology and for medical purposes as well as in the food industry sector as pH-modifier, flavoring or antimicrobial agent (Cukalovic and Stevens 2008).

Table 3.1 List of bio-succinate joint-ventures formed in the last years, the respectively applied strain and estimated production volumes for future bio-based succinate production.

Strategic alliance	Year	Microorganism	Product volume
BioAmber / **Mitsubishi Chemicals** (in JV with Ajinomoto since 2006)	2008	Yeast biocatalyst (BioAmber) / *B. flavum* or *C. glutamicum* (Mitsubishi Chemicals)	34,000 tons per year (Canada) / 65,000 tons per year (Thailand)
Succinity (BASF SE and Corbion Purac)	2009	*B. succiniciproducens*	50,000 tons per year (Spain)
Myriant / **ThyssenKrupp Uhde** & Showa Denko	2009	*E. coli*	77,000 tons per year (US)
Reverdia (Royale D.S.M & Roquettes)	2010	Yeast biocatalyst	30,000 tons per year (Italy)

Information according to Ajinomoto 2007; Beauprez et al. 2010; BioAmber 2011; BASF SE and CSM 2012; Bastidon 2012; Jansen et al. 2012; Myriant 2013a; Myriant 2013b; Roquette 2013

The brilliant properties have meanwhile driven the formation of different industry joint ventures (Table 3.1). These collaborations comprise prestigious global companies (Beauprez et al. 2010). Apparently, these strategic alliances aim at innovative and commercially competitive bioprocesses based on renewable feedstocks. For successful industrial scale production several benchmarks have to be reached. The key criteria involve a minimal productivity of 2.5 g L^{-1} h^{-1}, minimal nutrient supply combined with cheap substrates and high titers of 50 – 100 g L^{-1} (Werpy and Peterson 2004; Warnecke and Gill 2005). In particular, tailored production strains are needed that efficiently convert the raw material into succinate in a robust and reproducible process. Different microorganisms have been considered over the last years as potential succinate producers. Two strategies seemed most promising. First, bacteria from animal rumen such as *B. succiniciproducens*, *M. succiniciproducens* or *A. succinogenes* (Guettler et al. 1999; Lee et al. 2002; Scholten and Dägele 2008) have a high natural potential to synthesize succinate. On the other hand, recombinant strains of industrial well-known cell factories like *E. coli*, *C. glutamicum* or *S. cerevisae* can be built on excellent knowledge and synthetic biology methods for cellular engineering (Okino et al. 2008; Beauprez et al. 2010; Otero et al. 2013).

Table 3.2 Potential industrial hosts for bio-based succinate production.

Strain	Production host specific characteristics	
Escherichia coli	Physiology	Facultative anaerobic, Gram-negative, rod-shaped, mesophile
	Genome	Completely sequenced; 4.6 Mb (Blattner et al. 1997)
	Advantages	Short doubling time
		Wide substrate variety and well-studied nutrition requirements
		Fully established engineering tool-box
	Disadvantages	No natural producer (typically low anaerobic yields)
		Catabolite repression and strong regulation patterns
		PTS mediated substrate uptake
Corynebacterium glutamicum	Physiology	Aerobic, Gram-positive, pleomorphic, mesophile
	Genome	Completely sequenced; 3.3 Mb (Kalinowski et al. 2003)
	Advantages	GRAS-status
		Broad industrial feasibility
		Fully established engineering tool-box
	Disadvantages	No natural producer (biotransformation of succinate under oxygen deprivation (Okino et al. 2005; Inui et al. 2007))
Saccharomyces cerevisiae	Physiology	Eukaryotic, aerobic, round to ovoid cells, reproduction via budding, mesophile
	Genome	Completely sequenced; 12.2 Mb
	Advantages	GRAS-status
		High product tolerances
		Wide pH operation range
		Well-established engineering tool-box
	Disadvantages	No natural producer
		Lacking growth on pentose sugars (Hong and Nielsen 2012)
		Compartmented synthesis pathway
Actinobacillus succinogenes	Physiology	Facultative anaerobic, Gram-negative, pleomorphic, mesophile, capnophilic
	Genome	Completely sequenced; 2.3 Mb (McKinlay et al. 2010)
	Advantages	Natural producer of high succinate titers,
		PEP-carboxykinase mediated carbon dioxide fixation,
	Disadvantages	Auxotrophies for glutamate, cysteine and methionine
		Missing engineering tools
		No complete TCA cycle
Mannheimia succiniciproducens	Physiology	Facultative anaerobic, Gram-negative, pleomorphic, mesophile, capnophilic
	Genome	Completely sequenced; 2.3 Mb (Hong et al. 2004)
	Advantages	Natural producer of high succinate titers
		PEP-carboxykinase mediated carbon dioxide fixation
		Ferments wide variety of substrates and hydrolysates
		Specifically developed engineering tools
	Disadvantages	Pyrimidine auxotrophy
		Missing links in vitamin pathways and in methionine and cysteine pathway
Basfia succiniciproducens	Physiology	Facultative anaerobic, Gram-negative, pleomorphic, mesophile, capnophilic
	Genome	Partially sequenced (Kuhnert et al. 2010)
	Advantages	Natural producer of high succinate titers
		PEP-carboxykinase mediated carbon dioxide fixation
		Ferments wide variety of substrates and hydrolysates, e.g. glycerol
		No Auxotrophies
	Disadvantages	Poor availability of genetic tool knowledge

3.2 Succinate production by *Basfia succiniciproducens*

3.2.1 Physiology and basic properties

B. succiniciproducens strains were first isolated from bovine rumen juice during a selective study, aiming at succinate producing microorganisms (Scholten and Dägele 2008; Kuhnert et al. 2010). The BASF proprietary isolate *B. succiniciproducens* DD1 is a Gram-negative and facultative anaerobic bacterium characterized by a pleomorphic shape and tending to accumulate in clusters. It belongs to the family *Pasteurellaceae* a bacteria species primarily associated with the normal flora of vertebrate mucosal membranes. Multilocus sequence analysis revealed a strong genetic similarity to the patent strain *Mannheimia succiniciproducens* MBEL55E with a total of 2006 homologous ORFs and a comparable genome size of 2.3 Mb (Kuhnert et al. 2010). In contrast to other *Pasteurellaceae* members such as strains belonging to the genus *Haemophilus* or *Actinobacillus*, this bacterium is neither toxic nor pathogen enabling an unrestricted application in industrial production processes.

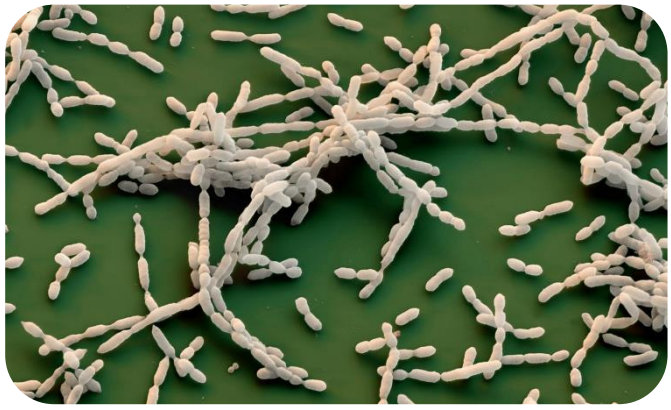

Figure 3.2 Scanning electron microscope picture of *B. succiniciproducens* DD1 (kindly provided by BASF SE)

B. succiniciproducens DD1 thrives under capnophilic conditions (Scholten and Dägele 2008; Stellmacher et al. 2010) based on the incorporation of the environmentally significant gas carbon dioxide into its metabolism. This preference is caused by the natural environment, since the bovine rumen contains about 65.5 mol % carbon dioxide in its gas atmosphere (Hong et al. 2004). Under these carbon dioxide rich conditions, the strain naturally produces substantial amounts of succinate, hence representing an ideal host for the rising bio-based succinate market. Primary production studies, based on several carbon sources such as glucose, sucrose or xylose, described a standard anaerobic fermentation product portfolio in addition to succinate containing lactate, formate and acetate

(Scholten and Dägele 2008) without production of gas (Kuhnert et al. 2010). Further approaches using crude glycerol as carbon source in continuously driven cultivations described highly anticipated yields (Scholten et al. 2009). This broad substrate utilization emphasizes the promising applicability of this strain in industrial production processes.

3.2.2 Biochemistry of succinate synthesis

The biosynthesis of succinate is a biological widespread process as the compound is an intermediate of the tricarboxylic acid (TCA) cycle, an almost ubiquitous pathway to provide cellular energy and building blocks. Succinate can generally be formed by three pathways, the oxidative branch and the reductive one, respectively and via the glyoxylate shunt. Under aerobic conditions succinate appears as intermediate of the oxidative TCA cycle and supplies electrons for the oxidative phosphorylation or regenerates the oxaloacetate pool (Cox et al. 2006) with a theoretical stoichiometric maximum yield of 1 mol succinate per mol glucose. Typically, it is not secreted in the medium to maintain cyclic operation of this pathway. Alternatively, succinate derives from the glyoxylate shunt by the cleavage of isocitrate to succinate and glyoxylate while by-passing decarboxylation steps (Raab et al. 2010). This pathway mainly serves to support growth on carbon two substrates and is found in different bacteria and in yeasts. In natural succinate producers the anaerobic pathway is favored while fumarate acts as final electron acceptor. This fermentative growth leads to substantial succinate release, thus exhibiting a tremendous potential to produce succinate.

Based on glucose, *B. succiniciproducens* predominantly runs the glycolytic pathway to convert the substrate to cellular building blocks and energy. However, some carbon is metabolized through the pentose phosphate pathway to serve for anabolic precursors while recycling excess carbon back into glycolysis (Becker et al. 2013). At the pyruvate node, supplied carbon is distributed towards the reductive TCA cycle by carboxylation of phosphoenolpyruvate (PEP). Obviously, it represents an integral part of the succinate synthesis by delivering required precursors. When supplemented with carbon dioxide the carboxylation is optimally driven by PEP carboxykinase as observed with other natural succinate producers (Van der Werf et al. 1997; Lee et al. 2006) and directly coupled to ATP formation. Additionally, this reaction affects the carbon flux towards pyruvate itself as secreted by-product or as precursor for other mixed fermentation by-products. Acetate and formate production particularly occurs synchronized as they both derive from formate C-acteyltransferase activity and growth coupled, while lactate accumulates during stationary phase (Stellmacher et al. 2010). This behavior can be presumably explained by growth associated gene expression and protein abundance (Lee et al. 2006) and unveils a high metabolic flexibility of *B. succiniciproducens* regarding the reallocation of carbon depending on the metabolic state of the cell. The TCA cycle is operated in a separated, bifurcated manner.

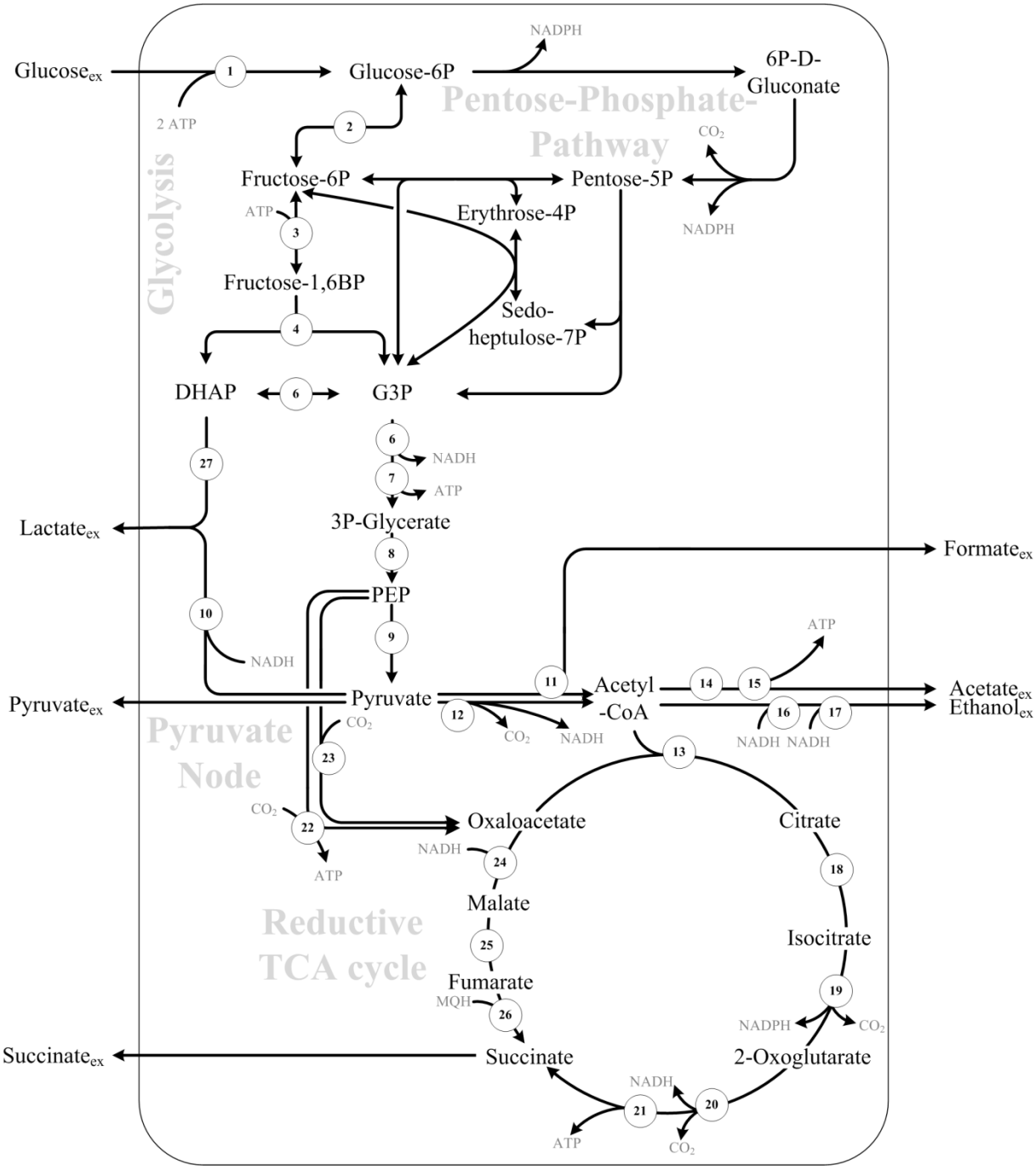

Figure 3.3 Overview of *B. succiniciproducens* carbon core metabolism involving glycolysis, pentose phosphate pathway, pyruvate node and TCA cycle. Glucose uptake is performed by (1) glucokinase. The enzymes coping with succinate precursor demand via glycolysis are (2) glucose-6-phosphate isomerase, (3) phosphofructokinase, (4) fructose-bisphosphate aldolase, (5) triosephosphate isomerase, (6) glyceraldehyde-3-phosphate dehydrogenase, (7) phosphoglycerate kinase, (8) phosphoglycerate mutase and (9) pyruvate kinase. At the pyruvate node, mixed fermentation products are generated via (10) lactate dehydrogenase, (11) formate C-actetyltransferase and (12) pyruvate dehydrogenase. Additionally, lactate can derive from (27) methylglyoxal pathway. Acetyl-CoA serves as precursor for the TCA cycle by its integration through (13) citrate synthase and for acetate and ethanol formation via (14) phosphate acetyltransferase, (15) acetate kinase and (16), (17) alcohol dehydrogenase, respectively. The oxidative TCA branch is further conducted by (18) aconitase, (19) isocitrate dehydrogenase, (20) 2-oxoglutarate dehydrogenase complex and (21) succinyl-CoA synthetase. Anaerobic succinate synthesis is primarily facilitated through (22) phosphoenolpyruvate carboxykinase, with (23) phosphoenolpyruvate carboxylase, and (24) malate dydrogenase, (25) fumarate hydratase and (26) fumarate reductase.

The reductive branch is exclusively used to synthesize succinate, while the oxidative part revealed only low utilization in *B. succiniciproducens* strains (Becker et al. 2013). Considering the redox balance and cofactor management of succinate synthesis, generation of succinate requires 2 molecules of reductants. In general NADH supply exceeds NADH consumption, while the *Pasteurellaceae* genus seems to struggle with sufficient NAPDH supply. Apparently, this likely suggest additional NADPH sources in *B. succiniciproducens* (Becker et al. 2013) as documented for *A. succinogenes* that employs a transhydrogenase or the malic enzyme, closing this gap in redox balancing (McKinlay et al. 2007). Unfortunately, the malic enzyme withdraws carbon from the reductive TCA branch and formed pyruvate is usually not converted back to oxaloacetate. The observed excess in ATP production is addressed to cellular maintenance and transport processes (McKinlay et al. 2007; Becker et al. 2013).

3.2.3 Optimal production performance

The primary desired feature of an industrial host is the efficient conversion of substrate to product. Therefore, the natural, in general non-optimal distribution of applied substrates throughout the metabolism can be externally affected by introduction of heterologous pathways or targeted regulation of cellular metabolic routes. Nevertheless, it is inevitable to gain information on these routes and their corresponding fluxes. Elementary flux mode analysis was used to search probable succinate producing phenotypes with a distinctive ratio of succinate production and biomass formation based on glucose (Becker et al. 2013). Applying a flux balance approach the phenotype with optimal succinate yield showed the ideal carbon distribution for succinate production, while rejecting any by-product or biomass formation (Figure 3.4). Obviously, the complete glucose is metabolized through glycolysis generating 2 mols PEP per mol glucose. At the pyruvate node, optimal flux distribution for succinate production revealed a branched TCA whereas 86 % of the carbon is carboxylated and subsequently used in the reductive TCA cycle. The rest is applied in the oxidative TCA cycle via pyruvate dehydrogenase and citrate synthase to generate sufficient NADH for running the reductive part. This is essential, since glycolysis produces 1 NADH per PEP, but reduction of OAA towards succinate requires 2 NADH. A maximal theoretical succinate yield of 1.71 mol per mol glucose under carbon dioxide atmosphere recommends the consideration of this network for innovative optimization approaches by e.g. metabolic engineering. Furthermore, the combination with additional reducing power such as hydrogen can yield 2 mol succinate per mol glucose (McKinlay et al. 2007).

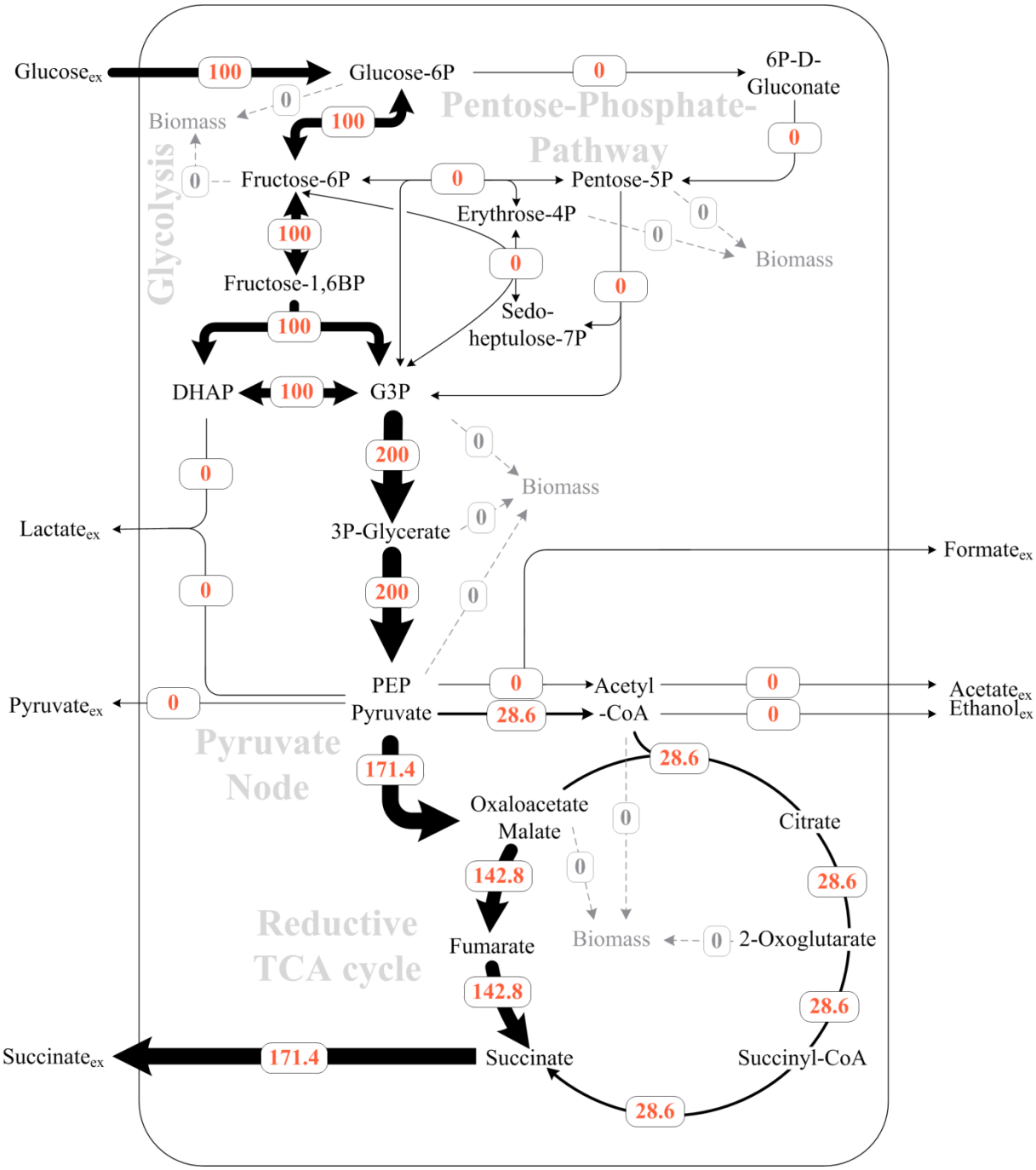

Figure 3.4 Metabolic fluxes of *B. succiniciproducens* for optimum succinate production by elementary flux mode analysis, based on a network model, containing all reactions for succinate production (Melzer et al. 2009; Becker et al. 2013). The fluxes are given as relative molar fluxes to the glucose uptake.

3.3 Key criteria for successful industrial production of succinate

Recent years upgraded the concept of biorefinery to become a mainstay of the future industrial landscape, considering valuable and innovative green products as substitutes for currently petrochemically derived compounds. The concept is similar to the traditional petroleum refinery, except its objective to convert biomass feedstocks into a myriad of applicable and industrial competitive products (Paster et al. 2004; Sauer et al. 2008; Cherubini 2010). This approach is forwarded to stepwise replace the global economy by a sustainable bioeconomy with bio-based products as one backbone among others. However, several key criteria have to be fulfilled to obtain an industrial platform for bio-based production processes, reaching competitive price margins. Succinate was reported with a selling price between $ 6 and 9 per kg and with production costs of about $ 1.1 per kg which have to be further reduced to $ 0.55 per kg in the future (Patel et al. 2006; Song and Lee 2006). This financial aspect has to be considered in terms of upstream and downstream sections as well as the fermentation part itself. Regarding the complete bioprocess costs, upstream processing covers 40 % of the overall succinate production costs, based on a raw sugar price of $ 0.40 per kg in 2013 (USDA), and desired succinate yields of about 90 %. Since downstream processes generally accounts for 50 % of the process costs, due to insufficient high product titers, complex mixtures of cell material and chemicals in the broth and desired final product purity (Wisbiorefine; Cheng et al. 2012), fermentation contributes to approximately 10 %. However, these three steps are closely intertwined (Figure 3.5), since substrate application specifies fermentation performance and subsequent recovery processes. The fermentation part affects both upstream and downstream processing by nutrition requirements of employed microorganisms and their respective product – by-product portfolio. Additionally, recovery strategies influence fermentation development, e.g. yield and productivity and the complexity of unit-operations (van Hoek et al. 2003). In this line, the effective cost allocation to each step is directly linked to decisions made for the other two process parts and represents major elements for improving the competitiveness of a bioprocess. Microbial hosts exhibit substrate preferences, limited tolerances towards components resulting from substrate pretreatment or need essential additives for cellular growth. Thus, low-cost media must be developed, preferably based on inexpensive raw material such as glycerol or lignocellulose hydrolysate. The fermentation process must feature high product yields and titers of above 100 g L^{-1} combined with efficient productivities of at least 2.5 g L^{-1} h^{-1}, while by-product formation must be kept to a minimum (Werpy and Peterson 2004; Patel et al. 2006). Efficient succinate recovery strategies have to be installed in an integrated bioprocess (Kurzrock and Weuster-Botz 2010; Cheng et al. 2012). Therefore, low pH fermentation will be advantageous considering cost savings for e.g. acidifying agents that are necessary for succinic acid recovery.

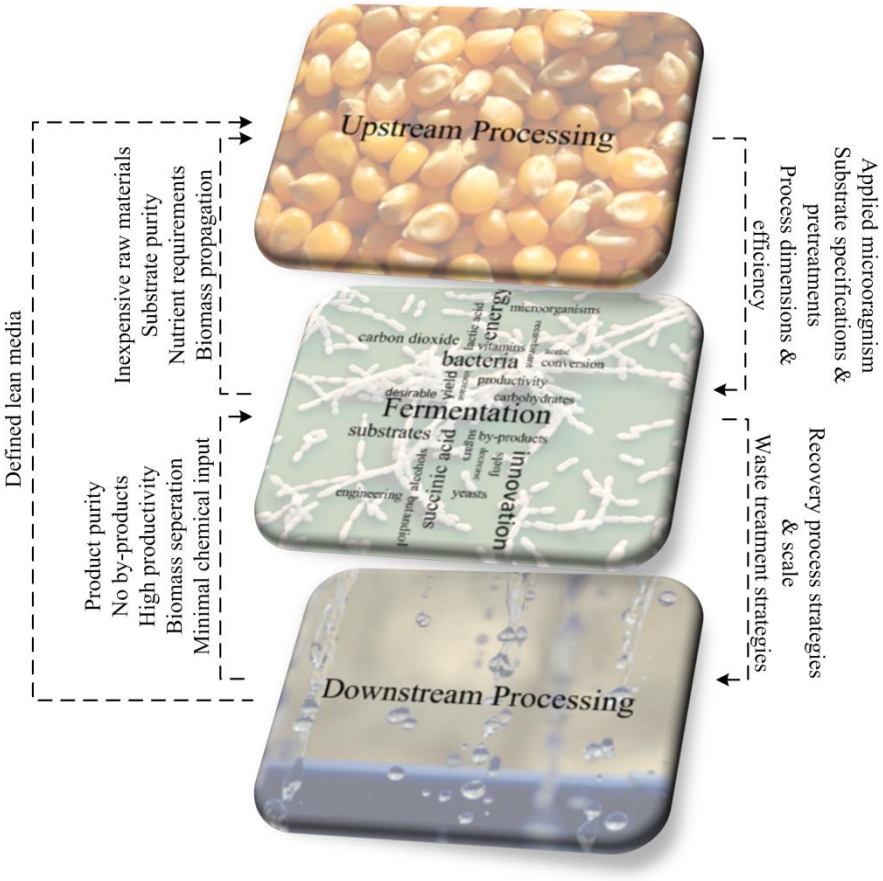

Figure 3.5 Schematic bioprocess model, considering the key criteria as dependencies and interactions between the fermentation and the pre- and post-fermentative phases. Dashed lines and respective arrows indicate prerequisites between the process parts.

3.4 Towards superior succinate production strains

3.4.1 Systems biotechnology approaches

Recently, industrial biotechnology broadened the field of study concerning optimization of bio-based production towards a holistic approach involving several biological disciplines. The generation of propitious cell factories is directly linked to evolving targets, unraveled by techniques like genomics (DNA), transcriptomics (RNA), proteomics (proteins), metabolomics and fluxomics (metabolites) (Kohlstedt et al. 2010), and phenomics (phenotype) (Bochner 2009). For optimization purposes regarding industrial aspects, it is not necessary to examine all levels of the omics-family to reveal beneficial modifications. Nevertheless, it can be helpful to combine various omics-techniques to draw a more accurate picture of the phenotype and its underlying interactions among functional layers.

In case of succinate production optimization, only few approaches combined two or more techniques. Most studies were built on *in silico* or *in vitro* tracking of carbon metabolism, accompanied by metabolic engineering of relevant targets to redistribute the carbon flux towards succinate (Lee et al. 2006; McKinlay et al. 2007; McKinlay and Vieille 2008; Becker et al. 2013). The underlying networks obviously derived from genome knowledge and annotations. This genomics tool is essential for the understanding of the nuts and bolts of the observed production phenotypic. By analysis of sequenced genomes, targets could be identified, that would contribute to an optimized phenotype by their amplification, deletion or introduction.

One level above, the adjustment of cellular metabolite synthesis and distribution can be mediated by two underlying regulatory mechanisms. On the one on hand, cells can probably switch on proteins or rather specify their activation state to direct fluxes towards desired metabolites. In this case, fluxes change according to varied conditions or modification implementation while gene expression patterns remain the same. The second option includes the fine tuning of RNA transcripts that has to be recruited for flux adjustment. Custom-made DNA microarray based gene expression analysis provides the possibility to gain a global view on the gene expression pattern of microorganisms. Thereby, different strains can be screened for global regulatory responses on various implemented genetic modifications. Furthermore, transcriptomic changes can be revealed under various conditions, e.g. high or low temperature. It is thus possible to unravel hindering metabolic bottlenecks that are mainly caused by non-optimal expression profiles of specific genes. On the other hand, modification based specific expression responses can be concluded from these datasets. A further approach allows for elucidation of gene expression concerning their participation in functional groups. This gene set enrichment analysis shows transcriptional responses according to several clustered genesets that share common biological function (Subramanian et al. 2005).

Metabolite fluxes represent the level above transcriptomics and proteomics and thus define the cellular metabolite state. The technique to visualize these fluxes, metabolic flux analysis (MFA), is a vital and widespread applied method throughout the industry related biotechnological landscape. MFA, combining an experimental part applying ^{13}C-carbon sources and a computational part with a genome-scale molecular network (Wittmann 2007), serves to gain information on metabolic turnover rates. The quantification of intracellular fluxes is realized by tracing the ^{13}C-carbon distribution throughout the network. It thus allows for the design of industrial valuable production hosts by pin-pointing specific targets like bottlenecks that cannot be clearly determined by phenotype observations. Successful industrial application of MFA was widely documented throughout recent literature, whereas a product spectrum was covered including relevant industrial products like amino acid, organic acids, vitamins, ethanol and antibiotics (Iwatani et al. 2008; Feng et al. 2010; Kohlstedt et al. 2010).

Cellular phenotypes are the most comprehensive features of microorganisms, since their biochemical and physiological properties are easily observable and the phenotype consequently results from gene expression and environmental influences. The recently described method of phenotypic microarray

analysis allows for specific phenotypic characterization of microorganisms with the aid of phenotypic microarrays (Bochner 2009). Based on the understanding of bacterial characterization through simple growth assays this approach is justified to describe various phenotypic alterations. Every microorganism is specially adapted towards its niche. Thus, the pattern of nutrient consumption or toxicity tolerance, based on this niche, varies between and defines them. Another interesting aspect in case of optimization approaches is the determination of loss of function or gain of function events. While gain of function is mostly beneficial and thus represents a desired feature of adapted phenotypes, loss of function can involve industrial detrimental characteristics, like the inability to metabolize a common substrate (Blaby et al. 2012).

3.4.2 Metabolic engineering of succinate production strains

Rational analysis, based on accessible knowledge of cellular pathways and kinetics, provides the opportunity for optimization that can be realized by molecular biological techniques. This systems metabolic engineering enables target-oriented implementation of genetic modifications thus leading to increased carbon fluxes and improved metabolite product yields (Stephanopoulos et al. 1998) while reconfiguring metabolic bottlenecks. Regarding succinate production the major engineering approach deals with increasing the succinate yield. In this line, the primary group of targets blatantly derives from the mixed fermentation characteristics of almost all microorganisms during anaerobic growth. For each industrial host, specific targets arise from their inherent set of by-products and their ratio to succinate. Since the metabolic optimization involves complete channeling of provided carbon towards succinate, targeted gene deletion is the most preferred method to realize the desired fluxes. Genes that were preferentially considered for this strategy encoded lactate dehydrogenase, formate C-acetyltransferase, acetate kinase or alcohol dehydrogenase (Bunch et al. 1997; Lee et al. 2006; Okino et al. 2008; Becker et al. 2013). Completing these tasks, succinate yields could be increased in natural succinate producing hosts. In primary aerobic industrial platform hosts, this strategy partially caused growth defects mainly due to the effect of completely linking cellular growth to succinate production and thus unbalancing the redox and energy capacities (Bunch et al. 1997; Stols and Donelly 1997; Sánchez et al. 2005; Jantama et al. 2008). Encouragingly, the introduction of the NAD generating malic enzyme in the respective host strain increased growth performance and succinate production (Stols and Donelly 1997). Considering the succinate biosynthesis pathway as target, the key reaction under optimal and thus anaerobic conditions is the carbon fixation step. Theoretically, three enzymes are capable of that reaction, whereas natural producers exhibit high specific enzyme activities for and carbon fluxes through the PEP carboxykinase (Podkovyrov and Zeikus 1993; Van der Werf et al. 1997; Kim et al. 2007; Becker et al. 2013). On the other hand, studies revealed the potential of non-ATP coupled PEP- and pyruvate carboxylase as carboxylation step (Vemuri et al. 2002; Sánchez et al.

2005; Litsanov et al. 2012), the latter one especially in context with PEP dependent substrate uptake systems, due to no losses in precursor supply (Shanmugam and Ingram 2008), while keeping in mind that carbon dioxide is essential to catalyze these thermodynamically unfavored reactions (Samuelov et al. 1991). Continuing with this pathway, the reductive TCA cycle directly emerges as target for pushing the carbon flux from oxaloacetate towards succinate by engineering the synthesis steps (Wang et al. 1998; Hong and Lee 2004; Lee 2009). This strategy is emphasized by observed accumulation of malic acid as pathway intermediate in engineered strains (Hong and Lee 2004; Lee et al. 2006). The additionally accumulating pyruvate represents an essential node in almost every metabolism (Sauer and Eikmanns 2005), but it is predestined to redirect its carbon via parts of the oxidative TCA cycle accompanied by the glyoxylate shunt (Lin et al. 2005; Raab et al. 2010; Scholten et al. 2010; Litsanov et al. 2012; Skorokhodova et al. 2013). Another crucial target comprises the balancing of the cellular redox capacities by e.g. implementation of heterologous genes (Hong and Lee 2001) or enzyme specific co-factor engineering (Wang et al. 2013). In this line, fine-tuned design approaches have to be followed by balancing the redox benefits and carbon loss, with e.g. the malic enzyme. Having in mind that all these strategies are mainly conducted regarding glucose based succinate production, it is inevitable to design microbial host that efficiently convert industrial desired raw materials, like molasses, hydrolysates or waste products into succinate. First studies elaborated the possibilities of glycerol conversion, exploiting the advantage of the higher reduced substrate for optimized redox balance (Blankschien et al. 2010; Scholten et al. 2009). Other approaches targeted the application of these mixed substrates in bioprocess refinements using both natural succinate producers and engineered platform microorganisms (Kim et al. 2004; Liu et al. 2008; Jiang et al. 2010; Chan et al. 2011; Borges and Pereira Jr 2011; Liu et al. 2012). However, these complex compounds often contain inhibitory substances to some extent that complicate optimization tasks. Overall, the sophisticated approach of understanding intracellular fluxes in combination with strain specific genome-scale models and molecular biology methods is highly suitable in context to industrial objectives like product formation, volumetric production or yield. Thus, rational analysis, based on accessible knowledge of metabolic pathways and their kinetics, provides the opportunity for optimization strategies. Nevertheless, engineering strategies for succinate production have to be exclusively adjusted to the respective microbial hosts, their specific networks and their physiological characteristics as natural producer or platform host. Thus, systems metabolic engineering indeed specifically alters basic production phenotypes that are mediated by just a few genes, but lacks the ability to select for robust strains (Blaby et al. 2012) and complex phenotypes. Moreover, many of these phenotypes remain largely inaccessible to this method due to difficulties in predicting the genotype-phenotype relationship.

3.5 Creating robust industrial phenotypes through evolutionary engineering

Under industrial aspects it is not very likely to design bioprocesses to the employed microorganisms. Nowadays, the development process is strongly interwoven with the capability of producing microorganisms that tolerate industrial preferred settings. Additionally, the industry is continuously searching for microorganisms that allow for a process, which features already existing facilities accompanied by low development costs. An answer to these driving forces is the application of multi-tolerant phenotypes that exhibit high tolerances for various stress triggers like temperature, product tolerances, pH, shear stress, osmolarity, nutrient supply, or toxicity (Table 3.3), called complex phentotypes.

Table 3.3 List of process step assigned industrially desired properties for competitive bioprocesses with their required complex phenotype.

Process step	Industrial requirements	Complex phenotype
Substrate supply	Implementation of substrate pre-processing (saccharification)	Temperature tolerance, tolerance towards impurities
	Application of industrial waste products and renewable ressources	Substrate metabolism
	Fluctuating substrate quality, impurities	Toxic residue tolerance
Plant facilities	Efficient energy policy	Temperature tolerance
	Spatial inhomogenities	High substrate tolerance, temperature tolerance, mechanical stress tolerance, pH tolerance, osmolarity tolerance, starvation tolerance
	Decrease contamination risk	Temperature tolerance, Phage tolerance
Fermentation process	High product titers	High substrate tolerance, product tolerance
	No by-product formation	Re-balancing of cellular redox metabolism
Downstream processing	Simple cell separation	Cell composition
	High product purity	Product tolerance
	Application of less purification agent	pH tolerance, solvent tolerance

These complex phenotypes distinguish themselves by their advanced polygenic response to stress triggers, since a single innovative product and its producing microorganism are not anywhere near sufficient to meet the overall criterions for an economic feasible and competitive production process. On that account, the last decades delivered various approaches to achieve methods for generating these specific microorganisms.

A classical method to forward these issues is mutagenesis (Figure 3.6), where the genetic material is iteratively exposed to mutagens. Surviving clones of this procedure are then selected for the specifically desired phenotype (Patnaik 2008). This method convinces by its simplicity but lacks the ability to modify microorganism target-oriented. Nonetheless, it gets attention due to the rapid and extensive development of high-throughput screening systems that enables quick and reliable phenotype characterization (Patnaik 2008). Considering industrial requirements for cultivation stability at high/low temperature or osmolarity or at mechanical stress, these complex or polygenic phenotypes need multiple coordinated changes to retain special features (Patnaik 2008). An option to

cope with these problems is nature itself with its most efficient method, the evolution. Evolution mimicking optimization strategies were already followed throughout the last years to gain new variants of proteins. This approach, called directed evolution, is performed in three steps: diversification, selection and amplification. In most cases, several rounds are conducted to achieve an improved feature.

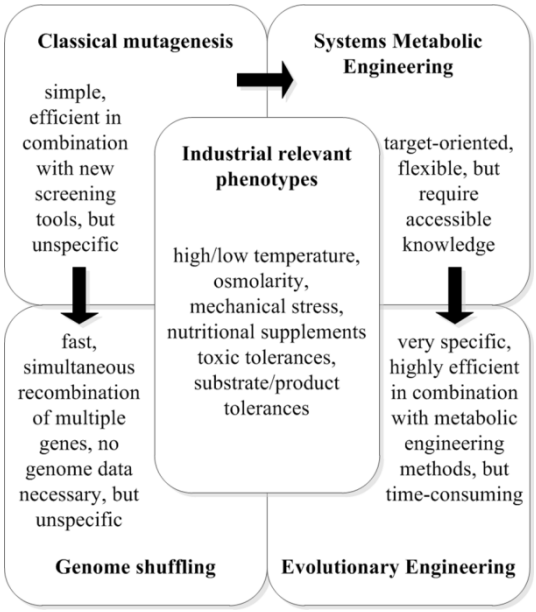

Figure 3.6 Several methods can be applied to generate industrially valuable phenotypes. The arrows depict that methods like systems metabolic engineering and genome shuffling emerged from the classical approach through increasing metabolic knowledge or more extensive recombination options. The evolutionary engineering developed from the combination of evolutionary adaptation with metabolic engineering strategies.

Based on this knowledge, further methods evolved in the last years, e.g. genome shuffling (Zhang et al. 2002) and were successfully applied to lactic acid production (John et al. 2010), respectively. However, most methods combine the need for separate screening steps and suffer the disadvantages of unspecific implementation of mutations or inaccessible genotype-phenotype knowledge. This will lead us to a straightforward, but very potent phenotype tailoring approach. During evolutionary adaptation in sequential batch or chemostat experiments, industrial conditions can be applied that specifically trigger the evolution to favorable phenotypes, which, naturally exhibit beneficial mutations. In combination with standard techniques of metabolic engineering, the evolutionary engineering can easily generate auspicious candidates for biotechnological processes. In a first step, known by-product pathways will be eliminated to restrict evolutionary adaptation towards desired products. Then, cells will be cultured under desired conditions to evolve potential phenotypes. At several time-points, single colonies will be isolated to access knowledge of genomic, transcriptomic or phenomic changes. Since most beneficial mutations mediate fitness advantage within the population, screening of these phenotypes is very efficient. Another great advantage is the convergence of developed phenotypes, whereby 6 out of 7 independently adapted *E. coli* lines were shown to exhibit similar phenotypic

characteristics, while the gene expression differed from each other (Fong et al. 2005). It was also shown that adapting genomes evolve in a near-linear fashion by accumulating mutations, while vigorously fitness improvements occur in the beginning of adaptive processes and distinctly decreases over time (Barrick et al. 2009). Combining these two facts, it is obvious that a parallel adaptation approach will yield highly efficient phenotypes in short time. Considering this method to be applied in strain optimization, four facts have to be kept in mind. First, the physiological limitations of the microorganism have to be studied to draw a picture of the complete criterion dependent performance space. This information will then be used to set up adaptation starting points, where growth is affected by the stressor, but still present. Second, the engineering level of the applied microorganism must be determined. Here, the wild-type easily comes to mind, but strains exhibiting definite genetic modifications, like gene deletion, will serve as a better host. Their metabolism is channeled to a specific product and often includes redox balance inconsistencies. This will narrow down the degrees of freedom for evolution and thus raise the odds on succeeding in desired phenotype improvement. Extensively modified production strains are unfavorable adaptation hosts. Indeed, a large number of implemented genetic changes like point mutation or promoter exchanges direct fluxes into product channels, but engender detrimental growth characteristics. However, the main crux lies in the evolutionary ability to remove these cellular undesired modifications and switch back to the wild-type allele. Thus phenotype generation is still possible but involves loss of industrial relevant production features. The third fact includes the question for the adaptation medium. Complex media facilitate faster growth but cause the accumulation of auxotrophies. Moreover these auxotrophies remain undetected during adaptation while increasing microbial fitness due to less metabolic costs for the cellular growth. As a consequence it is highly appreciated to apply minimal media, while their composition has to be adjusted for each approach. Fourth, it is necessary to setup the adaptation approach, which comprises the question for sequential batch or continuous cultivation, as well the fashion of stress induction. While batch experiments are simple structured, their effort for iteratively media preparation and inoculation exceeds continuous approaches, while they are running. Prior to the adaptation their configuration is much more elaborate. Considering the stress application, continuous approaches allow for constant cellular response documentation and subsequent counteracting. During sequential batches in small volume, these results can only be determined in between iterations. All things considered, evolutionary adaptation has to be well prepared to create conspicuous new phenotypes.

Temperature

The biological significance of temperature is undeniable. All organisms and their vital surroundings are directly or subtly influenced by it. The industrial interest in temperature adapted phenotypes can be easily linked to economic matters. Concerning specific enzymes, cold adapted proteins that exhibit

highest activities at low temperatures are state of the art nowadays in the detergent industry and rule the sales figures of companies. In contrast, the development of adapted whole cells for cultivation purposes is in its early stages. Improved microbial temperature stability is highly appreciated in fermentation processes to keep the cooling costs down. Furthermore, the extension of the growth optimum decreases the probability of external contamination that occur due to impracticalities in vessel sterilization, since the adapted strain exceeds in growth performance compared to standard contamination seeds. Another economic aspect is the combination of substrate pre-treatment steps with the following fermentation to a single step process (Turner et al. 2007). Along with it, enzyme kinetics, basically chemical reactions can be described by the Arrhenius equation. A generalization of this equation describes doubled reaction rate per 10 °C increased temperature. Thus, the industry aims for better growth and production performance of temperature adapted microorganisms at elevated temperatures. Interestingly, the Arrhenius equation was shown to be applicable for bacterial growth in their temperature optimum (Herendeen et al. 1979). However, rational approaches to design temperature tolerant microorganism were mainly based on random findings. In case of *E. coli*, the addition of methionine to a cultivation medium enabled for growth at a lethal temperature (Ron and Davis 1971). On closer inspection two specific amino acid sites were revealed in homoserine *o*-succinyltransferase, the first enzyme in methionine synthesis that stabilized the protein and thus *E. coli* growth at higher temperature. In general, the bacterial heat stress response is just partly understood caused by its magnitude of involved regulatory pathways. Since temperature represents a pervasive challenge for microorganisms, they developed a successful adaptation scheme to overcome this stress called heat shock response. This mechanism is mediated by organism specific transcription factors that are directly activated by the perturbant before damage or by the damage itself (DNA, mRNA, proteins). Afterwards ubiquitous existing chaperons and proteases are activated that deal with unfolded or misfolded proteins to preserve the protein homeostasis (Lim and Gross 2011). Other predicted strategies describe the maintenance of physiological rates achieved by a quantitative approach, where the concentration of enzymes is increased throughout adaptation. A qualitative approach comprises more stable enzyme variants, whereas the modulation approach minimizes the temperature effect by modifying the protein environment (Clarke 2003). Concluding this, it is inevitable to acquire tolerant phenotypes to facilitate the strategic tailoring of temperature tolerant microorganisms.

Product Tolerance

A common claim of biorefinery is a fermentation process yielding maximal titers, a key performance indicator. The crux in this claim is the fact that even though some industrial microorganisms show the potential of producing organic acids in extremely high titers they exhibit intolerances against the produced compounds to some extent (Loubiere et al. 1997; Song et al. 2008; Urbance et al. 2004),

which limits the commercial application. During a mixed organic acid fermentation secreted acids dissociate and cause a rapid decrease in pH. In case of non-regulated cultivation media the pH drops below the corresponding pK_a and the organic acids remain undissociated. These acids can then directly diffuse across cellular membranes (Warnecke and Gill 2005). They enter the cell unimpeded and accumulate intracellular. The neutral pH of the cytosol promotes the dissociation of these organic acids resulting in a severe pH decrease and thus decreased integrity of purine bases and severe protein denaturation (Warnecke and Gill 2005). At a neutral pH instead, the nearly equilibrium between intracellular and extracellular pH prevents from toxic accumulation of organic acids in the cell. Furthermore, at neutral pH organic acids dissociate into protons and acid residues, which can only be taken up via secondary transport. Anyhow, the rational understanding of these complex networks is limited by its broad spectrum. Microorganisms have developed several strategies to compensate for the problem of acid shock that is accompanied by a decrease of cytosolic pH. The proton permeability of membranes can be triggered through their composition (Booth 1999). A further response can be observed on the level of transport mechanisms. As recently reported, a succinate adapted *E. coli* exhibited strong changes on the level of transcriptomics for genes that contributes to several transport mechanisms. Additionally, higher expression patterns could be observed for genes that are involved in osmoprotectant biosynthesis (Kwon et al. 2011). Nevertheless, it was shown that not only growth associated organic acid production, but also organic acid salts impede cellular growth, both, for natural succinate producers and engineered microorganisms, when added to the medium prior to cultivation (Lin et al. 2008; Li et al. 2010; Hoon et al. 2010). Besides, organic acid tolerance depends on the respective organic acid. While succinate seems to be a mild stressor with high critical concentrations, formate severely ceases cell proliferation (Loubiere et al. 1997; Lin et al. 2008). It is therefore crucial to understand intracellular regulation pathways towards industrial oriented improvements in bio-succinate production. This effort can be minimized by creating and evaluating evolutionary derived complex phenotypes with beneficial features (Buschke et al. 2013).

pH Tolerance

Industrial bioprocesses are closely connected to economic production procedures and down-stream treatments. Considering the succinate production, a classic recovery method comprises the application of calcium salts and the subsequent acidification with sulfuric acid (Kurzrock and Weuster-Botz 2010), which accounts for a process relevant cost factor. Lower cultivation pH comprises lower investment costs due to less salt processing operations and lower variable costs caused by less salt acquisition. Thus regarding process sustainability, acidic pH increases the carbon footprint of succinate production (Jansen et al. 2012). Furthermore, applied calcium carbonate combines lower cultivation pH with buffer effect and carbon dioxide source. It is thus recommended to employ acidic pH tolerant microorganisms for production processes. By default, many microorganisms exhibit an

optimum at neutral pH with decreasing tolerance toward acidic pH, belonging to the neutralophilics. For organic acid producing bacteria the fermented products decrease extracellular pH that causes a transmembrane pH gradient shift. In the end organic acids accumulate in the cytosol and directly perturb the intracellular pH (Booth 1985). The response to that event is mediated by a passive and an active regulated homeostasis. The first one comprises low membrane permeability to protons and a cytoplasmic buffer capacity. The active mechanisms include controlled transport of cations across the membrane (Booth 1999). An additional response is the synthesis of proteins that forms neutral compounds from acidic ones or converts neutral ones to alkaline substances, in respect to the pH stress. Taking together, pH tolerance and organic acid tolerance are somewhat intertwined and cannot be clearly treated individually.

4 Material and Methods

4.1 Chemicals

Yeast extract, peptone and BHI (brain heart infusion) were purchased from Becton Dickinson (Heidelberg, Germany). Ninety-nine percent [1-^{13}C] glucose was obtained from Eurisotop (Saint-Aubin Cedex, France). All other chemicals were of analytical grade and purchased from Sigma Aldrich (Steinheim, Germany), Merck (Darmstadt, Germany), Roth (Karlsruhe, Germany) and Fluka (Buchs, Switzerland), respectively.

4.2 Growth media

4.2.1 Media for genetic engineering

B. succiniciproducens was grown in liquid BHI medium (Table 4.1) for genetic engineering purposes, i.e. for electroporation and during the regeneration step of transformation. Selection of plasmid carriage was performed on BHI-MOPS agar plates (Table 4.2) by adding chloramphenicol stock solution (30 g L^{-1}) to a final concentration of 5 mg L^{-1} prior to usage. Sucrose was added to 100 g L^{-1} for second recombination selection before autoclaving.

Table 4.1 Composition of BHI medium.

Component	Quantity [g]
BHI	37
ad 1 L aqua dest autoclaved (121 °C, 20 min)	

Table 4.2 Composition of BHI-MOPS agar plates.

Component	Quantity [g]
BHI	37
Agar	18
ad 750 mL aqua dest. autoclaved (121 °C, 20 min)	
MOPS	9.375
Bis-Tris	5.75
$Mg(OH)_2$	0.625
ad 250 mL aqua dest., stirred overnight	
$NaHCO_3$	1.79
sterile filtered, add 250 mL MOPS-Bis-Tris solution to 750 mL BHI agar medium	

E. coli TOP10 cultivations for plasmid amplification were performed in LB broth (Luria Bertani) or on LB agar plates (Table 4.3). For selection purposes, chloramphenicol was added to the respective medium to a final concentration of 50 mg L^{-1}. Agar plates were prepared by adding 18 g L^{-1} agar.

Table 4.3 Compositions of LB medium.

Component	Quantity [g]
Tryptone	10
Yeast extract	5
NaCl	5
ad 1 L aqua dest autoclaved (121 °C, 20 min)	

After heat shock, *E. coli* TOP10 cells were regenerated in SOC (super optimal broth (SOB) with catabolite repression) medium (Table 4.4).

Table 4.4 Composition of SOC medium.

Component	Quantity [g]
Tryptone	20
Yeast extract	5
NaCl	0.5
ad 970 mL aqua dest. autoclaved (121 °C, 20 min)	
$MgCl_2$ (1M) sterile filtered	10 mL
$MgSO_4$ (1M) sterile filtered	10 mL
Glucose (2M), autoclaved (121 °C, 20 min)	10 mL

4.2.2 Media for growth and succinate production

For all media, stock solutions were prepared separately (Table 4.5), subsequently sterile filtered and stored at room temperature. The vitamin solutions 1 and 2 were stored as aliquots at -20 °C. Prior to usage, the stock solutions were mixed at room temperature as needed. A complex medium A was applied for first pre-cultures of *B. succiniciproducens*. The second pre-culture and following main cultivations of *B. succiniciproducens* were conducted in respective media (Table 4.6 to Table 4.11).

Table 4.5 Composition of stock solutions for *B. succiniciproducens* cultivation.

Component	Quantity [g]
Glucose solution	
Glucose	500
ad 1L aqua dest., sterile filtered	
Maltose solution	
Maltose	500
ad 1L aqua dest., sterile filtered	
Glycerol solution	
Glycerol (99.5 %)	502.5
ad 1L aqua dest., sterile filtered	
Yeast extract solution	
Yeast extract	100
ad 1L aqua dest., sterile filtered	
Peptone solution	
Peptone	100
ad 1L aqua dest., sterile filtered	
Salt solution	
NaCl	100
$MgCl_2$	20
$CaCl_2$	20
ad 1L aqua dest., sterile filtered	
$(NH_4)_2SO_4$ solution	
$(NH_4)_2SO_4$	500
ad 1L aqua dest., sterile filtered	
K_2HPO_4 solution	
K_2HPO_4	500
ad 1L aqua dest., sterile filtered	
Amino acid solution	
L-valine	25
L-glutamate	25
ad 1L aqua dest., sterile filtered	
Vitamin solution 1	
Thiamin HCl (B_1)	3
Riboflavin (B_2)	6
Nicotinamide (B_3)	3
Pantothenic acid (B5)	10
Pyridoxine HCl (B6)	1
Biotin (B7)	0.5
each vitamin was individually dissolved, biotin and riboflavin were titrated with 2 M NaOH to complete dissolution, ad 1L aqua dest., sterile filtered	
Vitamin solution 2	
Cyanocobalamin (B_{12})	0.5
ad 1L aqua dest., sterile filtered	
Na_2CO_3 solution	
Na_2CO_3	200
ad 1L aqua dest., sterile filtered	

A total volume of 10 mL of each medium was freshly prepared from stock solutions (Table 4.5) for 30 mL scale serum bottles. Serum bottles were autoclaved prior to usage containing 0.5 g $MgCO_3$ (final concentration in medium of 50 g L^{-1}). Fermentations for $MgCO_3$ free preparation of cell pellets for RNA isolation were carried out in bioreactors using minimal medium E according to Table 4.10 in corresponding volumes. Cultivation experiments of *B. succiniciproducens* variants carrying expression vectors were conducted in described media A – F (Table 4.6 to Table 4.11), containing 5 mg L^{-1} chloramphenicol, respectively.

Table 4.6 Complex growth medium A for first pre-cultures.

Stock solution	Volume [mL]
Yeast extract	50
Peptone	50
Salt solution	10
$(NH_4)_2SO_4$	2
K_2HPO_4	6
Glucose	100
Aqua dest.	ad 1 L

Table 4.7 Complex glucose based growth medium B for succinate production.

Stock solution	Volume [mL]
Yeast extract	100
Na_2CO_3	20
$(NH_4)_2SO_4$	2
K_2HPO_4	6
Glucose	100
Aqua dest.	ad 1 L

Table 4.8 Industrial growth medium C for succinate production.

Stock solution	Volume [mL]
Yeast extract	100
Na_2CO_3	20
$(NH_4)_2SO_4$	2
K_2HPO_4	6
Glycerol	100
Maltose	40
Aqua dest.	ad 1 L

Table 4.9 Complex growth medium D for $MgCO_3$-free cultivations.

Stock solution	Volume [mL]
Yeast extract	100
Na_2CO_3	20
$(NH_4)_2SO_4$	2
K_2HPO_4	24
Glucose	100
Aqua dest.	ad 1 L

Table 4.10 Defined growth medium E for succinate production.

Stock solution	Volume [mL]
Amino acid solution	20
Salt solution	10
Vitamin solution 1	10
Vitamin solution 2	1
$(NH_4)_2SO_4$	2
K_2HPO_4	6
Glucose	100
Aqua dest.	ad 1 L

Table 4.11 Defined growth medium F for succinate production.

Stock solution	Volume [mL]
Amino acid solution	20
Salt solution	10
Vitamin solution 1	10
Vitamin solution 2	1
$(NH_4)_2SO_4$	10
K_2HPO_4	6
Glucose	100
Aqua dest.	ad 1 L

4.3 Genetic engineering

4.3.1 Strains and plasmids

The wild-type strain *B. succiniciproducens* DD1, the mutant *B. succiniciproducens* Δ*ldhA* Δ*pflD* and the mutant *B. succiniciproducens* Δ*ldhA* Δ*pflA* were obtained from BASF SE (Ludwigshafen, Germany) (Table 4.12). *E. coli* TOP 10 was acquired from Invitrogen (Karlsruhe, Germany) and used for plasmid amplification.

Table 4.12 Strains of *B. succiniciproducens* used in the present work

Strain	Modification(s)	Reference
B.succiniciproducens DD1	Wild-type	BASF SE
B.succiniciproducens DD3	DD1 + deletion of lactate dehydrogenase *ldhA* and formate C-acetyltransferase *pflD*	BASF SE
B.succiniciproducens DD5	DD1 + deletion of lactate dehydrogenase *ldhA* and formate C-acetyltransferase activator *pflA*	BASF SE
E. coli TOP 10	F- *mcrA* Δ(*mrr-hsdRMS-mcrBC*) φ80*lacZ*ΔM15 Δ*lacX*74 *recA*1 *araD*139 Δ(ara-leu)7697 *galU galK rpsL* (Str^R) *endA*1 *nupG*	Invitrogen

A *Pasteurellaceae* specific episomal replicating expression vector (Frey 1992) was applied for *B. succiniciproducens* transformation. The vector had a size of 8.1 kb, contained an origin of replication for *E. coli* and *B. succiniciproducens*, a multiple cloning site for site specific insert integration and a chloramphenicol acetyltransferase gene for antibiotic resistance (Cm^R) as selection marker. Genome-based transformation was realized using the pClik int *sacB* Cm integrative vector. It had a size of 4.3 kb, contained an origin of replication for *E. coli*, a multiple cloning site, the chloramphenicol resistance and the gene *sacB* encoding levansucrase of *Bacillus subtilis*. Cm^R and *sacB* served as selection marker for first and second homologous recombination events during genome integration.

Table 4.13 Plasmids used for targeted genetic modification of *B. succiniciproducens*.

Plasmid	Specification(s)	Reference
pJFF224-XN	Episomal vector with ORI for *E. coli*, *mob*, Cm^R as selection marker and MCS	BASF SE
pClik *sacB* Cm	Integrative transformation vector for *B. succiniciproducens* with MCS, ORI for *E. coli*, and Cm^R and *sacB* as selection markers	BASF SE

Transformation vectors were constructed by using respective DNA fragments, which were amplified via polymerase chain reaction employing site-specific primer pairs. End primers were artificially modulated by insertion of appropriate restriction sites for specific integration into the vector. Purified DNA fragments were restricted with two appropriate enzymes and ligated into the MCS of the vector.

4.3.2 Isolation of chromosomal DNA from *B. succiniciproducens*

Cells from a cryogenic stock were incubated overnight in BHI medium. The culture broth was centrifuged (16,000 x g, 4 °C and 5 min) and the supernatant was discarded. Then, 400 µL lysis buffer (DNeasy Plant Minikit; Qiagen, Hilden, Germany) and 4 µL RNase solution (100 mg mL^{-1}) were added to the cell pellet. The suspension was vortexed and incubated for 15 min at room temperature. In the next step, 130 µL neutralization buffer was added to the suspension. The mixture was kept on ice for 5 min. Afterwards 600 µL Roti®-Phenol/Chloroform/Isoamylalcohol (Carl Roth GmbH, Karlsruhe, Germany) were added, followed by vigorous mixing and subsequently centrifugation (16,000 x g, 4 °C and 10 min). The upper phase was transferred to a sterile 1.5 mL reaction tube, mixed with 600 µL Chloroform/Isoamylalcohol (24:1) and again centrifuged (16,000 x g, 4 °C and 10 min). Then, the upper phase was transferred to a sterile 1.5 mL reaction tube, followed by the addition of 50 µL sodium acetate (3 M, pH 5.5) and 1 mL pure ethanol. The precipitated DNA was then pelleted by centrifugation (16,000 x g, 4 °C and 10 min). After that the supernatant was discarded. Subsequently, 1 mL of icecold 70 % ethanol was added. The washed DNA pellet was harvested by centrifugation (16,000 x g, room temperature and 1 min). Right after removing the supernatant the pellet was dried at room temperature for 10 min. Finally, the pellet was dissolved in 200 µL sterile aqua dest..

During strain construction and screening steps, DNA was routinely isolated by following a fast preparation protocol. In this case, cells were disrupted using glass-beads (0.10 – 0.25 mm; Retsch, Haan, Germany) and a mixer mill (30 sec, 30 s^{-1}; Mikro-Dismembrator S, Sartorius Stedim, Göttingen, Germany). Cell debris was removed by centrifugation (16,000 x g, room temperature and 1 min) and the supernatant, containing the DNA, was transferred into a sterile 1.5 mL reaction tube.

DNA quantity and quality were measured using the Nanodrop®-Spectrophotometer ND-1000 (Thermo Fisher Scientific Inc., Waltham, MA, USA). DNA samples exhibiting a 260/280 ratio of 1.8 to 2.0 were considered to be pure DNA. For genome sequencing the DNA integrity was validated with an 0.8 % agarose gel. Isolated DNA was stored at 4 °C.

4.3.3 Polymerase chain reaction

The polymerase chain reaction (PCR) was performed in a Mastercycler Eppgradient (Eppendorf, Hamburg, Germany). A Phusion® polymerase (New England Biolabs, Frankfurt, Germany), exhibiting a proof-reading function, was applied for genetic engineering purposes and for sequencing supported verification of specific nucleotide exchanges. The validation of engineered strains was completed using PCR master (Roche Applied Science, Mannheim, Germany), which employed the *Taq* polymerase.

Table 4.14 PCR profiles for Phusion® polymerase and PCR master (annealing temperature and elongation time were chosen primer specifically).

		Phusion® polymerase		**Taq polymerase**	
	Step	**Temperature [°C]**	**Time [sec]**	**Temperature [°C]**	**Time [sec]**
1 x	Denaturation	98	120	95	120
	Denaturation	98	10	95	30
30 x	Annealing	52 – 59	30	52 – 59	30
	Elongation	72	30 per kb	72	60 per kb
1 x	Elongation	72	5	72	7
	End	10	∞	15	∞

Appropriate primers were designed with the Primer3 tool (http://biotools.umassmed.edu/bioapps/primer3_www.cgi). Afterwards, relevant restriction sites were added to the designed primers. The calculation of primer annealing temperature was performed using the NEB T_m Calculator Tool (https://www.neb.com/tools-and-resources/interactive-tools/tm-calculator=). All primers were purchased from Life Technologies (Carlsbad, CA, USA). Purified genomic DNA, fast prepared genomic DNA and purified plasmid DNA were used as PCR templates according to following schemes (Table 4.15 and Table 4.16).

Table 4.15 Reaction setup for a PCR with Phusion® polymerase.

Component	Volume [µL]	Final concentration
Phusion® HF buffer (5x)	10	1 x
dNTPs	1	200 µM
Forward primer	0.5	1 µM
Reverse primer	0.5	1 µM
Template DNA	Variable	~ 200 ng
Phusion® polymerase	0.5	1 U
Nuclease free water	ad 50 µL	

Table 4.16 Reaction setup for a PCR using Taq polymeras.

Component	Volume [µL]	Final concentration
Forward primer	0.2	1 µM
Reverse primer	0.2	1 µM
Template DNA	Variable	~ 200 ng
Master	10	1 x
Nuclease free water	ad 20 µL	

PCR amplified products were purified with the illustra GFX™ PCR DNA & Gel Band Extraction Kit (GE Healthcare, Solingen, Germany). A list of all primers, applied in the present work, can be found in the appendix (Table 9.10).

4.3.4 Gel electrophoresis

Gel electrophoresis was performed to analyze PCR products and RNA integrity using agarose gels (0.8 % w/v and 1.5 % w/v in 1 x TAE buffer, respectively). Electrophoresis was realized at 100 – 120 V for 1 to 1.5 h in an Owl B1A easy cast mini or D2 wide gel system (Thermo Fisher Scientific, Waltham, MA, USA) with the Power Pack P25T (Biometra, Göttingen, Germany) in 1 x TAE buffer, freshly prepared from a 50 x TAE buffer stock solution (Table 4.17). RNA integrity gels were carried out with the Biometra Compact XS/S system, applying the Power Pack P25 (Biometra, Göttingen, Germany).

Table 4.17 Composition of 50 x TAE buffer for gel electrophoresis.

Component	Quantity
Tris	242.28 g
EDTA (0.5 M, pH 8)	100 mL
Acetic acid	52 mL
ad 1 L aqua dest.	

Prior to gel loading, samples were mixed with 10 x orangeG dye (Table 4.18) or 6 x loading dye (Fermentas, St. Leon-Rot, Germany).

Table 4.18 Composition of orangeG gel loading buffer.

Component	Quantity
Glycerol (60 %)	50 mL
EDTA (0.5 M, pH 8)	100 mL
OrangeG	75 mg

Visualization of DNA fragments was performed by gel staining in an ethidium bromide bath (0.5 mg L^{-1} ethidium bromide). Appearing DNA-ethidium bromide complexes were illustrated under UV light with the Gel iX Imager (Intas Imaging Instruments GmbH, Göttingen, Germany). For size estimation of DNA and RNA fragments, a 1 kb ladder and a 100 bp ladder were used, respectively (GeneRuler™, Fermentas, St. Leon-Rot, Germany).

4.3.5 Construction of transformation vectors

B. succiniciproducens specific expression and integrative vectors were constructed by insertion of PCR amplified fragments into the MCS of empty vectors pJFF224-XN and pClik *sacB* Cm, respectively (Table 4.13). Two distinct restriction sites served as integration points, since vector and fragment were digested with appropriate restriction enzymes (FastDigest, Fermentas, St. Leon-Rot, Germany) (Table 4.19).

Table 4.19 Restriction enzyme digestion setup for insert and vector.

Component	Volume [µL]	Final concentration
Restriction enzyme A	1	
Restriction enzyme B	1	
FastDigest buffer (10 x)	2	1 x
DNA	Variable	0.2 µg (insert); up to 1 µg (vector)
ad 20 µL nuclease free water Incubation for 30 min at 37 °C		

Afterwards, the digested vector was treated with shrimp alkaline phosphatase (SAP) to prevent self-ligation (Table 4.20). Then, the dephosphorylated vector was directly applied in the following ligation reaction (Table 4.21). Both steps were conducted using the Rapid DNA Dephos & Ligation Kit (Roche Diagnostic, Mannheim, Germany). The ligation reaction mix was directly transformed into *E. coli* TOP10 cells by heat shock or stored at -20 °C.

Table 4.20 Reaction setup for vector dephosphorylation.

Component	Volume [µL]	Final concentration
Vector DNA	Variable	up to 1 µg
rAPid Alkaline Phosphatase Buffer (10 x)	2	1 x
SAP	1	1 unit
ad 20 µL nuclease free water		
Incubation for 10 min at 37 °C and deactivation for 2 min at 75 °C		

Table 4.21 Reaction setup for ligation of vector and insert.

Component	Volume [µL]	Final concentration
Vector DNA	Variable	50 ng
Insert DNA	Variable	150 ng
Dilution buffer (10 x)	2	1 x
ad 10 µL nuclease free water		
Ligation buffer (2 x)	10	1 x
T4 DNA ligase	1	5 units
Mix thoroughly		
Incubation for 20 min at room temperature		

4.3.6 Transformation

E. coli

Competent *E. coli* TOP10 cells were transformed by heat shock. Aliquoted cell suspension (50 µL) was thawed on ice and subsequently mixed with 5 µL ligation mixture. After 30 min incubation on ice, cells were shocked for 45 sec at 45 °C in a thermo block (Thermomixer comfort, Eppendorf, Hamburg, Germany). Afterwards, cells were cooled down immediately and kept on ice for 2 min. For regeneration, the transformed cells were incubated for 1 h at 37 °C and 600 rpm in SOC medium. Then, the cells were harvested (16,000 x g, room temperature and 1 min). The supernatant was discarded, except a residual volume of about 200 µL, which was used for resuspension of the cell pellet. Transformed *E. coli* Top10 cells were streaked out on LB^{Cm} agar plates and incubated for 24 h at 37 °C.

B. succiniciproducens

Cells from a cryogenic stock were incubated overnight in BHI medium (10 mL, 37 °C and 130 rpm). The main culture (100 mL, 37 °C and 130 rpm), initially started with an optical density (OD_{600}) of 0.3, was grown until OD_{600} of 0.8 and cells were then harvested by centrifugation (10,000 x g, 4 °C and 5 min). After washing with sterile, ice-cold glycerol (10 %), the cells were resuspended in 6 mL glycerol (10 %) per gram cell wet weight. The electroporation time was determined by using cell

suspension without plasmid DNA. If the electroporation time of the control was lower than 8 ms, the cell suspension was further diluted with glycerol (10 %). The transformation of *B. succiniciproducens* was conducted with the GenePulser XCell (Bio-Rad, Hercules, CA, USA) at 2 kV, 400 Ω and 25 µF after mixing 200 µL cell suspension with 2 and 5 µg of integrative plasmids or 200 and 500 ng of episomal plasmids in a 2 mm electroporation cuvette. After the electroporation pulse, cells were regenerated for 2 h or 1h for episomal plasmids in BHI medium at 37 °C and 600 rpm (Thermomixer comfort, Eppendorf, Hamburg, Germany). Afterwards, the cell suspension was plated on BHI-MOPS^{Cm} agar plates and incubated for 2 – 3 days at 37 °C. Cells carrying the episomal plasmid and cells that successfully past the first recombination by integration of the integrative vector were selected for growth via the antibiotic resistance. The existence of desired inserts was then confirmed by PCR. In case of integrative plasmids, a second recombination was needed. Here, positive clones of the first recombination were incubated in 2 mL liquid BHI medium for 1 – 2 days at 37 °C and 130 rpm. 200 µL of a 1:100 dilution was then streaked out on BHI-Sac agar plates and incubated at 37 °C overnight, selecting for clones which have lost the *sacB* gene. Additionally, to increase the recombination probability, 50 µL of this cell suspension was used to inoculate 2 mL liquid BHI-Sac medium overnight at 37 °C and 130 rpm. This step was repeated 4 times to generate 5 generations of second recombination clones. Two clones from each recombination generation, validated by sucrose resistance, were used to validate the integration of the desired modification via PCR or sequencing.

4.3.7 Plasmid DNA purification

The GeneJET Plasmid Miniprep Kit (Thermo Fisher Scientific, Waltham, MA, USA) was used for purification of plasmid DNA from *E. coli* cells. This was performed from 3 mL overnight culture of a single *E. coli* colony in a total of 5 mL liquid LB^{Cm} medium at 37 °C and 130 rpm. The isolation was conducted according to the manufacturer's protocol. Plasmid DNA concentration was measured spectrophotometrically (see 4.3.2) and the plasmid was subsequently checked for the desired inserts by digestion or PCR.

4.4 Cultivation

4.4.1 Strain conservation

Cells from a cryogenic stock were cultivated in complex medium (LB for *E. coli* and medium A for *B. succiniciproducens*). Exponentially growing cells were harvested, and 500 µL cell culture was mixed with 500 µL sterile glycerol (86 %). The suspension was subsequently stored at -80 °C in 2 mL cryo culture tubes.

4.4.2 Batch cultivation in serum bottles

First pre-cultures of *B. succiniciproducens* were grown in pre-sterilized serum bottles (30 mL, sealed with gas-tight butyl rubber stopper) filled with 0.5 g $MgCO_3$ as buffering agent and 10 mL of complex medium A. The filled bottles were inoculated from cryo stocks, amended with CO_2-rich atmosphere of 0.8 bar overpressure after 10 automatic flushing steps and then incubated on a rotary shaker (37 °C, 130 rpm; shaking diameter 50 mm; Certomat BS-1, Sartorius Stedim S.A., Göttingen, Germany). During exponential growth, cells were harvested by centrifugation (16,000 x g, 4 °C and 5 min) including a washing step with the afterwards applied medium (Table 4.6 to Table 4.11). The obtained cell suspension was then used for inoculation of the second pre-culture. The conditions of the incubation differed depending on experimental needs, as specified below. In all cases, exponentially growing cells were harvested and washed with fresh medium as described above and applied as inoculum for the main culture, which was carried out with three biological replicates. The initial cell concentration was adjusted to an OD_{600} of 0.3. For fluxome studies, naturally labeled glucose was replaced by 99 % [1-^{13}C] glucose in second pre- and main cultures, respectively.

4.4.3 Sequential batch fermentation in serum bottles for evolutionary adaptation

For adaptive evolution the serum bottle batch experiments (see 4.4.2) were extended to sequential batch approaches. Hereby, exponentially growing cells from a first main culture in minimal glucose medium served as starting culture for the adaptation. During the adaptation experiment, proliferating cells were harvested and washed with fresh minimal medium and subsequently employed for inoculating serum bottles of the next batch generation applying the same medium. The initial cell concentration was always adjusted to OD_{600} of 0.3. The cultivation was conducted in a rotary shaker (see 4.4.2) and adaptation parameters were set according to experimental needs. Cellular adaptation

was monitored with OD_{600} and cells were sampled at an OD_{600} of about 5. This procedure was identically repeated for all iterations, each one conducted as triplicate from the respectively best grown culture.

4.4.4 Sequential batch fermentation in small scale bioreactors for evolutionary adaptation

Cultivation was performed in a SixFors fermenter system (Infors AG, Bottmingen, Switzerland) to monitor and control the pH (Mettler Toledo, Gießen, Germany). Cells from a serum bottle main culture (see 4.4.2) using minimal glucose medium were taken as starting culture for adaptation purposes and prepared by a washing step in fresh minimal medium. Initial cell concentration was adjusted to an OD_{600} of 0.3 and the starting pH was set to experimental needs by adding 0.5 M H_3PO_4. During cell proliferation the pH of the broth was maintained at a desired value by automatically controlled addition of 1 M Na_2CO_3. The added volume was calculated by measuring the pumping time. Cultivation was operated at a temperature of 37 °C, a stirrer speed of 500 rpm and a constant CO_2-sparging at 0.1 NL h^{-1}. Each iteration was conducted as a single experiment, during which the cell density and thus evolutionary progress was monitored by measuring OD_{600}.

4.4.5 Bioreactor cultivation

Alternatively, *B. succiniciproducens* was cultivated in 1 L bioreactors (DASGIP AG, Jülich, Germany) with a working volume of 300 mL employing a 6-blade Rushton impeller. The DASGIP control 4 software (DASGIP AG, Jülich, Germany) was applied for online monitoring. Temperature of 37 °C was controlled by the bioblock temperature control system TC4 (DASGIP AG, Jülich, Germany). A constant pH of 6.5 was maintained by on-line measurement with a pH electrode (Mettler Toledo, Gießen, Germany) in combination with the system PH4PO4 and 1 M Na_2CO_3 applying the miniature peristaltic pump of module MP8 (DASGIP AG, Jülich, Germany). The pumped volume was automatically monitored during batch fermentation. Anaerobic conditions, i.e. dissolved oxygen levels below 2 %, were adjusted by CO_2-sparging with 0.1 NL h^{-1}. The conditions were verified by a pO2 electrode (Visiferm™ DO sensor, Hamilton, Bonaduz, Switzerland) using the DASGIP system PH4PO4. The cultivation was operated at 37 °C, 500 rpm and a controlled pH set-point of 6.5. The applied minimal medium E was inoculated with freshly grown cells from 100 mL serum bottles, containing 50 mL cultivation broth with 30 g L^{-1} $MgCO_3$. The cells were harvested (8500 x g, 4 °C and 5 min), washed with prepared fresh culture minimal medium and subsequently used as inoculum. Batch fermentations were started at an optical density of 0.3.

4.5 Analytical procedures

4.5.1 Cell concentration

During cultivation, the cell concentration was measured as optical density by spectrometry (Libra S11, Biochrome, Cambridge, UK) at 600 nm (OD_{600}) in 1.6 mL semi-micro cuvettes (Sarstedt, Nümbrecht, Germany). To remove residual $MgCO_3$ and to obtain optical density values between 0.05 and 0.3, cells were appropriately diluted with 1 M HCl. Exact dilution factors were determined gravimetrically on an analytical balance (CP225D, Sartorius, Göttingen, Germany).

4.5.2 Quantification of glucose

Supernatants from culture broth were obtained by centrifugation (16,000 x g, 4 °C and 5 min). The analytical quantification of glucose concentration was carried out enzymatically using the STAT 2300 Plus™ (YSI Life Sciences, Yellow Springs, OH, USA) after diluting samples with water as described above.

4.5.3 Quantification of organic acids

Culture supernatants were prepared as described above. Organic acids and ethanol were quantified using HPLC (LaChromElite, VWR Hitachi, West Chester, PE, USA) employing an Aminex HPX-87H column (300 x 7.8 mm; BioRad, Hercules, CA, USA) as stationary phase and 12 mM H_2SO_4 as mobile phase at 0.5 mL min^{-1} and 45 °C. The compounds were detected using refractive index (RI).

4.5.4 Quantification of intracellular amino acids

Intracellular amino acids were quantified from cell extracts (see 4.5.8) with α-aminobutyric acid as internal standard. The analysis was performed by HPLC (Agilent Series 1200; Agilent Technology, Waldbronn, Germany) as previously described (Krömer et al. 2005). Analytes were derivatized prior to injection, using o-phthaldialdehyde (OPA) and subsequently separated on a RP column (Gemini 5µ C18 110A, 150 x 4.6 mm; Phenomenex, Aschaffenburg, Germany) equipped with a precolumn (Gemini C18, MAX-RP, 4 x 3 mm; Phenomenex, Aschaffenburg, Germany) as stationary phase.

Table 4.22 Profile of mobile phase gradient applying eluent A (40 mM NaH_2PO_4, pH 7.8) and eluent B (45 % acetonitrile, 45 % methanol, 10 % MilliQ) for separation and quantification of intracellular amino acids.

Time [min]	Eluent A [%]	Eluent B [%]
0.0	100.0	0.0
40.5	59.5	40.5
41.0	39.0	61.0
43.0	39.0	61.0
57.5	0.0	100.0
59.5	0.0	100.0
60.5	25.0	75.0
61.5	50.0	50.0
62.5	75.0	25.0
63.5	100.0	0.0
65.5	100.0	0.0

Separation of amino acids was obtained by a gradient (Table 4.22) of applied mobile phase A (40 mM NaH_2PO_4, pH 7.8) and B (45 % acetonitrile, 45 % methanol, 10 % MilliQ) at 1 mL min^{-1} and 40 °C. OPA-derivated amino acids were detected using a fluorescence detector (340 nm excitation, 540 nm emission; Agilent, Waldbronn, Germany).

4.5.5 Analysis of mass isotopomers by GC/MS

The mass isotopomer fractions of proteinogenic amino acids from biomass and of succinate from culture broth supernatant were determined by GC-MS (Wittmann et al. 2002). About 1 mg biomass, harvested from exponentially growing cells, was washed with 1 M HCl until $MgCO_3$ was completely removed. The cells were then hydrolyzed in 100 µL 6 M HCl for 24 h at 105 °C. Insoluble matter was cleared by filtration (Ultrafree-MC filter devices, 0.22 µm durapore membrane; Millipore, Billerica, MA, USA). Afterwards, the filtrate was dried under ambient nitrogen stream, resuspended in 50 µL dimethylformamid (0.1 % pyridine) and derivatized with 50 µL N-methyl-N-tert-butyl-dimethylsilyl-trifluoracetamid (MBDSTFA; Macherey-Nagel, Düren, Germany) for 30 min at 80 °C. Possible salt precipitates were eliminated by centrifugation (1,177 x g, room temperature and 1 min). The labeling pattern of succinate was measured from dried culture supernatants (Becker et al. 2013), which were processed analog to the biomass procedure. The measurement of mass isotopomers was conducted with a GC/MS system, consisting of a HP 6890 gas chromatograph (Hewlett Packard, Paolo Alto, California, USA) employed with an HP-5MS GC column (5%-Phenyl-methylpolysiloxane; 30 m x 0.25 mm x 0.25 µm; Agilent, Waldbronn, Germany) and a quadrupole MS 5973 (Agilent, Waldbronn, Germany) for detection. Helium was applied as carrier gas with a flow rate of 1.7 mL min^{-1}. The inlet temperature was set to 250 °C, interface and quadrupole temperature were set to 280 °C. Electron ionization was performed at 70 eV. The injection volume was 1 µL and each sample was measured in duplicate. A potential isobaric interference of the analytes and matrix components was checked by first measurements in scan mode. Labeling patterns of amino acids were then determined by selective ion

monitoring (SIM) of preferred ion clusters after GC-separation using a temperature gradient (Table 4.23).

Table 4.23 Temperature profile of GC oven for measurements of labeling patterns of amino acids and succinic acid.

Time [min]	Temperature [°C]
0.0	120
2.0	120
12.0	200
24.5	325
27.0	325

Table 4.24 Mass fragments of analytes as MBDSTFA derivates used for flux calculation.

Analyte	M_0 (m/z)	Fragment	Carbon atoms
Alanine	260	M-57	$C_1 - C_3$
	232	M-85	$C_2 - C_3$
Glycine	246	M-57	$C_1 - C_2$
	218	M-85	C_2
Aspartate	418	M-57	$C_1 - C_4$
	390	M-85	$C_2 - C_4$
Threonine	404	M-57	$C_1 - C_4$
	376	M-85	$C_2 - C_4$
Serine	390	M-57	$C_1 - C_3$
	362	M-85	$C_2 - C_3$
Phenylalanine	336	M-57	$C_1 - C_9$
Tyrosine	466	M-57	$C_1 - C_9$
Succinate	289	M-57	$C_1 - C_4$

Amino acids and succinate were identified via retention time and fragmentation pattern from a standard of amino acids and succinate, respectively. The fragments [M-57] and [M-85] specific for MBDSTFA derivatization were taken for flux determination (Table 4.24).

4.5.6 Genome sequencing of *B. succiniciproducens* strains

Next generation sequencing was performed by the company BaseClear B.V. (Leiden, Netherlands). In a first step, 50 bp single reads were generated using the Illumina HiSEQ2500 platform and compiled to FASTQ sequence reads applying Illumina Casava pipeline (version 1.8.2), accompanied by two quality assessments (Illumina Chastity filtering and FASTQC quality control 0.10.0). Subsequent *de novo* assembly was performed with CLC Genomics Workbench (version 5.0; Aarhus, Denmark). Afterwards, the DD1 contigs (reference) were annotated using Genostar's IOGMA based on the MicroB database (Montbonnet, France) integrating several online databases. All other genomes were aligned to the DD1 genome and subsequently, polymorphisms were analyzed using CLC Genomics

Workbench (version 5.1; Aarhus, Denmark). The calling of false positive was reduced by minimizing the variant frequency to 75 % and setting the coverage to five.

4.5.7 Gene expression analysis

Preparation of total RNA

During bioreactor cultivation, cells were harvested and 14 mL cell suspension was mixed with 2 mL RNA Later® (Ambion® Life Technologies, Darmstadt, Germany) and subsequently aliquoted to 2 mL reaction tubes. After centrifugation (16,000 x g, room temperature and 20 sec) the supernatant was carefully discarded. The cell pellet was immediately frozen in liquid nitrogen and stored at -80 °C until further processing. The column based RNA preparation was performed with the RNeasy® Plus Mini Kit (Qiagen, Hilden, Germany). The individual steps of the purification were performed according to the manufacturer's protocol. Prior to RNA extraction, cell pellets were lyophilized overnight (Alpha 1-4 LD plus, Christ, Osterode, Germany). The dried cell pellets were then transferred into 1 mL cryo-tubes (Nalgene Nunc, Rochester, NY, USA) each containing a grinding ball (diameter: 10 mm; Sartorius Stedim, Göttingen, Germany), and cooled in liquid nitrogen. The biomass was then homogenized using a laboratory ball mill (Mikro-Dismembrator S, Sartorius Stedim, Göttingen, Germany) at 3000 min^{-1} for 10 sec. The disrupted cells were resuspended in 600 µL lysis buffer (RLT Plus, containing 1 % v/v ß-mercaptoethanol), gently mixed by inversion and transferred into a new 1.5 mL reaction tube, followed by 2 min incubation at 56 °C. The complete lysis solution was then transferred to a QiaShredder™ column (Qiagen, Hilden, Germany) and centrifuged (10,000 x g, room temperature and 30 sec). The flow-through was directly transferred to a gDNA eliminator column and centrifuged (10,000 x g, room temperature and 30 sec), followed by the addition of 600 µL ethanol (70 %). After mixing carefully, the solution was transferred in two steps to an RNeasy mini column and centrifuged (10,000 x g, room temperature and 15 sec). The flow through was discarded and the column was washed once with RW1 buffer. A volume of 80 µL of a freshly prepared DNase solution (10 µL DNase I stock solution plus 70 µL RDD buffer; Qiagen, Hilden, Germany) was added to the column, which was placed into a new 1.5 mL reaction tube and subsequently incubated (600 sec^{-1}, 28 °C and 30 min). Afterwards, the column was washed with 350 µL RW1 buffer, placed into a new 2 mL reaction tube, followed by three additional washing steps applying 500 µL buffer RPE (10,000 x g, room temperature and 2 min). RNA was eluted into a sterile 1.5 mL reaction tube by centrifugation (10,000 x g, room temperature and 2 min) within three steps using each 20 µL RNA free water. Purified RNA was stored at -80 °C. RNA quantification was performed using the Nanodrop®-Spectrophotometer ND-1000 (Thermo Fisher Scientific Inc., Waltham, MA, USA), followed by an 1.5 % agarose gel based quality control. Specific RNA quality was controlled using the

RNA 6000 Nano LabChip Kit with the 2100 Bioanalyzer (Agilent, Santa Clare, CA, USA). Quality criteria were set to a 23S/16S ratio higher than 1.5 and a RNA integrity number (RIN) above 8.

DNA microarray analysis

Comparative gene expression analysis was realized by application of a customized DNA microarray. For this purpose, all annotated genes derived from *B. succiniciproducens* genome sequencing were compiled and used for the array design in the online software Agilent eArray (https://earray.chem.agilent.com/). The employed format was an 8 x 15 k slide containing 8 arrays with a maximum of 15,000 probes. The oligonucleotide probe design was carried out applying following parameters: (i) preferred probe length of 60 bp, (ii) 3 probes per target gene, (iii) double coverage of all target genes, (iv) antisense probe orientation, and (v) melting temperature of 80 °C. The customized DNA microarray featured 14152 probes, whereas 536 Agilent probes served as control and 13616 probes represented three replicates of each target gene in twofold coverage. Fluorescence labeling was completed via direct chemical labeling of 1 µg purified RNA using the ULS Fluorescent Labeling Kit (Kreatech Diagnostics, Amsterdam, Netherlands) according to its protocol. Quality control of labeling degree was obtained with the Nanodrop®-Spectrophotometer ND-1000 (Thermo Fisher Scientific Inc., Waltham, MA, USA) after removing residual labeling agent with KREApure columns (Kreatech Diagnostics, Amsterdam, Netherlands). 300 ng of the Cy3 or Cy5 labeled RNA were fragmented in blocking agent and fragmentation buffer (Agilent, Santa Clare, CA, USA) for 30 minutes at 60 °C. The competitive hybridization was obtained by mixing equal amounts of differently labeled RNA, priorly diluted in 25 µL hybridization buffer, respectively. Then, 40 µL of a total of 50 µL mixture were used to load a gasket well on the gasket slide. After completing this step for all samples, the gasket slide was assembled with the microarray and hybridized (10 rpm, 65 °C and 17 h). After incubation, the microarray was disassembled and washed for 1 min in gene expression buffer 1 (Agilent, Santa Clare, CA, USA), followed by 1 min incubation in pre-warmed gene expression buffer 2. Microarray analysis was performed with the Agilent C Scanner (Agilent, Santa Clare, CA, USA) at 532 nm and 635 nm. Scanning and extraction was conducted using the Agilent Scan Control and Feature Extraction software (Agilent, Santa Clare, CA, USA). Extracted raw data was further processed using R programming language and bioconductor (Yang and Paquet 2005). For gene specific data interpretation, genes from three biological replicates exhibiting a p value < 0.05 combined with a $|\log_2 FC| > 0.8$, describing a 1.7 fold change, were considered to be differentially expressed concerning operon regulation. Single gene expression relevance was set to a fold change of 2.0. A global perspective of gene expression was gained using the gene set enrichment analysis (GSEA) tool (Subramanian et al. 2005) comprising all COG assigned genes according to *M. succiniciproducens* annotation (Hong et al. 2004). For this purpose 2291 designated gene sequences were taken from the DNA chip design, whereof 1900 genes could be assigned to proposed

gene clusters. For each GSEA analysis, 1000 permutations were conducted with the gene set as permutation type, while the genes were ranked according to the metric log_2 values. Significantly changed gene sets were determined by p-values below 0.01 and a false discovery rate below 5 %.

4.5.8 Metabolome analysis

Sampling by fast filtration

Intracellular amino acids were sampled by fast filtration, adapted from a validated protocol for other microorganisms (Bolten et al. 2007). Hereby, 2 mL exponentially growing cells from minimal glucose medium cultures were harvested by vacuum filtration (cellulose nitrate filter, 0.2 µm pore size, diameter 25 mm; Sartorius, Göttingen, Germany). Sampling included an additional washing step with 5 % NaCl solution. The whole procedure was finished in less than 30 sec. Sampling was conducted at two cell concentrations, corresponding to OD_{600} of 3 and 5, respectively. Cultivations were performed with two biological replicates.

Metabolite extraction

The filter with attached cells was used for metabolite extraction. For this purpose, it was incubated for with 2 mL α-aminobutyric acid (200 µM) as internal standard for quantification in a sealable plastic cup (15 min in boiling water). Subsequently, the extraction mix was cooled down on ice. The suspension was transferred into a sterile 2 mL reaction tube and centrifuged (13,000 x g, 4 °C and 5 min). Finally, the obtained extract was directly used for intracellular amino acid quantification or stored at -20 °C until further processing.

4.5.9 Enzyme activity assays

Preparation of crude cell extract

Cells were harvested by centrifugation (10,000 x g, 4 °C and 5 min). To avoid residual $MgCO_3$, cells pelleting above the insoluble $MgCO_3$ from the medium, were removed with a spatula and washed with ice-cold 250 mM citric acid. A second washing step was then conducted, whereby the washing solution was chosen according to the need of the subsequent assay. Afterwards, cells were resuspended in the respective buffer. Cell disruption was carried out after adding two spatula tips of glass beads (0.10 – 0.25 mm; Retsch, Haan, Germany) to 500 µL of cell suspension in 2 mL reaction tubes with a laboratory ball mill (30 sec^{-1} for 30 sec; Mikro-Dismembrator S, Sartorius Stedim,

Göttingen, Germany). The cell debris was separated by centrifugation. The obtained supernatant was then used for enzyme assays and quantification of protein concentration.

Determination of protein concentration

Protein concentration of crude cell extracts was determined with the Pierce™ BCA Protein Assay Kit (Thermo Fisher Scientific, Waltham, MA, USA). For calibration purposes, a bovine serum albumin stock solution was diluted according to the protocol. Cell extracts were diluted 1:10. Samples and standards were subsequently mixed with prepared working reagent. After incubation (37 °C and 30 min) the absorption was measured by spectrometry at 562 nm. The respective protein concentration was calculated with the slope of a standard curve, obtained by plotting the measurement of each standard versus its concentration.

Pyruvate kinase activity assay

The washing buffer consisted of 100 mM TRIS HCl (pH 7.0). Pyruvate kinase activity assays were performed at 37 °C in a total volume of 200 µL in 96-well plates employing the micro titer plate reader SUNRISE (Tecan, Crailsheim, Germany). The reaction mix contained 15 mM $MgCl_2$, 1 mM ADP, 0.25 mM NADH, phosphoenolpyruvate (PEP), 5.5 U mL^{-1} lactate dehydrogenase and 2.5 µL cell extract. For enzyme kinetic studies, PEP was added to a final concentration of 1, 2.5, 5, 10, 25, 50 and 75 mM, respectively. Negative controls were carried out without PEP and without cell extract, respectively. The decline of NADH extinction was monitored at 340 nm (Magellan™ data analysis software; Tecan, Crailsheim, Germany). All experiments were carried out with three biological replicates. The extinction coefficient for NADH at 340 nm is 6,220 M^{-1} cm^{-1}. One unit of enzyme activity correlates to the amount of enzyme catalyzing the conversion of one micro mole of substrate per minute.

4.5.10 Metabolic flux analysis

Metabolic flux experiments were carried out with [1-^{13}C] glucose as tracer substance and with two biological replicates. For minimizing effects of unlabeled biomass, the second pre-culture was already conducted on [1-^{13}C] glucose. The metabolic network for *B. succiniciproducens* was taken from Becker et al. 2013. It contained all essential reactions for succinate formation based on glucose. Reversible reactions were defined as netto fluxes. Pyruvate and PEP, as well as oxaloacetate (OAA) and malate (Mal), respectively, were lumped into joint metabolite pools each, because the fluxes

between the single pools could not be resolved by the applied tracer substance [1-^{13}C] glucose (Wittmann and Heinzle 2001a). Anabolic precursor demand was calculated from cellular composition of *B. succiniciproducens* biomass (Becker et al. 2013). The labeling data of the proteinogenic amino acids and of succinate from culture supernatant (Table 4.24), respectively, were combined with stoichiometric data (biomass yield, succinate yield, by-product yields and glucose uptake) from at least three biological replicates for calculation of metabolic fluxes. The simulation of metabolic fluxes was performed with an OpenFlux implementation (Quek et al. 2009) in MATLAB 7.6 (Mathworks Inc., Natick, MA, USA). OpenFlux directly corrected the raw mass spectrometry data for natural isotope abundance and fitted unknown flux parameters from the labeling data by isotopomer and metabolite balancing. The iterative fitting process finally generates a set of fluxes with minimized deviation between simulated and measured isotopomers, which was considered as best calculated intracellular flux distribution (Wittmann et al. 2002; Wittmann 2007). Statistical evaluation of the fluxes was conducted by a Monte-Carlo approach. Flux estimation from 50 independent calculations was used to determine 90 % confidence intervals for the flux parameters.

4.5.11 Phenotypic microarray analysis

Phenotypic characterization of *B. succiniciproducens* was conducted by the Omnilog® PM system (Biolog, Hayward, CA, USA), using the carbon source plates PM1 and PM2 provided by the manufacturer. Cells were obtained by overnight incubation in liquid BHI medium. Then, 100 µL of the suspension was plated on BHI-MOPS agar plates and incubated for 24 h at 37 °C. Further processing was conducted according to the manufacturer's protocol using the Redox Dye Mix D (Biolog, Hayward, CA, USA). 100 µL cell suspension was pipetted into each well. The prepared plates were wrapped in gas-tight bags (Biolog, Hayward, CA, USA), equipped with CO_2Gen paper sachets (Oxoid, Thermo Fisher Scientific, Waltham, MA, USA) to create a carbon dioxide rich atmosphere and subsequently sealed with tape. Data acquisition was carried out for 48 h at 37 °C. Each type of plate was incubated as duplicate and the metabolic activity was analyzed by the area under curve (AUC) applying the opm package implemented in R (Vaas et al. 2012).

5 Results and Discussion

The present work aimed at the development of superior strains of *B. succiniciproducens* for bio-succinate production. Beyond previous rational, metabolic engineering strategies for reduced by-product formation and enhanced product yield (Becker et al. 2013), this bacterium should be improved towards better process robustness, a key to its successful implementation into industrial production. As molecular mechanisms, that could provide enhanced tolerance to specific process configurations, are unknown, an evolutionary strategy was chosen to design superior phenotypes of interest.

5.1 Production performance and basic physiological properties of *B. succiniciproducens*

First experiments focused on the characterization of basic physiology of *B. succiniciproducens*. Its tolerance to extreme temperature, product concentration and pH-values should provide an insight into its natural robustness and possible strategic points for evolutionary adaptation.

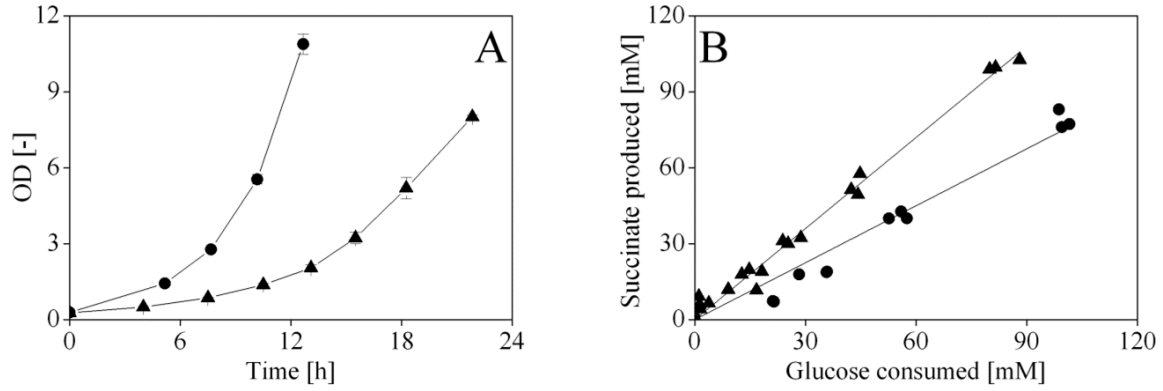

Figure 5.1 Growth (A) and production (B) performance of (●) *B. succiniciproducens* DD1 and its engineered derivative (▲) *B. succiniciproducens* DD3 in minimal glucose medium. Data and standard deviations derive from three biological replicates.

The comparison of *B. succiniciproducens* DD1 and DD3, grown in minimal media, clearly illuminates the advantage of the rational strain development (Figure 5.1). The specific succinate yield of DD3 was increased by about 50 %, as compared to the wild-type (Table 5.1). Unfortunately, this improvement went along with detrimental growth effects. Deletion of lactate and formate pathways unbalanced the metabolic redox state, which is obviously linked to biomass formation, as observed from the decreased specific biomass yield and specific growth rate.

Table 5.1 Physiology of *B. succiniciproducens* DD1 and DD3. The data comprise specific growth rate (μ), biomass yield ($Y_{X/S}$), succinate yield ($Y_{Suc/S}$), formate yield ($Y_{For/S}$), acetate yield ($Y_{Ace/S}$), lactate yield ($Y_{Lac/S}$), ethanol yield ($Y_{EtOH/S}$), pyruvate yield ($Y_{Pyr/S}$) and maximal succinate productivity (P_{Suc}). Data represent values from three biological replicates during exponential growth in complex and in minimal glucose medium with corresponding standard deviations.

	Complex medium		**Minimal medium**	
	DD1	DD3	DD1	DD3
μ [h^{-1}]	0.64 ± 0	0.19 ± 0.01	0.29 ± 0.01	0.16 ± 0.01
$Y_{X/S}$ [g mol^{-1}]	62.4 ± 3.1	43.7 ± 3.3	35.6 ± 0.2	29.8 ± 2.5
$Y_{Suc/S}$ [mol mol^{-1}]	0.77 ± 0.02	1.18 ± 0.03	0.76 ± 0.03	1.13 ± 0.04
$Y_{For/S}$ [mol mol^{-1}]	0.97 ± 0.02	< 0.01	0.58 ± 0.02	< 0.01
$Y_{Ace/S}$ [mol mol^{-1}]	0.83 ± 0.05	0.34 ± 0.01	0.57 ± 0.01	0.21 ± 0.06
$Y_{Lac/S}$ [mol mol^{-1}]	< 0.01	< 0.01	0.03 ± 0	< 0.01
$Y_{EtOH/S}$ [mol mol^{-1}]	0.15 ± 0.01	< 0.01	0.03 ± 0	< 0.01
$Y_{Pyr/S}$ [mol mol^{-1}]	< 0.01	22.6 ± 0.02	< 0.01	0.16 ± 0.03
P_{Suc} [g L^{-1} h^{-1}]	1.31 ± 0.05	1.12 ± 0.07	1.42 ± 0.04	0.76 ± 0.01

The yields were determined by linear fitting of the concentration of biomass and product with that of the substrate.

Regarding the evolutionary adaptation approach, DD3, exhibiting a high specific yield for succinate seemed to be the most promising candidate. In addition, deletion of by-product pathways narrowed the degrees of freedom of the selection pressure down, i.e. cells can no longer adapt by redirection of flux into non-beneficial redox balancing.

Impact of high temperature

The cultivation temperature is a relevant process parameter. It strongly affects overall production costs by the linkage to microbial kinetics, i.e. productivity and by the efforts for cooling needs. In addition, temperatures beyond the growth optimum of contaminants can minimize the contamination risk.

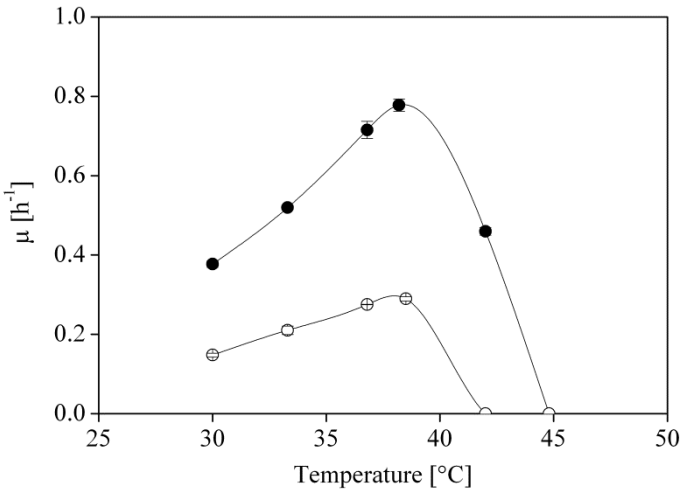

Figure 5.2 Influence of temperature on growth of the wild-type *B. succiniciproducens* DD1 in (●) complex medium A and (○) minimal medium F. The data represent mean values of three biological replicates with standard deviations. The growth is given as exponential growth rate at each temperature (μ).

To this extent, the influence of temperature on *B. succiniciproducens* DD1 was evaluated in growth experiments in serum bottles and within a temperature range of 30 °C to 45 °C (Figure 5.2). Hereby, complex and minimal medium were applied. Temperatures below 37 °C decreased DD1 proliferation. At 30 °C, the specific growth rate was only 50 % of that at 37 °C. However, the strain was able to grow exponentially in complex and minimal medium, respectively, while producing succinate as main fermentation product. The maximal performance, regarding growth rate, succinate yield and productivity was observed between 37 and 39 °C reflecting the temperature of bovine rumen, the natural habitat of the bacterium. Under these conditions, DD1 produced almost 30 g L^{-1} succinate in 24 h, while additionally forming lower amounts of acetate, formate and lactate. A cultivation temperature of 42 °C fully inhibited growth in minimal medium. Here, only an initial increase in cell concentration could be observed. Complex medium still enabled growth at 42 °C, however, at a drastically reduced growth rate. This implies specific metabolic pathways that probably relate to biosynthesis, which fail at 42 °C, but can be compensated by complex medium ingredients. This would also fit to the initial phase of growth in minimal medium. Here, intracellular pools of affected metabolites, derived from pre-cultures, could provide a reservoir, which then rapidly depletes. At 45 °C, DD1 showed no growth in both media. The obtained results agreed with the growth behavior of other mesophilic bacteria, obviously linked to the natural habitat of *B. succiniciproducens* and its phylogenetic relatives (Scholten and Dägele 2008; Lee et al. 2002). The increased temperature tolerance by complex nutrients appeared promising with regard to the planned evolutionary adaptation, as the bacterium showed basic robustness with selective sensitive pathways.

As shown, *B. succiniciproducens* DD1 revealed severe growth problems when cultivated in minimal medium at elevated temperatures (Figure 5.2). Considering this effect, the support of growth performance was first rationally analyzed by adding defined compounds (Table 5.2). The chosen amino acids have been previously identified as stimulatory or even essential for *M. succiniciproducens* MBEL55E (Song et al. 2008). Methionine seemed promising, since the first enzyme in methionine synthesis, homeserine O-transsuccinylase, is heat-sensitive in *E. coli* (Ron and Davis 1971; Mordukhova et al. 2008). In addition, compatible solutes were selected, due to the mediation of temperature tolerance in bacteria (Arakawa and Timasheff 1985; Lippert and Galinski 1992; Caldas et al. 1999; Bourot et al. 2000).

None of the amino acid could restore growth at 42 °C (Table 5.2). Among the compatible solutes, only glycine betaine enabled growth of DD1 at 42 °C, whereas the other supplements had no effect. This is coherent with observations that glycine betaine prevents temperature-induced protein aggregation (Caldas et al. 1999) and induces increased thermal stability (Arakawa and Timasheff 1985; Lippert and Galinski 1992).

Table 5.2 Impact of specific medium ingredients on growth of *B. succiniciproducens* DD1 at 42°C in defined glucose-based medium.

Compound	Concentration [mM]	Growth
Alanine	5	-
Asparagine	5	-
Aspartic acid	5	-
Cystein	5	-
Methionine	5	-
Proline	5	-
Glycine betaine	1	+
Ectoine	1	-
Hydroxyectoine	1	-

This finding suggested that temperature sensitivity of *B. succiniciproducens* DD1 was mainly caused by denatured proteins. Recapitulating, the addition of glycine betaine that is already applied in animal feedstuff and agro industry (Mäkelä 2004), appeared as one straightforward possibility to improve process performance of *B. succiniciproducens*. But, as this would add extra costs to the process, evolutionary adaptation was performed next to eventually create a new temperature phenotype.

Impact of high succinate levels

The product titer represents a key performance indicator of industrial competitiveness of bioprocesses and is highlighted in various reports as major prerequisite, i.e. desired values of about 100 g L^{-1} (Werpy and Peterson 2004; Patel et al. 2006; Bastidon 2012). In this line, product tolerance displays a target for improvements. Indeed, succinate producers show sensitivity to high levels of succinate (Table 5.3) and the inhibition can be described by a linear relationship (Equation 1) (Lin et al. 2008).

Table 5.3 Succinate tolerance of succinate producing bacteria.

Strain	Medium	Succinate [g L^{-1}]	Reference
Actinobacillus succinogenes	Complex (Glc, YE, Vit)	104.6 [a]	(Lin et al. 2008)
Actinobacillus succinogenes 130Z	Complex (Glc, Cas, SP)	50 [b]	(Li et al. 2010)
Escherichia coli AFP111	Complex (Glc, YE, T)	80 [b]	(Li et al. 2010)
Mannheimia succiniciproducens MBEL55E LPK7	Complex (Glc, YE)	5.1 [a]	(Hoon et al. 2010)
Basfia succiniciproducens DD3	Minimal (Glc, Vit)	19.1 [a]	this work

Medium components: Glc: glucose, YE: yeast extract, Cas: pancreatic digested casein, SP: soy peptone, T: tryptone, Vit: vitamins.
[a] depicts calculated critical succinate concentration according to Lin et al. 2008
[b] shows experimental data for tolerated final concentration of succinate for the growth according to Li et al. 2010

$$\mu = \mu_{max}\left(1 - \frac{C_{Pi}}{C_{Pi}^{*}}\right) \qquad \text{(Equation 1)}$$

Product tolerance was estimated for the producing strain *B. succiniciproducens* DD3 by conducting serum bottle experiments on minimal medium buffered with $MgCO_3$. Succinate was added from a stock solution, after neutralization with 1 M NaOH, to a level of 2.5, 5, 7.5, 10, 15, and 20 g L^{-1}, respectively, prior to inoculation.

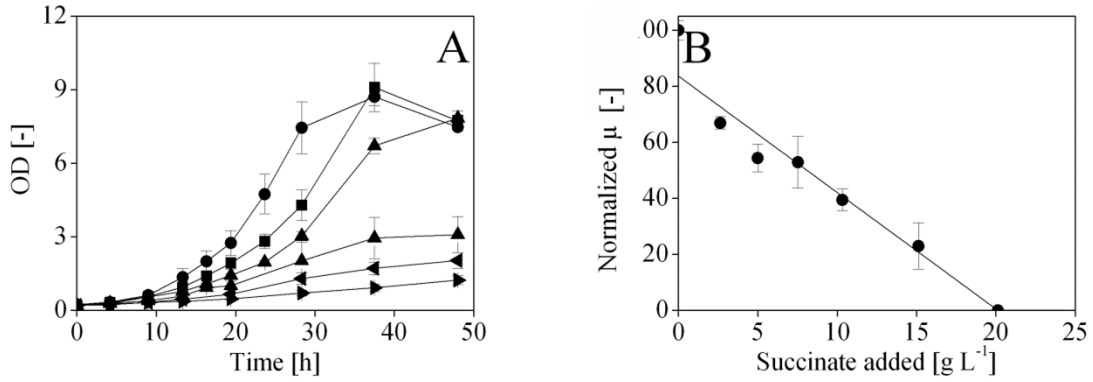

Figure 5.3 Influence of succinate on growth of *B. succiniciproducens* DD3 in minimal medium with (●) no, (■) 2.5 g L^{-1}, (▲) 5 g L^{-1}, (▼) 7.5 g L^{-1}, (◄) 10 g L^{-1}, and (►) 15 g L^{-1} succinate (A) and linear correlation between growth, pictured by normalized specific growth rate at each succinate level, and the succinate concentration (B). Maximal observed specific growth of 0.16 h^{-1} was set to 100 %. Data represent mean values from three biological replicates with corresponding standard deviations.

As can be seen, cell growth was significantly inhibited by increasing succinate levels (Figure 5.3). With 20 g L^{-1} succinate, cells did not grow. Obviously, the resulting growth rate correlated linearly with the level of succinate (Figure 5.3), yielding a critical concentration ($\mu = 0$) of nearly 20 g L^{-1}, calculated according to the generalized Equation 1. Compared to other succinate producing microorganisms, *B. succiniciproducens* DD3 exhibited a moderate succinate tolerance (Table 5.3). Care has to be taken, because all other studies were carried out in complex media (Lin et al. 2008; Hoon et al. 2010; Li et al. 2010), while here, DD3 was cultivated in a minimal, defined medium. As discussed above, complex media can cover metabolic imbalances, since they provide ready to use substrates and enable basically interrupted or retarded pathways and thus facilitate more robustness. In comparison with *M. succiniciproducens* MBEL55E, the closest relative, *B. succiniciproducens* revealed a higher tolerance.

Impact of low pH-value

The industrial relevance of the pH-value results from specific downstream processing needs for organic acids. These are typically recovered from fermentation broth using calcium salts for precipitation (Kurzrock and Weuster-Botz 2010). After precipitation, the calcium salt of succinic acid has to be acidified for further preparations. This step requires large amounts of sulfuric acid, which can be reduced by a lower final fermentation pH. In special cases, calcium carbonate can be applied, which advantageously combines pH buffer function and carbon dioxide supply. This is beneficial for fermentative succinate production, but causes a slightly acidic pH of 5.8 in the medium under carbon dioxide saturated conditions.

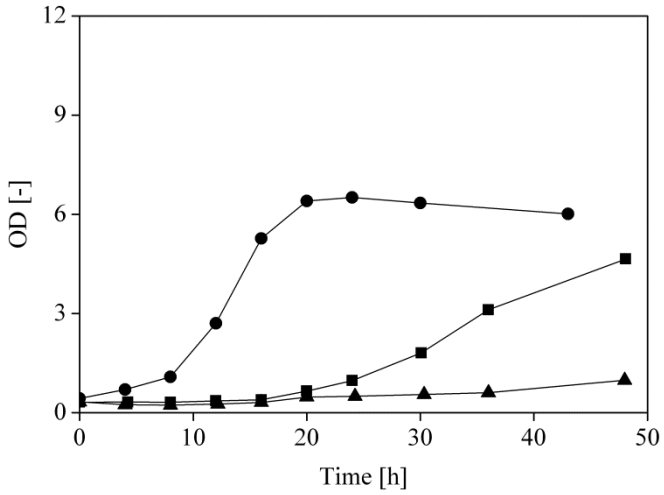

Figure 5.4 Growth of *B. succinicproducens* at (●) pH 6.0, (■) pH 5.5 and (▲) pH 5.3 in defined medium F during a pH-controlled cultivation.

To unravel the influence of an acidic pH on the growth behavior of *B. succiniciproducens*, the producing strain DD3 was grown at different pH-values in pH-controlled bioreactors applying minimal medium (Figure 5.4). While pH 6.0 allowed reasonable growth, pH 5.5 caused a pronounced lag-phase of about 15 h and slower growth. At a pH of 5.3, growth was almost fully inhibited. Further decrease to pH 5.0 completely eliminated growth of the cells. In addition to growth, the succinate production was severely inhibited by low pH. Whereas about 33 g L^{-1} succinate were achieved at pH 6.0, only 9 g L^{-1} were produced at pH 5.5. No succinate production occurred at the lowest pH-value of 5.3.

5.2 Evolutionary adaptation of *B. succiniciproducens* DD3 towards high temperature

5.2.1 Evolutionary adaptation towards a new temperature phenotype

The addition of single media supplements indicated the complexity of temperature sensitivity, since no single substance could overcome the growth inability at 42 °C. In this line, growth recovery at elevated temperatures was tackled by evolutionary adaptation. This approach generates novel phenotypes, which emerge under specific imposed conditions by natural selection of the fittest. As starting point, the double knockout mutant *B. succiniciproducens* DD3, lacking the *ldhA* and *pflD* genes to eliminate formation of lactate and formate appeared most promising. Despite its slower growth performance, DD3 has a 50 % increased succinate yield as compared to the wild-type (Becker et al. 2013). In this regard, DD3 possessed a high potential for valuable phenotype improvement. The lack of by-product forming pathways to lactate and formate reduced the adaptation probability of redirecting carbon flux into undesired redox balancing pathways. The following evolutionary adaptation was conducted in minimal medium to avoid accumulation of side-mutations in bio-synthetic pathways that would not have been recognized in complex medium. In order to realize the evolutionary adaptation, *B. succiniciproducens* DD3 was cultivated applying a repeated batch method. The formed cell concentration served as criterion to evaluate the adapted population. The cultivation time of each of the batches was extended until a cell concentration was reached, equivalent to OD_{600} of 5. The adaptation was started at 40 °C. Initial cell growth was remarkably retarded, which was validated by low specific growth rates (Figure 5.5).

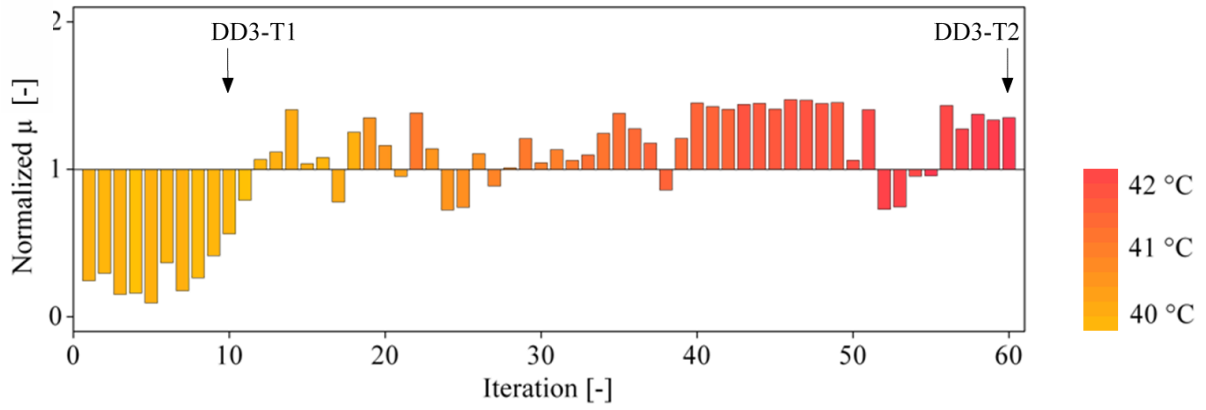

Figure 5.5 *B. succiniciproducens* DD3 adaptation towards 42 °C. The color legend visualizes the temperature during each batch of the evolutionary adaptation from 40 °C to 42 °C. The bar-chart represents the normalized specific growth rate, referring to the standard cultivation of DD3 in minimal medium (μ = 1) at 37 °C.

After 10 iterations however, the growth rate increased substantially. At this point, five clones were isolated from the heterogenic culture and briefly screened for their performance. As they showed identical growth properties, one of the clones, determined as DD3-T1, was chosen for further adaptation. A second adaptation round was started with the new *B. succiniciproducens* isolate DD3-T1, by now gradually increasing the temperature to 42 °C. The sequential batch strategy was continued for 50 additional iterations. While increasing the temperature, a significant improvement was observed for cell growth (Figure 5.5). At 42 °C, the heterogenic culture was able to grow with a nearly constant performance over several batches. Here again, clones were isolated and one of them was designated DD3-T2. The wild-type strain could not grow under these conditions (Figure 5.2). The overall adaptation was not extended beyond 50 iterations since most beneficial mutations accompanied by significant phenotypic impacts occur early during adaptation, while the fitness trajectory strongly decelerates over time (Barrick et al. 2009). Taken together, two clones with improved temperature tolerance, i.e. DD3-T1 (40 °C) and DD3-T2 (42 °C) were created by the adaptive approach.

5.2.2 Physiological characterization of evolutionary derived phenotypes

It was now relevant to study the growth and production performance of the novel phenotypes. Comparative cultivation studies were conducted with both isolates *B. succiniciproducens* DD3-T1 and DD3-T2, and the parent strain DD3 as control (Figure 5.6). All strains were cultivated in serum bottles in minimal glucose medium. First, potential evolutionary trade-offs were investigated by testing all strains at 37 °C. The isolate DD3-T2 showed a significantly increased growth rate, whereas no difference was observed between DD3 and DD3-T1 (Table 5.4). At the end of the exponential growth phase all strains reached a similar cell concentration. The improved growth of DD3-T2 at 37 °C could result from the prolonged adaptation to the minimal medium, as a consequence of its continuous use during the adaptation process. For *E. coli*, similar effects have been described during adaptive approaches (Blaby et al. 2012; Jantama et al. 2008). Most important, the optimized performance did not occur at the expense of the succinate yield. The high yield of the DD3 strain could be fully maintained in both isolates (Figure 5.6). Slight changes were found regarding the formation of acetate and pyruvate, both originating from the phosphoenolpyruvate/pyruvate (PEP/Pyr) node. This branch point represents a metabolic switch in various microorganisms (Sauer and Eikmanns 2005). The fast growth and the high product yield of DD3-T2 resulted in an attractive succinate productivity of 1.09 g L^{-1} h^{-1}, whereas DD3 and DD3-T1 exhibited lower productivities of about 0.76 g L^{-1} h^{-1} each (Table 5.4). Obviously, the adapted strains accumulated beneficial mutations. The defined medium hereby prevented the accumulation of detrimental auxotrophies as previously observed in *E. coli* LB-medium adaptations (Blaby et al. 2012).

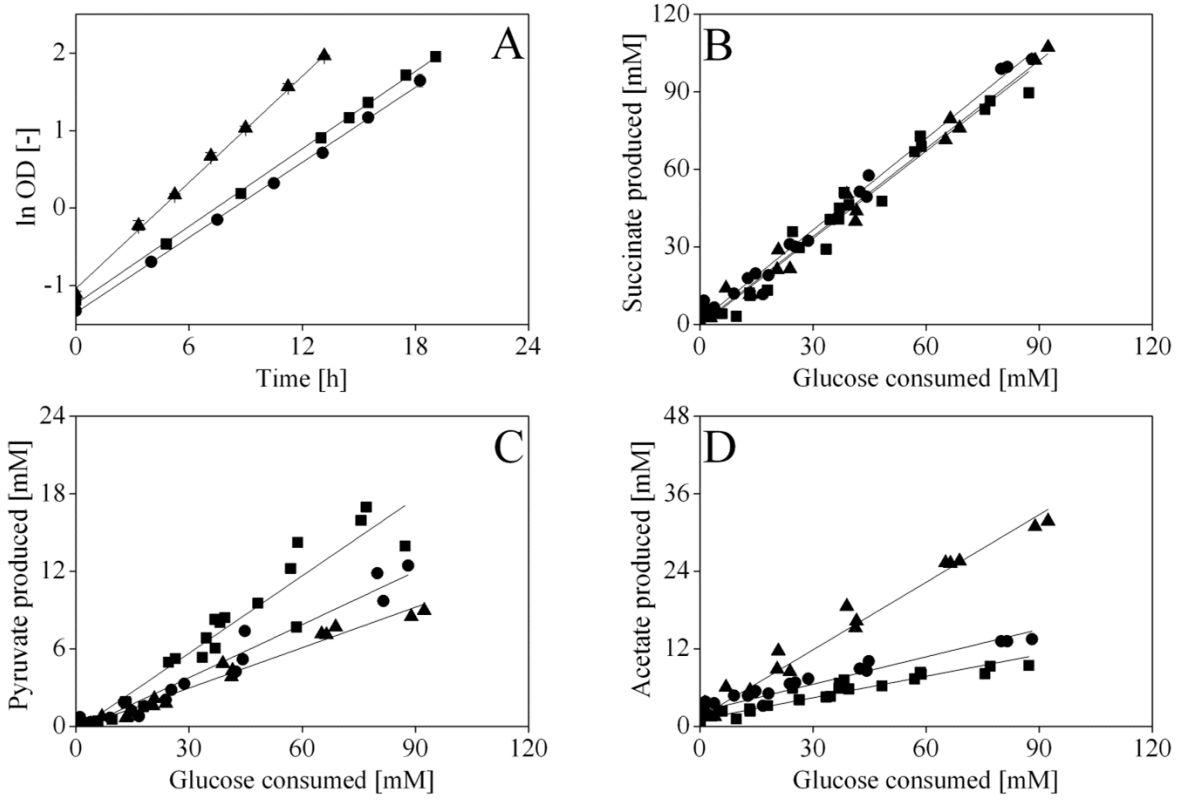

Figure 5.6 Physiological characterization of the adapted *B. succiniciproducens* strains (■) DD3-T1 and (▲) DD3-T2 compared to the parent strain (●) DD3 at 37 °C in minimal medium F in serum bottles. The data shown comprise specific growth rate (A), the yield for succinate (B), the yield for pyruvate (C), and the yield for acetate (D) during exponential growth phase of three biological replicates, respectively.

A more detailed insight into the metabolic changes, e.g. loss of function or gain of function was next screened applying phenotype microarrays.

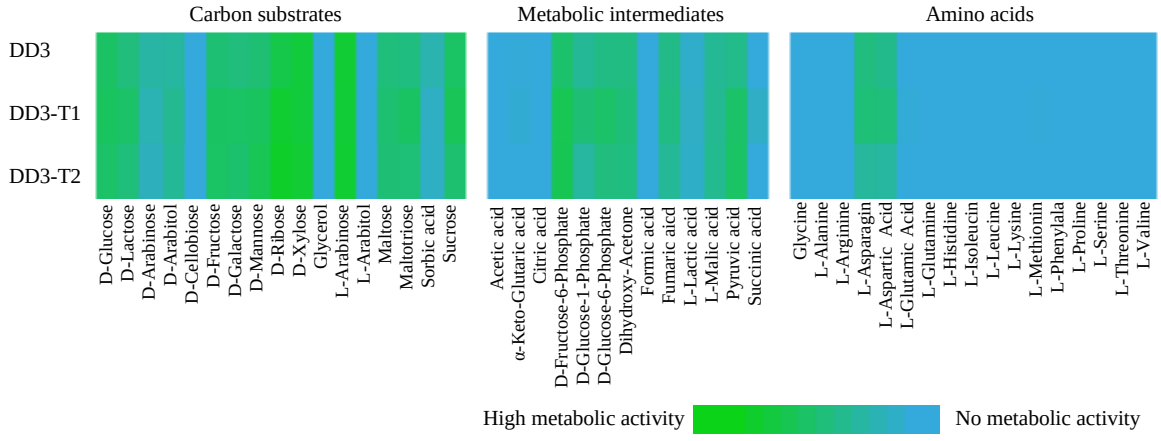

Figure 5.7 Phenotypic fingerprint of *B. succiniciproducens* DD3 as well as DD3-T1 and DD3-T2. The heat map pictures metabolic activity, whereas blue indicates no metabolic activity and green indicates high metabolic activity. The values represent the area under the measured curve of increasing redox dye coloration. Experiments were conducted with two biological replicates.

For this purpose, the adapted *B. succiniciproducens* strains were evaluated for metabolic defects or benefits by screening for their substrate potential (Figure 5.7). The obtained phenotypic patterns showed no significant differences and revealed that the evolutionary adaptation of *B. succiniciproducens* towards increased temperature was not linked to the use of specific substrates or their energetic metabolism. This implies a more subjacent adapting pattern, on the basis of regulatory pathways. However, it was important to prove that no loss of function was observed for industrially relevant substrates, such as glucose, maltose or sucrose.

In a next set of experiments, the fitness gain in growth and production performance of DD3-T1 and DD3-T2 was compared to the parental DD3 at higher temperature. As evolved, DD3 was cultivated at 40 and 42 °C, respectively. DD3 grew at 40 °C, although at a reduced specific growth rate of 0.10 h^{-1}. The adapted variant DD3-T1 grew almost twice as fast (μ = 0.17 h^{-1}; Figure 5.8).

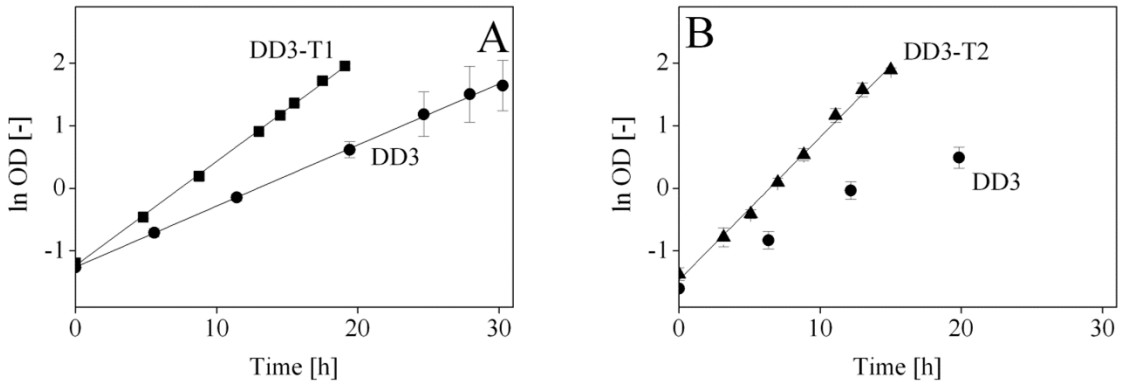

Figure 5.8 Growth of (●) *B. succiniciproducens* DD3 at 40 °C (A) compared to (■) DD3-T1 and at 42 °C (B) compared to (▲) DD3-T2. All cultivations were conducted as three biological replicates.

Table 5.4 Growth and production characteristics of *B. succiniciproducens* DD3 and the temperature adapted strains DD3-T1 and DD3-T2 during exponential phase of batch cultivations at different temperatures in glucose minimal medium. The data given are specific growth rate (μ_{max}), biomass yield ($Y_{X/S}$), succinate yield ($Y_{Suc/S}$), formate yield ($Y_{For/S}$), acetate yield ($Y_{Ace/S}$), lactate yield ($Y_{Lac/S}$), ethanol yield ($Y_{EtOH/S}$), pyruvate yield ($Y_{Pyr/S}$) and maximal succinate productivity (P_{Suc}). The values represent mean values of three biological replicates with corresponding standard deviations.

	DD3			**DD3-T1**		**DD3-T2**	
	37 °C	40 °C	42 °C	37 °C	40 °C	37 °C	42 °C
μ_{max} [h^{-1}]	0.16 ± 0.01	0.10 ± 0.02	-	0. 17 ± 0	0.15 ± 0	0.23 ± 0	0.23 ± 0
$Y_{X/S}$ [g mol^{-1}]	29.8 ± 2.5	28.5 ± 3.1	19.2 ± 2.2	29.2 ± 0.8	28.0 ± 0.4	29.2 ± 1.0	28.9 ± 0.5
$Y_{Suc/S}$ [mol mol^{-1}]	1.13 ± 0.04	1.11 ± 0.02	1.08 ± 0.12	1.14 ± 0.03	1.09 ± 0.06	1.12 ± 0.04	1.10 ± 0.05
$Y_{For/S}$ [mol mol^{-1}]	< 0.01	< 0.01	< 0.01	< 0.01	< 0.01	< 0.01	< 0.01
$Y_{Ace/S}$ [mol mol^{-1}]	0.21 ± 0.06	0.28 ± 0.05	0.29 ± 0.02	0.11 ± 0.01	0.17 ± 0.01	0.28 ± 0.05	0.39 ± 0.03
$Y_{Lac/S}$ [mol mol^{-1}]	< 0.01	< 0.01	< 0.01	< 0.01	< 0.01	< 0.01	< 0.01
$Y_{EtOH/S}$ [mol mol^{-1}]	< 0.01	< 0.01	< 0.01	< 0.01	< 0.01	0.02 ± 0.01	< 0.01
$Y_{Pyr/S}$ [mol mol^{-1}]	0.16 ± 0.03	0.07 ± 0.00	0.11 ± 0.01	0.22 ± 0.01	0.13 ± 0.01	0.15 ± 0.03	0.09 ± 0.02
P_{Suc} [g L^{-1} h^{-1}]	0.76 ± 0.01	0.33 ± 0.12	0.16 ± 0.02	0.76 ± 0.01	0.55 ± 0	1.09 ± 0.03	1.02 ± 0.04

Yields were determined by linear fitting of the concentration of biomass and product with that of the substrate.

At 42 °C, DD3 did not grow, whereas DD3-T2 still propagated. Overall, succinate production significantly declined with increasing cultivation temperature (Table 5.4). Interestingly, DD3-T2 performed identical at 42 and 37 °C and even showed superior production performance to its parent strain. As a result of the evolutionary adaptation, the maximal temperature for succinate production could be increased to 42 °C in minimal medium, using DD3-T2. Since no loss of function was detected for this strain, it seemed a promising candidate for further evaluation toward its industrial performance.

5.2.3 Metabolic pathway fluxes of *B. succiniciproducens* DD3-T2

The evolutionary adaptation yielded the isolation of a new, well performing production mutant, which exceeds the performance of the parent strain regarding growth and succinate productivity. Towards a better understanding of the molecular mechanisms that mediated the obviously improved performance, the isolate was next analyzed by using ^{13}C fluxomics and transcriptomics. Thereby, fluxomic analysis was recruited by using isotopic substrates to unravel the *in vivo* carbon flux distribution throughout the core metabolism of *B. succiniciproducens* (Becker et al. 2013).

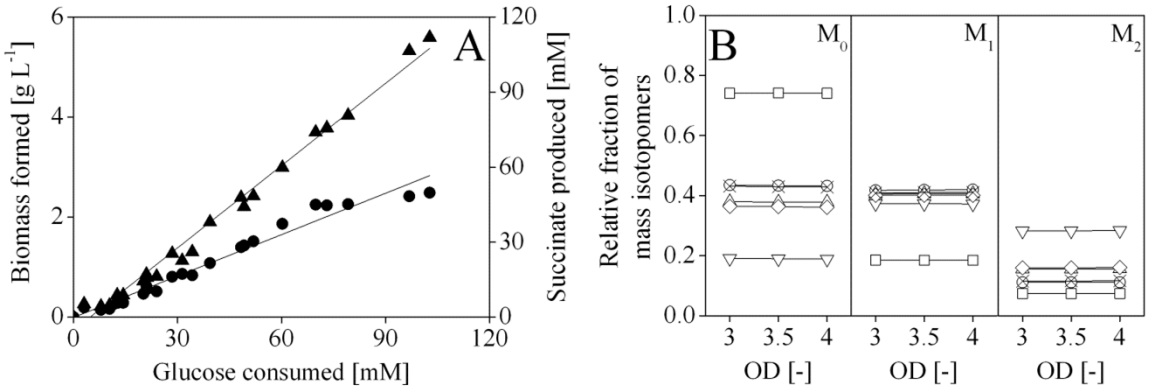

Figure 5.9 Growth balance during labeling experiments with *B. succiniciproducens* DD3-T2 was verified by metabolic (A) and isotopic (B) steady state. Metabolic steady state was determined from linear correlation between (●) biomass and (▲) succinate formation, respectively, and glucose consumption. Isotopic steady state was assessed by constant labeling patterns of proteinogenic amino acids and succinate. Hereby, exemplary shown amino acids and succinate stem from different parts of the metabolic network. M_0 (non-labeled), M_1 (single labeled) and M_2 (double labeled) represent the relative fraction of corresponding isotopomers of (○) alanine, (□) glycine, (Δ) serine, (▽) phenylalanine, (◊) aspartate, and (x) succinate.

B. succiniciproducens DD3-T2 producing significant amounts of succinate at 42 °C, strongly differed from its performance from DD3 and also from its direct predecessor DD3-T1 (Table 5.4). Labeling data of proteinogenic amino acids from the cultivations with [1-^{13}C] glucose, together with stoichiometric data of biomass and product formation (Table 5.4) and of anabolic demands (Table 9.1) were used to compute the fluxes. The excellent fit of experimental and simulated labeling data

indicated a high consistency of the obtained fluxes (Table 9.2). The calculated flux distributions of both setups were directly compared to recently published data of DD3 (Becker et al. 2013). Metabolic steady state was enforced by constant growth and product formation over time (Figure 5.9). Isotopic steady state could be assessed from constant ^{13}C labeling patterns of proteinogenic amino acids (Figure 5.9).

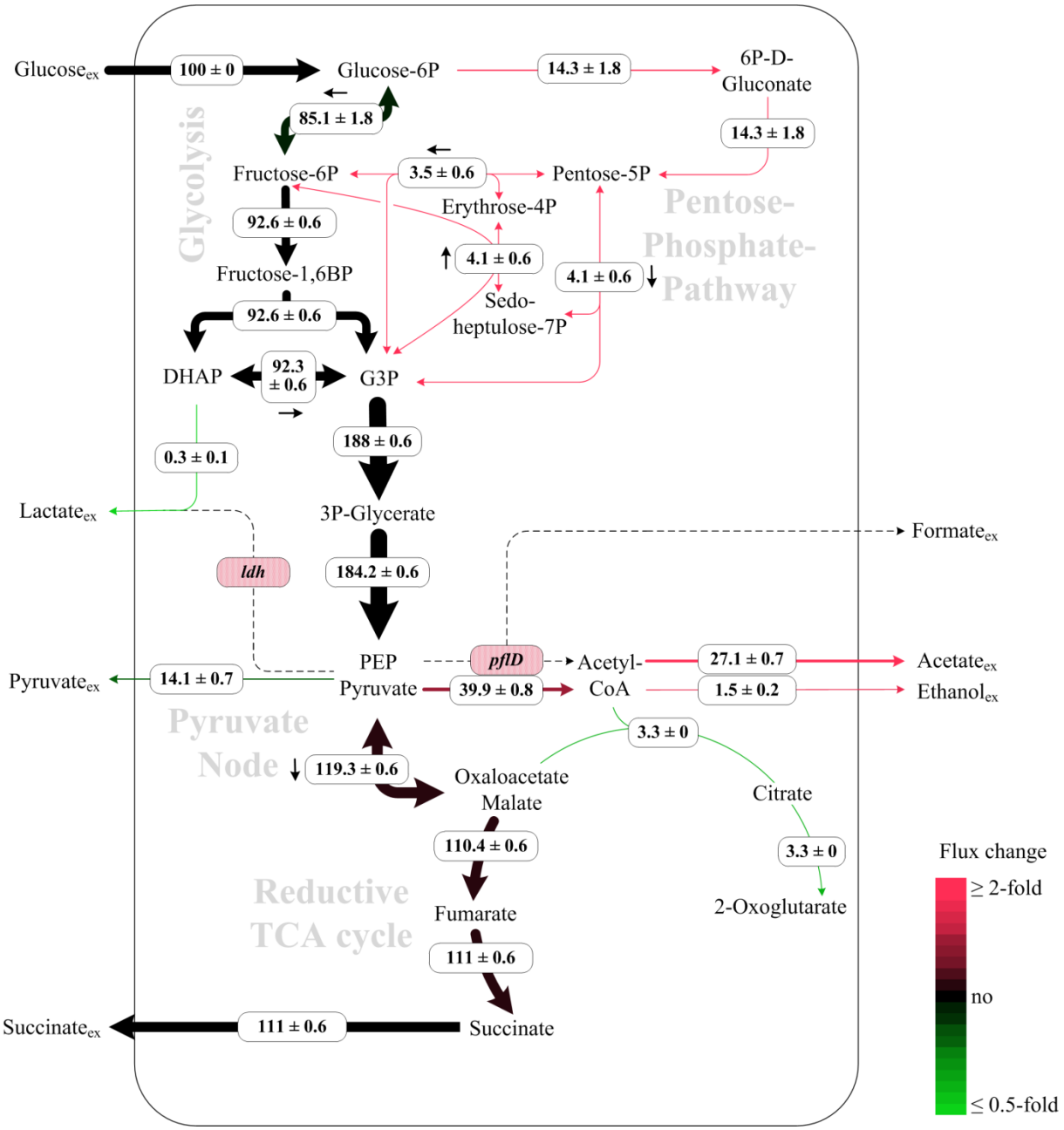

Figure 5.10 *In vivo* carbon flux distribution of the central carbon metabolism of *B. succiniciproducens* DD3-T2 during growth on glucose minimal medium at 37 °C. The fluxes are given as percentage of the specific glucose uptake rate of q_{Glc} = 8.2 mmol g^{-1} h^{-1}, that was set to 100 %. Net flux direction is indicated by small arrows. Rationally, prior to evolutionary adaptation deleted pathways are shown by a dashed line with corresponding gene name in a red box. Comparative metabolic flux response of the evolved mutant DD3-T2 to its parental strain DD3 is differentially visualized according to the color legend. Underlying fold changes of carbon flux were calculated based on data from DD3 taken from Becker et al. 2013 corrected for the specific glucose uptake rate (Table 9.4). The errors reflect 90 % confidence intervals.

As the temperature tolerant mutant DD3-T2 revealed an increased flux into the pentose phosphate pathway (PPP) (Figure 5.10), this might coincide with enhanced growth, because the PPP generates NADPH, required for various biosynthetic routes (Becker et al. 2013). For *Pasteurellaceae* growth, its supply even seemed to be the limiting factor (McKinlay, Shachar-Hill, et al. 2007). An increased PPP flux could thus support better growth, as observed with the mutant. One could propose strategies to increase NADPH supply by rational genetic engineering as previously done for the soil bacterium *C. glutamicum* regarding industrial lysine production (Becker et al. 2007). The flux through the upper glycolysis was decreased by 10 %, but the flux through the lower glycolysis remained largely unaffected, as the PPP replenished carbon into their routes at the fructose 6-phosphate (F6P) and glyceraldehyde 3-phosphate (GAP) node, respectively. At the PEP/Pyr node, the flux to acetate formation increased. In more detail, the flux via pyruvate dehydrogenase (PDH) was increased by 48 % to support the more than twofold increase in acetate flux by simultaneously reducing the flux towards pyruvate derived by-products (Table 9.4). In DD3, PDH is essential for acetyl-CoA formation due to the lack of the *pflD* gene, which predominantly accounts for acetyl-CoA synthesis in the wild-type (Becker et al. 2013). Synthesis of acetate comprises the enzymes *Pta* and *AckA* and leads to the formation of ATP. In the close relative *M. succiniciproducens* MBELL55E LPK7, this pathway mainly contributes to acetate production. Deletion of these genes negatively affected cell growth, possibly due to ATP shortage (Lee et al. 2006). Thus, the observed flux shift towards acetate could provide more energy from carbon (Figure 9.2), beneficial for biomass formation, while maintaining succinate yield. Concerning the TCA cycle, the reductive and the oxidative branch, respectively, showed no significant change in carbon flux.

It was now of interest to study the fluxes of the novel mutant DD3-T2 at 42 °C, as compared to DD3 at 37 °C. Again, the mutant revealed an increased PPP flux (Figure 5.11). A major shift in carbon flux was observed around the highly flexible PEP/Pyr node. Flux was redirected to the formation of acetate, at the expense of pyruvate and other pyruvate derived products (Table 9.4). This could also be due to an enhanced need for ATP under stress conditions. The high temperature is particularly linked to a higher energy requirement to maintain cellular processes, such as protein homeostasis (synthesis and degradation), chaperone expression and cell-cycle control (DNA repair and cell constituent biosynthesis) (Clarke 2003). Taken together, obvious changes in carbon fluxes of DD3-T2 indicate a gain in function considering industrial implementation of this tolerant mutant. Furthermore, first suggestions could be made regarding possible targets for metabolic engineering. As shown, a higher glucose 6-phosphate (G6P) flux into the oxidative PPP for NADPH generation might contribute to faster and thus more efficient growth. In addition, intracellular provision of energy (ATP) could increase stress tolerance and thus improve strain robustness.

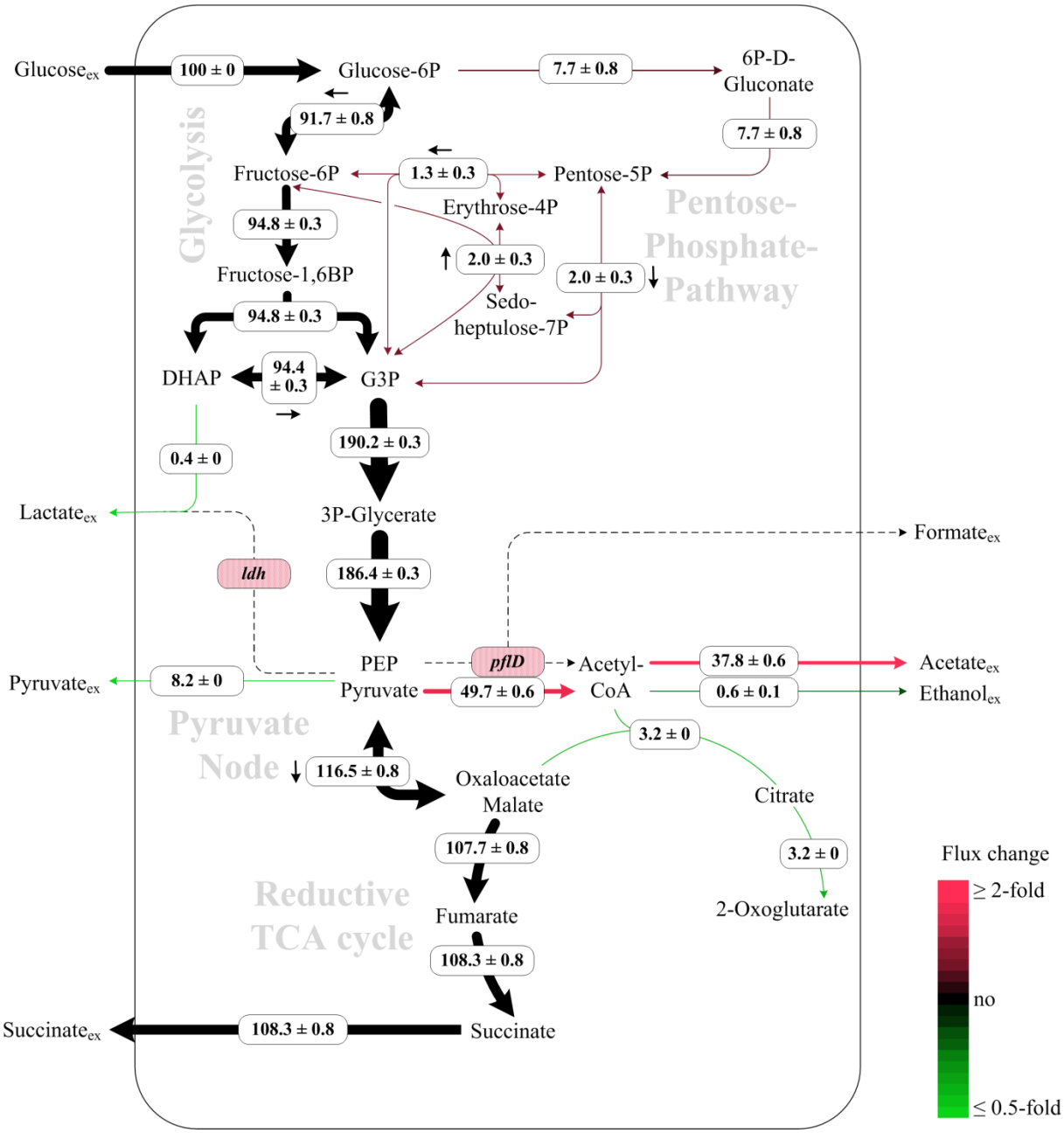

Figure 5.11 *B. succiniciproducens* DD3-T2 *in vivo* carbon flux distribution of the central carbon metabolism during growth in glucose minimal medium at 42 °C. Specific glucose uptake rate q_{Glc} = 9.1 mmol g^{-1} h^{-1} is set to 100 % and all fluxes are given as percentage thereof. Strain specific deleted pathways are shown as dashed line with corresponding gene names in red boxes, respectively. The flux changes are visualized as differential map, according to the color legend. Underlying fold changes of carbon flux were calculated based on data from DD3 taken from Becker et al. 2013, corrected for the specific glucose uptake rate (Table 9.4). The errors reflect 90 % confidence intervals.

Regarding redox balancing, NAD(P)H supply was improved with *B. succiniciproducens* DD3-T2, as compared to the ancestor (Figure 9.1). However, a higher cultivation temperature revealed redox patterns similar to these observed for DD3 under standard conditions. This indicates a metabolic stabilization as consequence of evolutionary adaptation.

5.2.4 Gene expression profile of the temperature tolerant mutant *B. succiniciproducens* DD3-T2

For gene expression profiling, a custom-made DNA microarray was designed and gene expression analysis was established for *B. succiniciproducens*, comprising 2291 annotated genes from the *B. succiniciproducens* genome sequence with a total of five probes per gene. For data analysis, the obtained expression profiles were ranked according to the metric log2 fold change and individually assigned to specific gene sets, so called clusters of orthologous groups (COG) (Tatusov et al. 2000). This gene set enrichment analysis (GSEA) (Subramanian et al. 2005) is frequently used to identify gene clusters that are ostensibly involved in the formation of phenotypes. The assignment of annotated genes to gene clusters was taken from literature (Hong et al. 2004) and subsequently implemented into the GSEA software tool. Experiments were conducted in pH-controlled bioreactors, preventing perturbing effects of $MgCO_3$. Biomass samples were taken at a cell concentration equivalent to OD_{600} of 2 – 3. The obtained expression data were analyzed by GSEA (Subramanian et al. 2005) to provide first information on favored or selectively preferred gene sets that contribute to the adaptation process. Analysis of the DD3-T2 transcriptome revealed three enriched gene clusters with significant statistics (Table 5.5), which positively correlate with the evolved phenotype. Surprisingly, the genes covered metabolic core functions to a larger extent. They imply that temperature adaptation is closely linked to intracellular exploitation of carbon and thus adapting the efficiency towards the required features.

Table 5.5 Gene sets affected towards the evolutionary adaptation of *B. succiniciproducens* DD3-T2 compared to the gene expression patterns of the parent strain DD3. Data comprise the normalized enrichment score (NES), the nominal p-value (NOM p-val) and the false discovery rate (FDR) (Subramanian et al. 2005). Data derive from triplicate bioreactor cultivations in minimal glucose medium.

Gene sets	NES	NOM p-val	FDR
Enriched in DD3-T2 vs. DD3			
Carbohydrate metabolism and transport	1.98	< 0.001	0.001
Signal transduction	1.81	0.005	0.004
Energy production and conversion	1.54	0.004	0.041

In *B. succiniciproducens* DD3-T2, 63 genes were significantly up- or down-regulated, as compared to the parental strain DD3, whereby 36 genes were at least twofold induced. Within the group of affected genes, operons were identified that exhibited concerted transcriptional regulation (Table 9.5). They were related to carbon core and energy metabolism and pointed out the essential role of these functional groups in the improved phenotype. The strongest expression change was observed for a hexose phosphate phosphorelay system (MS2284-87) consisting of a conserved histidine kinase-like regulatory system and a hexose phosphate permease (Weston and Kadner 1988). One might speculate that the modified expression level of this regulatory and transport operon may contribute to an

optimized substrate uptake, leading to more efficient growth and production. In this line, other carbon transport related genes were induced, such as a monosaccharide transporting ATPase (Table 5.6) and a phosphotransferase operon (Table 9.5). In addition, gene expression was changed for genes of the pyruvate metabolism. The genes coding for pyruvate dehydrogenase (MS1333-35) revealed an averaged 4.2-fold increased expression. This could explain the observed flux increase from pyruvate towards acetyl-CoA (Figure 5.10). Acetyl-CoA, supplied by pyruvate dehydrogenase complex, is an essential building block for cellular growth and biomass production. Its enhanced supply could contribute to the improved growth rate of DD3-T2 (Table 5.4), and also trigger the formation of acetate, which was indeed produced at a higher yield, as compared to DD3.

Table 5.6 Impact of evolutionary adaptation towards 42 °C on gene expression of *B. succiniciproducens*. Data comprise genes, up- and down-regulated in DD3-T2, as compared to the parental strain DD3 (corrected p-value < 0.05).

Systematic name[a]	Gene[a]	Fold change	Description[b]	Operon number[c]	Function[d]
MS1335	*aceF*	4.6	Pyruvate dehydrogenase complex, E2 component	2	Energy production and conversion
MS1334	*lpd*	4.4	Pyruvate dehydrogenase complex, E3 component	2	
MS1336	*ace*	3.8	Pyruvate dehydrogenase complex, E1 component	2	
MS1992	*glpQ*	2.4	Glycerophosphoryl diester phosphodiesterase		
MS2293	*pckA*	2.4	Phosphoenolpyruvate carboxykinase (ATP)		
MS1988	*glpK*	2.3	Glycerol kinase		
MS1984	*aspA*	3.8	Aspartate ammonia-lyase		Amino acid metabolism and transport
MS0787	*metF*	2.2	5,10-methylenetetrahydrofolate reductase		
MS0941	*metE*	2.1	Methionine synthase II		
MS2284	*uhpT*	39.5	Hexose phosphate permease		Carbohydrate metabolism and transport
MS1236	*amyA*	4.1	Trehalose-6-phosphate hydrolase		
MS2287	*uhpC*	3.8	Hexose phosphate sensor protein		
MS1237	*ptsG*	3.8	Phosphotransferase system, trehalose-specific, EIIBC components		
MS1991	*uhpC*	3.0	Glycerol-3-phosphate transporter		
MS1612	*rbsB*	2.9	Monosaccharide-transporting ATPase		
MS1615	*fbp*	2.7	Fructose-1,6-bisphosphatase		
MS1990	*glpF*	2.5	Glycerol uptake facilitator		
MS1607	*dAK1*	2.3	Dihydroxyacetone kinase, C-terminal	3	
MS1606	*dAK1*	2.3	Dihydroxyacetone kinase, N-terminal	3	
MS1608		2.1	Phosphotransferase system, dihydroxyacetone kinase-dependent, phosphotranferase subunit	3	
MS0618		2.1	Phosphotransferase system, mannose/fructose/N-acetylgalactosamine-specific component EIIAB	1	
MS0373	*ung*	2.2	Uracil DNA glycosylase, BER initiating		Replication, recombination and repair
MS0185	*himA*	2.0	DNA-binding protein HU		
MS2289		2.3	N-acetyltransferase	4	Cell wall, membrane, envelope biogenesis
MS0740	*ompW*	2.1	Outer membrane protein W		
MS2285	*uhpA*	8.6	UhpB-UhpA (hexose phosphate uptake) two-component regulatory system, transcriptional regulator	4	Signal transduction
MS2286	*uhpB*	5.6	UhpB-UhpA (hexose phosphate uptake) two-component regulatory system, sensory component	4	
MS2288	*narQ*	2.5	Signal transduction histidine kinase	4	
MS0349	*uspA*	2.1	Universal stress protein UspA homolog	4	

MS1823		-	2.0	Glycerol-3-phosphate acyltransferase		Energy production and conversion
MS0551	*proX*	-	3.2	ABC-type proline/glycine betaine transport systems, periplasmic components	5	Amino acid metabolism and transport
MS0549	*proV*	-	2.9	ABC-type proline/glycine betaine transport system, ATPase component	5	
MS0550	*proW*	-	2.7	ABC-type proline/glycine betaine transport system, permease component	5	
MS0227	*betT*	-	2.6	Glycine betaine transporter		
MS0353	*alsT*	-	2.4	Na^+/alanine or glycine symporter		
MS1797	*avtA*	-	2.3	Aminotransferase AlaT		
MS1790	*aroQ*	-	2.0	3-dehydroquinate dehydratase II		
MS1510	*fruB*	-	5.6	Phosphotransferase system, Phosphocarrier protein HPr		Carbohydrate metabolism and transport
MS1509	*ptsA*	-	2.8	Phosphotransferase system, PEP-protein kinase, EI component		
MS2073	*glgP*	-	2.2	Glycogen phosphorylase	9	
MS1795	*menF*	-	3.4	Menaquinone specific isochorismate synthase	6	Coenzyme metabolism
MS1794	*mend*	-	3.2	2-succinyl-5-enolpyruvyl-6-hydroxy-3-cyclohexene-1-carboxylate synthase	6	
MS1793	*mhpC*	-	2.6	2-succinyl-6-hydroxy-2,4-cyclohexadiene-1-carboxylate synthase	6	
MS1826	*lipA*	-	2.5	Lipoic acid synthetase		
MS1791	*dgoA*	-	2.4	O-succinylbenzoate synthase	6	
MS1792	*menB*	-	2.3	Dihydroxynaphthoic acid synthase	6	
MS1821	*rluD*	-	2.0	Pseudouridylate synthases, 23S RNA-specific	8	Translation
MS1820	*nrfG*	-	2.7	Outer membrane assembly lipoprotein		Cell wall, membrane, envelope biogenesis
MS1808	*artI*	-	2.0	Membrane-bound lytic murein transglycosylase		
MS1801	*nhaA*	-	2.7	Na^+/H^+ antiporter		Inorganic ion transport and metabolism
MS1818	*nrfB*	-	2.6	Formate-dependent nitrite reductase, penta-heme cytochrome c	7	
MS1816	*nrfD*	-	2.6	Formate-dependent nitrite reductase, membrane component	7	
MS1819	*nrfA*	-	2.5	Formate-dependent nitrite reductase, periplasmic cytochrome c552 subunit	7	
MS1817	*nrfC*	-	2.4	Formate-dependent nitrite reductase, 4Fe-4S subunit	7	
MS1341	*modB*	-	2.3	ABC-type molybdate transport system, permease component		

[a] Gene entries and names are given in accordance with KEGG annotations for *M. succiniciproducens* MBELE55.
[b] Information are adopted from Hong et al. 2004 and/or NCBI database using BLASTP swissprot (sequence coverage of 50 % and amino acid sequence homologies above 30 %) in combination with annotations from KEGG.
[c] Operons and their corresponding genes were assigned according to the Database of prOkaryotic OpeRons (Dam et al. 2007; Mao et al. 2009) and the Prokaryotic Operon DataBase (Taboada et al. 2012) for *M. succiniciproducens* MBELE55 predictions (see Table 9.5).
[d] Functional grouping was taken from literature (Hong et al. 2004).

The gene for the major anaplerotic carboxylation in *B. succiniciproducens*, PEP carboxykinase (PEPCK), was induced 2.4-fold. This probably re-directed the carbon flux towards the reductive TCA cycle and succinate (Figure 5.10). PEPCK was proven as a valuable engineering target towards tailor-made succinate producing *E. coli* (Millard et al. 1996; Kim et al. 2004; Zhang et al. 2010) and represents the most important enzyme in anaerobic succinate production. The amplified expression of PEPCK might be correlated to the efficient formation of succinate throughout the whole evolutionary adaptation process and in the final isolate DD3-T2. Beyond carbon core metabolism, several stress-related genes were induced at the level of RNA expression, comprising e.g. a DNA glycosylase (Table

5.6), mainly responsible for the base excision repair (Krokan et al. 1997) and the DNA stabilizing protein HU alpha (Kamashev and Rouviere-Yaniv 2000).

Interestingly, menaquinone biosynthesis genes were among the 27 repressed genes, despite menaquinone's presumed function in anaerobic fumarate reductase reaction towards succinate. Regarding the slightly increased carbon flux through the reductive TCA cycle (Figure 5.10), this down-regulation, however, seemed not limiting for the improved succinate formation with DD3-T2.

5.2.5 Genome sequencing reveals distinct mutations evolved during temperature adaptation in *B. succiniciproducens* DD3-T2

As shown, the evolutionary derived temperature tolerant mutant DD3-T2 exhibited altered metabolic fluxes. Furthermore, the adaptation process obviously affected gene expression. It was now relevant to identify the underlying mutations. For this purpose, both adapted strains, DD3-T1 and DD3-T2 were sequenced and compared to wild-type *B. succiniciproducens* DD1. Polymorphism significance was covered by a sequence coverage > 50 and a variant frequency set to 75 %.

Table 5.7 Single nucleotide polymorphisms (SNP) and deletion – insertion – polymorphisms (DIP) are listed with their respective position specific nucleotide (Nt ex) and amino acid (AA ex) exchange in the temperature adapted strains *B. succiniciproducens* DD3-T1 and DD3-T2. The wild-type genome was annotated, according to the published *M. succiniciproducens* MBEL55E genome (Hong et al. 2004) and served as reference for detection of mutations in the adapted phenotypes.

Strain	Systematic name	Nt ex	AA ex	Pm	Gene	Function
DD3-T1	MS0136	1435C>T	Pro479Ser	SNP	*nhaP*	Monovalent cation:H^+ antiporter
	MS2084	919G>T	Gly307Cys	SNP	*lysA*	Meso 2,6-diaminopimelate decarboxylase
	MS2286	586C>A	Gln196Cys	SNP	*baeS/uhpB*	Glucose-6-phosphate specific two-component signal transduction system
	MS2286	599C>T	Pro200Leu	SNP	*baeS/uhpB*	
DD3-T2	MS0136	1435C>T	Pro479Ser	SNP	*nhaP*	Monovalent cation:H^+ antiporter
	MS0213	692C>A	Thr231Lys	SNP	*rpoC*	β' prime subunit of RNA polymerase
	MS0911	46A>C	Thr16Pro	SNP	*rfe*	UDP-GlcNAc:undecaprenyl-phosphate GlcNAc-1-phosphate transferase
	MS2084	919G>T	Gly307Cys	SNP	*lysA*	Meso 2,6-diaminopimelate decarboxylase
	MS2286	586C>A	Gln196Cys	SNP	*baeS/uhpB*	Glucose-6-phosphate specific two-component signal transduction system
	MS2286	599C>T	Pro200Leu	SNP	*baeS/uhpB*	
	MS1237	-70C>A	-	SNP	P_{ptsG}	Promoter of trehalose (maltose)-specific transporter subunit IIBC of PTS
	MS1336	-207insA	-	DIP	P_{aceE}	Promoter of pyruvate dehydrogenase subunit E1

Pm: type of occurring polymorphism

The genome sequence of the temperature adapted strains *B. succiniciproducens* DD3-T1 and DD3-T2 revealed four and eight mutations, respectively (Table 5.7). The mutated genes, identified in DD3-T1, were attributed to energy and carbon metabolism and amino acid metabolism and transport. All these modifications were still present in DD3-T2 and, thus, were obviously kept during the further

adaptation process (Figure 5.12). This maintenance indicates their apparent metabolic value. The mutations, additionally present in DD3-T2, belonged to the transcription machinery, carbon metabolism and cell wall composition. Most relevant, the number of mutations mediating the superior phenotype was rather low. This promised metabolic engineering targets for rational improvement of increased temperature tolerance in *B. succiniciproducens*.

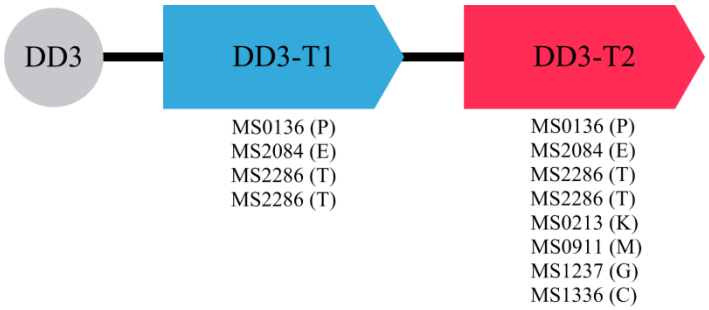

Figure 5.12 Overview on mutations evolved during temperature adaptation to 40 °C (DD3-T1) and 42 °C (DD3-T2) in *B. succiniciproducens* DD3. Systematic name and COG identifier (in brackets) are taken from *M. succiniciproducens* MBEL55E annotation (Hong et al. 2004). For further information on the single modifications, see Table 5.7.

Taken together, *B. succiniciproducens* DD3 was successfully adapted to a higher temperature level. The finally adapted strain DD3-T2 was proven at high temperature, initially inhibiting growth performance of the ancestor DD3 and the wild-type strain. Careful growth experiments and system biology approaches revealed a complex picture of tolerance underlying mechanisms. The increased tolerance might result from re-orientation of carbon fluxes, regulated at the level of transcriptomics and genomics. Regarding a rational engineering approach towards improvement of *B. succiniciproducens*, it appeared most relevant to analyze the impact of mutations, acquired during the adaptation process. In particular, mutations that contribute to straight-forward metabolic reactions seemed promising with regard to an industrial performance.

5.3 Increasing succinate tolerance in *B. succiniciproducens*

5.3.1 Sequential batch adaptation of *B. succiniciproducens* DD3 towards high succinate stress

It has been proposed that an efficient production process for succinate has to achieve a product titer above 100 g L^{-1} (Patel et al. 2006). Clearly, such performance relies on the robustness and tolerance of the producing microorganism to elevated levels of the product. Unfortunately, individual genetic targets that mediate such a tolerance are primarily not known. In particular organic acid tolerance, such as succinate, cannot be tailored by rational strain design, since the respective phenotype requires polygenic modifications to exhibit this higher stress tolerances (Patnaik 2008). In order to improve tolerance to succinate, *B. succiniciproducens* DD3, lacking *ldhA* and *pflD* to eliminate formation of the by-products lactate and formate, was chosen for the evolutionary process by exposing it to high succinate concentration in a minimal medium based sequential batch approach. At the starting point of the evolutionary adaptation, the external succinate concentration was set to 5 g L^{-1}, and was gradually increased further on. The batch interval was adjusted to cell growth, i.e. cells were harvested from a batch culture only when they had reached a cell density corresponding to an OD_{600} of 5 to ensure an appropriate adapted cell population prior to inoculating the next batch at an even higher succinate level. In case of a slow cell proliferation, the cultivation was simply extended to allow for the formation of sufficient biomass for the next following batch. During the first two adaptive rounds DD3 struggled with the external amount of 5 g L^{-1} succinate (Figure 5.13). It took about 24 h to reach notable cell growth. The third batch, still at 5 g L^{-1} succinate, showed a distinct improvement of growth. Suddenly, the cells revealed similar growth performance as observed for DD3 under standard conditions, i.e. without added succinate. The specific growth rate almost reached 0.1 h^{-1}. The specific succinate productivity advanced to nearly 1 g L^{-1} h^{-1} (Figure 5.13). Based on this sudden improvement, single clones were isolated from the population of this round three. One of the clones, selected for further analysis, was designated DD3-Suc1. Subsequently, the succinate concentration in the medium was stepwise increased throughout the following iterations. Each round of the further adaptation was accompanied by a significant improvement of growth, compared to the parental strain (Figure 5.13). In response to each further increase in externally added succinate, the cells were able to compensate for the extracellular stress. Two more superior strains were isolated. The designated strain DD3-Suc2 was isolated after 15 iterations, due to the remarkably increased specific growth rate and succinate productivity (Figure 5.13). It was interesting to note that the adapted cells performed well at almost 20 g L^{-1} of initially added succinate. This level was previously found to fully inhibit the parental strain (Figure 5.3).

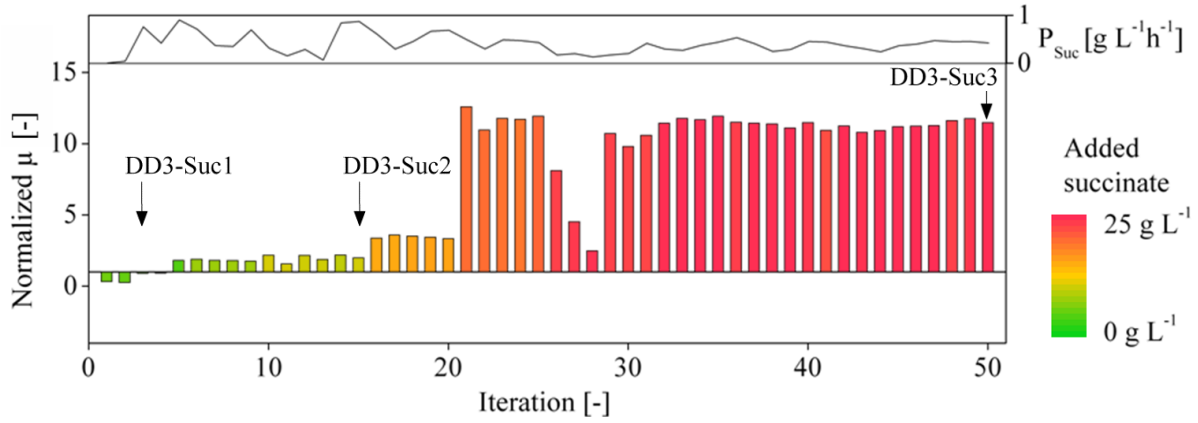

Figure 5.13 Evolutionary adaptation of *B. succiniciproducens* DD3 to high levels of succinate, visualized according to the color legend. The bar chart shows the normalized specific growth rate, referring to standard cultivations of un-adapted DD3 at respective succinate levels in minimal glucose medium (μ = 1). The top level indicates the specific succinate productivity during each batch. The data were estimated from the time specific succinate production of each round, after correcting for the initially added succinate (see color legend).

At the 25th iteration, succinate was supplemented at 25 g L^{-1}. Obviously, this imposed pronounced stress, clearly visible by a sudden decrease of growth and productivity, affected the performance (Figure 5.13). However, during the subsequent rounds the cells could recover and exhibited efficient growth and improved succinate productivity. From cultures that tolerate 25 g L^{-1} succinate, the clone DD3-Suc3 was isolated for further studies. At the higher succinate levels, succinate productivity never reached the values, observed for the parent strain DD3 without imposed succinate stress, but still remained at reasonable levels.

5.3.2 Physiological characterization of *B. succiniciproducens* DD3-Suc1, DD3-Suc2 and DD3-Suc3 adapted towards higher succinate levels

In order to gain information on the newly isolated succinate tolerant phenotypes, comparative cultivations were carried out with the parent strain *B. succiniciproducens* DD3 and with the mutants DD3-Suc1, DD3-Suc2 and DD3-Suc3. The focus was first set on evaluation of fermentation performance. Cultivation experiments were conducted in serum bottles at 37 °C. All adapted strains showed faster growth, as compared to DD3, and enhanced succinate production (Figure 5.14). Succinate productivity could be increased by about 30 % with DD3-Suc1 and DD3-Suc2, considering DD3 standard performance (Table 5.4).

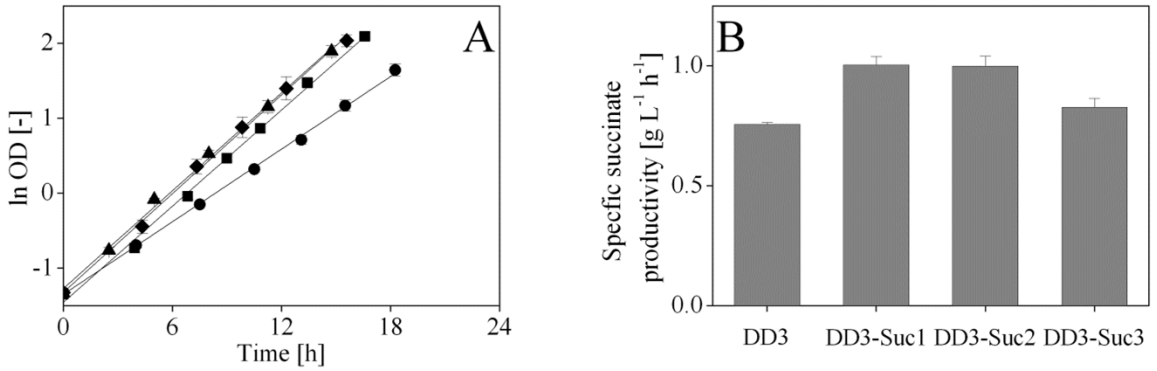

Figure 5.14 Growth physiology of the three succinate tolerant strains *B. succiniciproducens* (▲) DD3-Suc1, (■) DD3-Suc2 and (♦) DD3-Suc3 compared to their parental strain (●) DD3 (A) and maximal specific succinate productivity during 48 h cultivation period (B). The data points represent mean values from three biological replicates with their corresponding standard deviations. All cultivations were performed in minimal glucose medium E at 37 °C.

In addition to these observed improvements, the mutants revealed a pronounced change in their by-product spectrum (Table 5.8). All succinate tolerant mutants showed enhanced formation of pyruvate (Table 5.8). This organic acid is more tolerable according to inhibition studies with *A. succinogenes*, another succinate producing bacterium (Lin et al. 2008). The increased formation of pyruvate obviously went to the expense of succinate and acetate (Table 5.8).

Table 5.8 Growth and production characteristics of succinate adapted strains *B. succiniciproducens* DD3-Suc1, DD3-Suc2 and DD3-Suc3, compared to their parent strain DD3 at 37 °C in minimal glucose medium E. The data given are specific growth rate (μ_{max}), biomass yield ($Y_{X/S}$), succinate yield ($Y_{Suc/S}$), formate yield ($Y_{For/S}$), acetate yield ($Y_{Ace/S}$), lactate yield ($Y_{Lac/S}$), ethanol yield ($Y_{EtOH/S}$), pyruvate yield ($Y_{Pyr/S}$) and maximal succinate productivity (P_{Suc}). Data represent mean values of three biological replicates with their corresponding standard deviations.

	DD3	**DD3-Suc1**	**DD3-Suc2**	**DD3-Suc3**
μ_{max} [h^{-1}]	0.16 ± 0.01	0. 22 ± 0.01	0.22 ± 0.01	0.22 ± 0.01
$Y_{X/S}$ [g mol^{-1}]	29.8 ± 2.5	30.5 ± 1.0	30.1 ± 2.4	30.7 ± 4.0
$Y_{Suc/S}$ [mol mol^{-1}]	1.13 ± 0.04	1.09 ± 0.05	0.96 ± 0.04	0.90 ± 0.03
$Y_{For/S}$ [mol mol^{-1}]	< 0.01	< 0.01	< 0.01	< 0.01
$Y_{Ace/S}$ [mol mol^{-1}]	0.21 ± 0.06	0.14 ± 0.01	0.15 ± 0.03	0.28 ± 0.03
$Y_{Lac/S}$ [mol mol^{-1}]	< 0.01	< 0.01	< 0.01	< 0.01
$Y_{EtOH/S}$ [mol mol^{-1}]	< 0.01	< 0.01	< 0.01	< 0.01
$Y_{Pyr/S}$ [mol mol^{-1}]	0.16 ± 0.03	0.33 ± 0.01	0.27 ± 0.01	0.23 ± 0.02
P_{Suc} [g L^{-1} h^{-1}]	0.76 ± 0.01	1.00 ± 0.04	1. 00 ± 0.04	0.83 ± 0.04

The yields were determined by linear fitting of the concentration of biomass and product with that of the substrate.

A next round of experiments now evaluated the joined tolerance to increased succinate levels. For this purpose, *B. succiniciproducens* DD3, DD3-Suc1, DD3-Suc2 and DD3-Suc3 were cultivated under external addition of succinate to the growth medium, i.e. succinate was added prior to inoculation at concentrations of 5, 7.5, 10, 15 and 25 g L^{-1} (Figure 5.15).

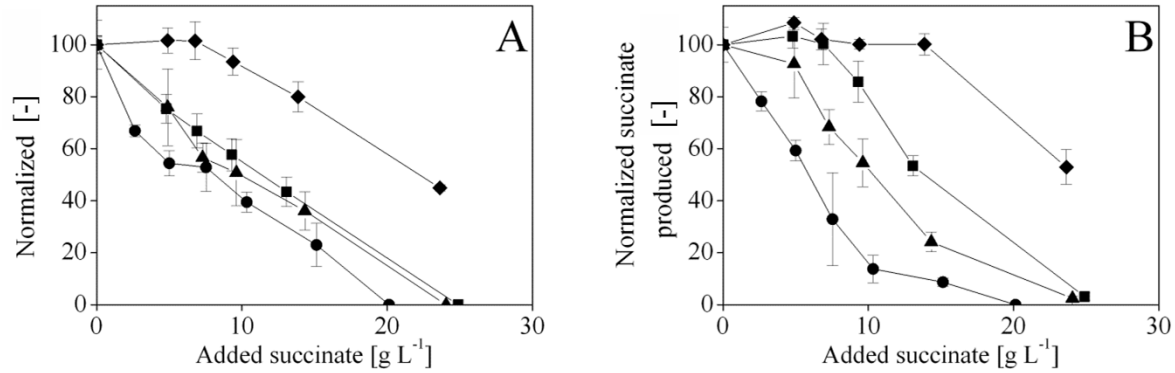

Figure 5.15 Succinate tolerance studies of *B. succiniciproducens* (■) DD3-Suc1, (▲) DD3-Suc2 and (♦) DD3-Suc3 compared to the parental strain (●) DD3 for specific growth (A) and final succinate titer, corrected for initially added succinate (B). Growth (μ) and succinate production of DD3 at standard conditions, i.e. 37 °C and no imposed succinate stress, were set to 100 %. Cultivations were conducted in minimal glucose medium with the addition of five succinate concentrations. Data represent three biological replicates with corresponding standard deviations.

Taken together, the isolated clones from the evolutionary adaptation revealed a remarkably increased tolerance towards external succinate (Figure 5.15). The parent strain DD3 was strongly inhibited in growth and responded to higher succinate levels with a drastic decrease in succinate formation. In contrast, all mutants were much more robust. The final isolate, DD3-Suc3 was almost unaffected in growth and succinate production at levels of 10 and 15 g L^{-1} added succinate, respectively. This was an exceptional performance when compared to that of DD3, the starting point of the evolutionary adaptation. The potential to adapt to higher succinate levels can be regarded as an important feature of *B. succiniciproducens* towards industrial succinate production.

5.3.3 Metabolic pathway fluxes in the succinate-tolerant *B. succiniciproducens* strains DD3-Suc2 and DD3-Suc3

The cellular tolerance to organic acids is complex and its regulation is barely understood (Warnecke and Gill 2005). Throughout the evolution, extremophile bacteria adapted to harsh environmental conditions, including organic acids and coupled pH stress, by developing various techniques (Booth 1985). The promising *B. succiniciproducens* mutants were now analyzed by systems biology approaches to shed some light upon the underlying molecular mechanisms in succinate tolerance and adaptation. To this end, metabolic flux analysis (fluxomics), metabolomics and transcriptomics, respectively, was conducted for the obtained isolates. Additionally, the mutants were sequenced to unravel correlations between phenotype and genotype.

Metabolic pathway fluxes for *B. succiniciproducens* DD3-Suc2 and DD3-Suc3 were determined by tracer cultivations, using [1-^{13}C] glucose as carbon source. On the basis of the obtained stoichiometric data (Table 5.8), ^{13}C labeling patterns of proteinogenic amino acids and succinate (Table 9.2) and anabolic demands (Table 9.1), the intracellular flux distribution was estimated using the Open Flux Tool (Quek et al. 2009). Metabolic and isotopic steady-state, an important prerequisite for the flux approach, was obtained for both adapted strains (Figure 5.16). An excellent fit of the labeling data was achieved during flux estimation (Table 9.2) underlining the consistency of the obtained fluxes. The statistical evaluation of the flux partitioning showed a high precision, so that flux differences to the parent strains could be attributed to strain-specific differences.

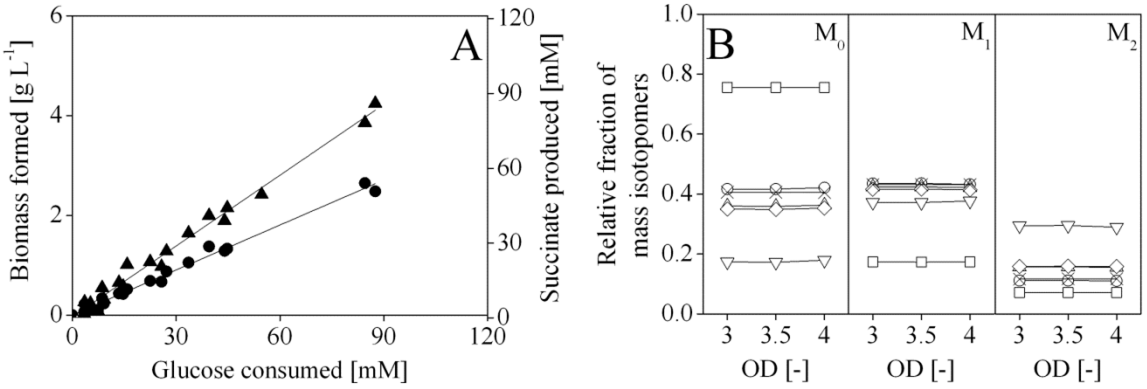

Figure 5.16 Metabolic (A) and isotopic (B) steady state during labeling experiments with *B. succiniciproducens* DD3-Suc2. The metabolic steady state was verified from linear correlation between (●) biomass and (▲) succinate formation, respectively, and glucose consumption. Constant labeling patterns of proteinogenic amino acids confirmed isotopic steady state. Hereby, exemplary shown amino acids and succinate stem from different parts of the metabolic network. M_0 (non-labeled), M_1 (single labeled) and M_2 (double labeled) represent the relative fraction of corresponding isotopomers of (○) alanine, (□) glycine, (Δ) serine, (▽) phenylalanine, (◊) aspartate, and (x) succinate.

Both succinate-adapted mutants showed an increased flux into the oxidative PPP, as compared to their ancestor DD3 (Figure 5.17 and Figure 5.18). This might relate the superior growth performance of the evolved phenotypes that could benefit from enhanced supply of NADPH via the PPP. The enhanced flux into the PPP was also observed in the temperature-tolerant strain DD3-T2, which also showed improved growth (see 5.2.2). NADPH presumably supports the biomass formation and is a limiting factor for *Pasteurellaceae* growth (McKinlay et al. 2007). Interestingly, the two independent adaptation approaches, towards high temperature and elevated succinate levels, respectively, induced both the same increased flux into the PPP.

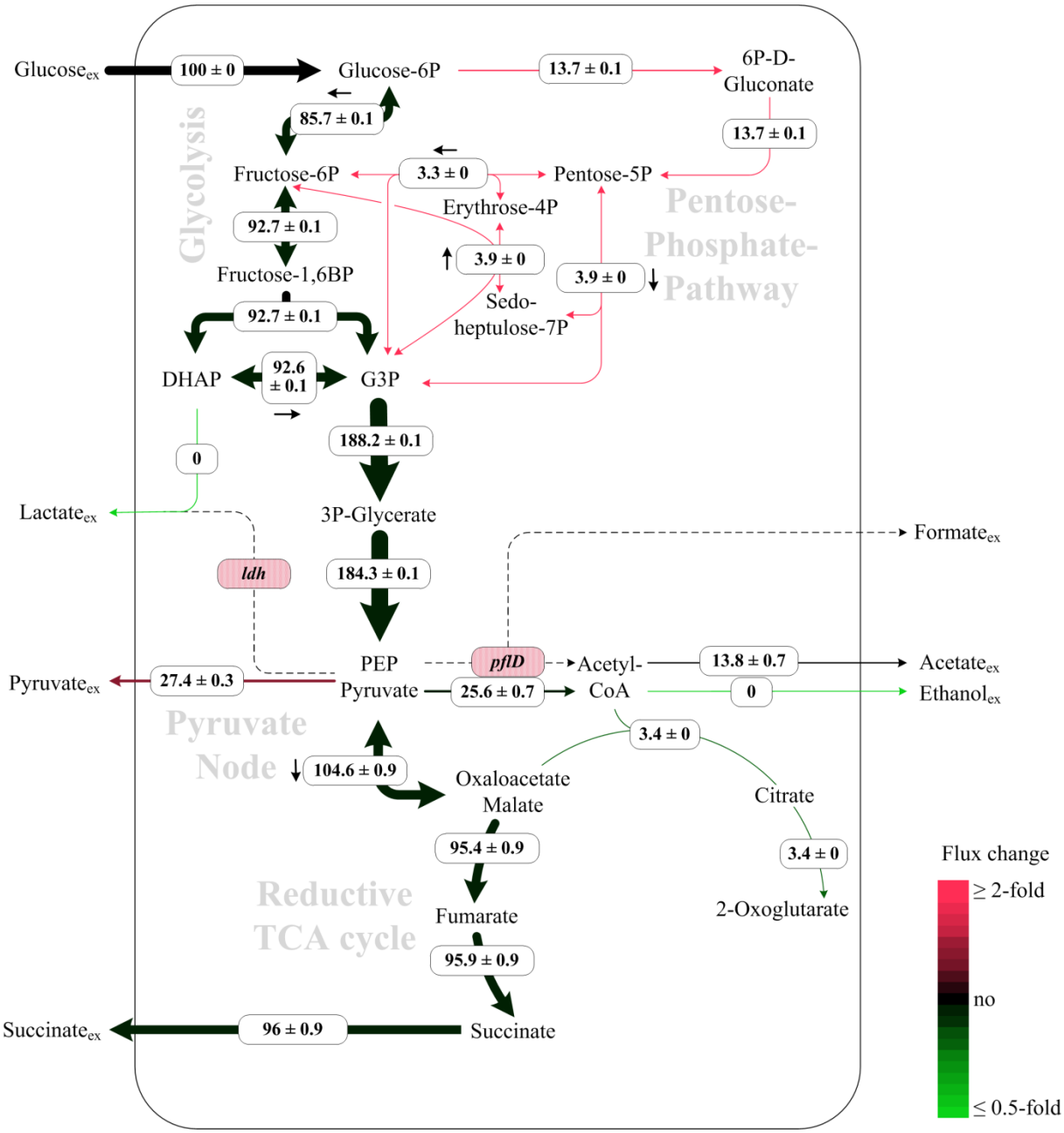

Figure 5.17 *In vivo* carbon flux distribution of *B. succiniciproducens* DD3-Suc2 during growth in minimal glucose medium. Fluxes are shown as percentage of the specific glucose uptake rate q_{Glc} = 7.8 mmol g^{-1} h^{-1} that was set to 100 %. Small arrows indicate net flux direction. Dashed lines show rationally deleted pathways prior to evolutionary engineering with their respective genes (red boxes). Flux fold change (Table 9.4) was estimated from specific glucose uptake rate corrected data from DD3 (Becker et al. 2013) and DD3-Suc2 and differentially visualized according to the color legend. The errors reflect 90 % confidence intervals.

Taken together, this flux re-distribution at the G6P-node could reflect an indirect response to provide extra redox power to cover an enhanced need as observed for other bacteria (Wittmann and Heinzle 2001b; Wittmann and Heinzle 2002). One might suggest, on basis of this molecular switch, rational engineering of the PPP flux in order to improve growth performance of *B. succiniciproducens*. However, enhanced growth would have to be carefully balanced with product formation, due to their direct link to each other (Becker et al. 2013).

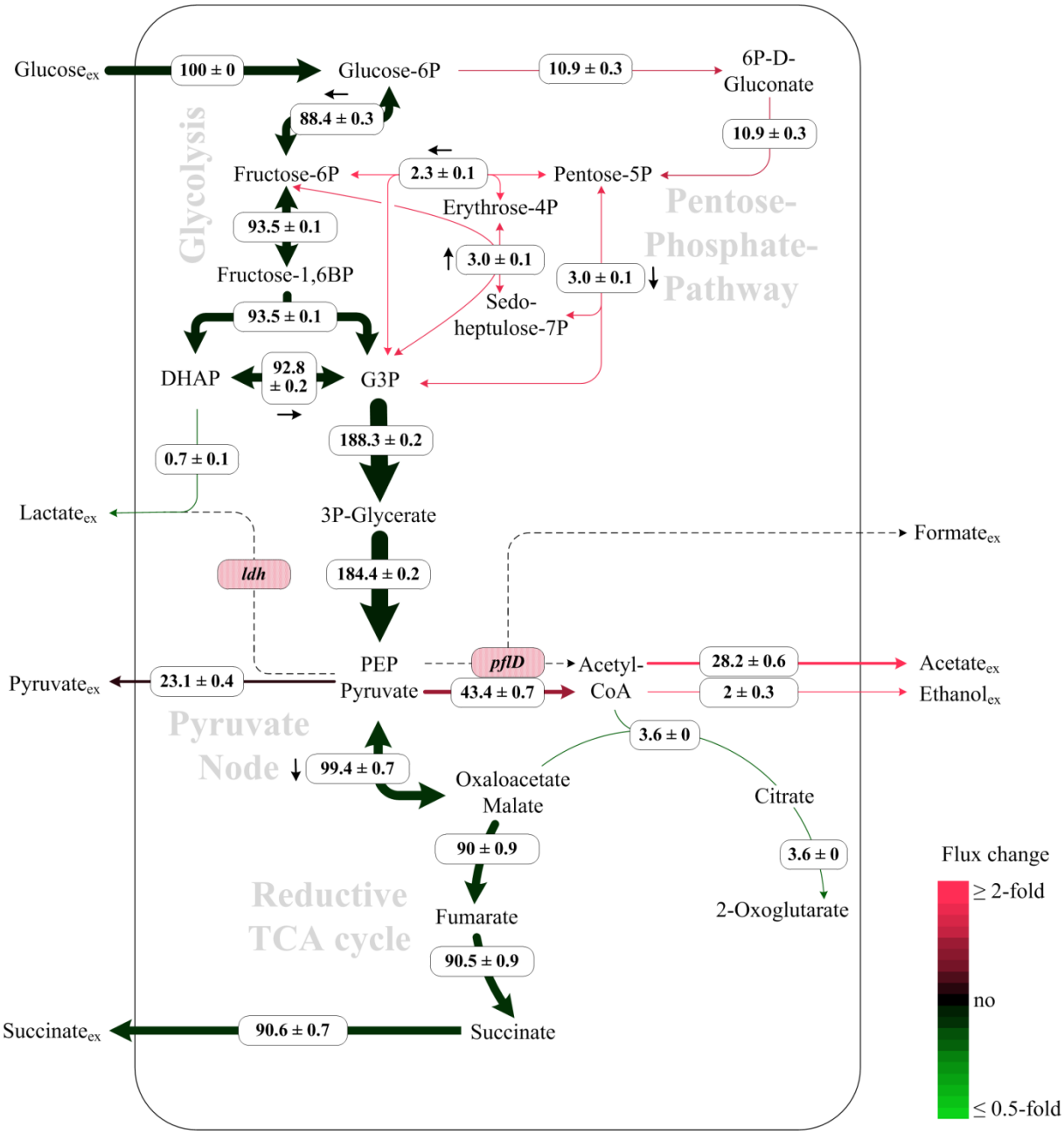

Figure 5.18 *In vivo* carbon flux distribution of *B. succiniciproducens* DD3-Suc3 during growth in minimal glucose medium. Specific glucose uptake rate q_{Glc} = 7.6 mmol g^{-1} h^{-1} is set to 100 % and all further fluxes are given as percentage. Net flux direction is indicated by small arrows. Rationally deleted pathways, i.e. *ldhA* and *pflD*, are shown by dashed lines. Comparison of specific glucose uptake rate corrected carbon fluxes of DD3 (Becker et al. 2013) and DD3-Suc3 is differentially visualized according to the color legend. The errors reflect 90 % confidence intervals.

The fluxes at the PEP/Pyr node showed a more complex picture. DD3-Suc2 redirected carbon flux from PDH and reductive TCA cycle towards pyruvate secretion (Figure 5.17), possibly favoring pyruvate's less toxic impact as compared to other organic acids (Lin et al. 2008). In contrast, DD3-Suc3 showed decreased pyruvate flux, but rather channeled the carbon into acetate production (Figure 5.18). This was supported by enhanced flux through the PDH. Here, the oxidative TCA cycle flux remained nearly unchanged, so that the formed acetyl-CoA was fully used for acetate synthesis. The

acetate production pathway generates ATP, which obviously supports the higher requirements under stress, as it was also observed during temperature adaptation (Figure 5.10). Taken together, *B. succiniciproducens* seems to exploit different mechanism to achieve a higher robustness. The shifts to less toxic by-products (i.e. pyruvate) and to energy-providing metabolic routes (i.e. acetate) seemed to be involved in this adaptation, so that the rearrangement of the by-product spectrum probably bears a substantial metabolic flexibility of *B. succiniciproducens*. The flux towards succinate production was decreased by 9 % in DD3-Suc2 and by 13 % in DD3-Suc3, respectively. Despite the necessity of this pathway for redox balancing, its reduction seemed to be linked to the adaptation process to higher external succinate concentrations. The flux through PEPCK, the driving force for anaerobic succinate formation in other microorganisms (Lee et al. 2006; McKinlay et al. 2010), is coherently reduced with increased tolerance against succinate (Figure 5.19). The reduced succinate formation as response to the stress becomes also obvious from the decreased succinate yields in the mutants (Table 5.8). Apparently, reduced succinate production itself supported the adaptation.

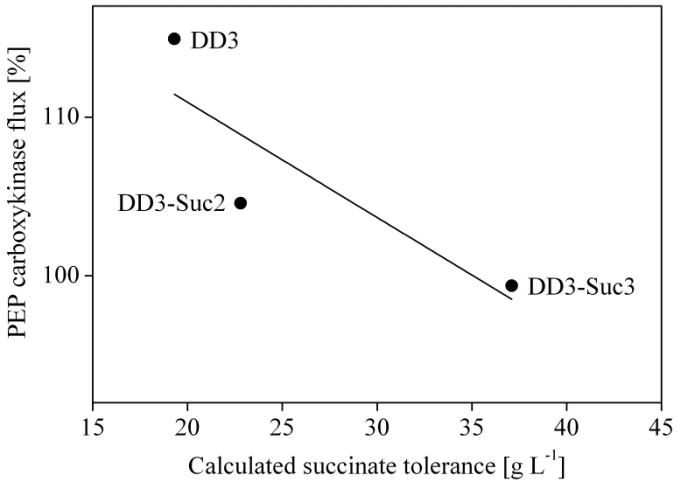

Figure 5.19 Correlation of succinate tolerance and relative carbon flux through phosphoenolpyruvate carboxykinase in *B. succiniciproducens* DD3, DD3-Suc2 and DD3-Suc3. The flux from PEP/Pyr towards the reductive part of the TCA was attributed to the reaction of the PEP carboxykinase, known as major anaplerotic enzyme in succinate producing microorganisms (Lee et al. 2006; McKinlay et al. 2010). The tolerance was determined from linear fit between specific growth rates at different succinate levels. The values given relate to the critical concentration ($\mu = 0$).

The decreased flux through the reductive TCA cycle branch finally resulted in lower regeneration of NAD^+, as this route accounts for 80 to 90 % of total NADH consumption in *B. succiniciproducens* (Becker et al. 2013). Obviously, this led to increased redox imbalances, as observed by supply and consumption of NADH in both mutants, as compared to DD3 (Figure 9.1).

5.3.4 Intracellular amino acid pools in succinate-tolerant *B. succiniciproducens* DD3-Suc3

Clearly, elevated succinate concentrations causes osmotic stress, so that the phenotypic response may involve the activation of mechanisms for osmotic protection, observed for other succinate producing microorganisms (Andersson et al. 2009; Fang et al. 2011). As example, proline has been identified as compatible solute in other bacteria (Brill et al. 2011). To this end, the intracellular pools of free amino acids were compared between the most tolerant strain *B. succiniciproducens* DD3-Suc3 and the wild-type strain DD1 (Figure 5.20).

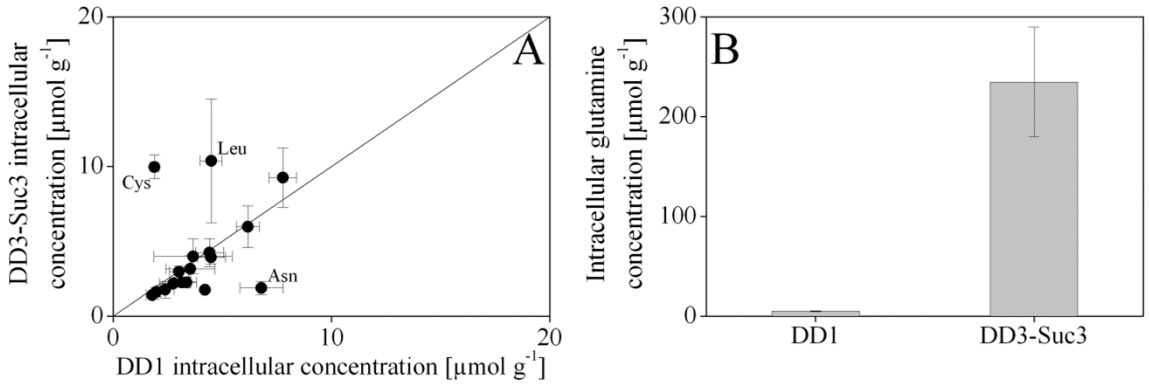

Figure 5.20 Intracellular amino acid (A) and glutamine (B) pools of *B. succiniciproducens* DD1 and DD3-Suc3. Data represent mean values with corresponding standard deviations from two biological replicates, each with two technical replicates, obtained during exponential growth phase on minimal glucose medium by applying an appropriate fast filtration.

As major difference, the succinate adapted strain DD3-Suc3 revealed an extreme up-regulation of intracellular glutamine (Figure 5.20). Indeed, glutamine has been found as compatible solute during moderate osmoadaptation (Frings et al. 1993; Goude et al. 2004). It was interesting to note that this compatible solute like amino acid was present without externally imposed stress. That might reflect a constitutive protection activated during the adaptation. Proline instead was observed in similar amounts in DD3-Suc3 as compared to DD1. Cysteine was increased 5-fold. It is reported to facilitate tolerance against oxidative stress (Turnbull and Surette 2010). This can be accredited to its function as precursor molecule for glutathione, an antioxidant. Glutathione-supplemented *M. succiniciproducens* MBEL55E fermentations revealed increased growth and productivity (Hoon et al. 2010). Cysteine is also known to be an essential compound for *M. succiniciproducens* MBEL55E growth (Song et al. 2008). The reduced intracellular asparagine pool might be explained by the reduced flux through the reductive TCA cycle in the succinate-tolerant mutant DD3-Suc3. Leucine was increased about twofold. This seemed not to be linked to enhanced tolerance, but due to the lack of *ldhA* and *pflD* in the mutant. In consequence of these deletions, *B. succiniciproducens* DD3 accumulates pyruvate-based metabolites, such as leucine and leucine specific precursors (Becker et al. 2013).

5.3.5 Gene expression profile in succinate-adapted *B. succiniciproducens* DD3-Suc2 and DD3-Suc3

In order to obtain more information on changes of the regulatory network, linked to the adaptation, gene expression studies were conducted with the adapted strains. For DD3-Suc2, adapted to 10 g L^{-1} succinate (Figure 5.13), significant changes were found for two gene groups (Table 5.9), i.e. the nucleotide metabolism and the translation. Both are crucial processes of living cells. Moreover, a direct link to the evolved tolerance is difficult to extract. Apart from that, the evolved strain DD3-Suc3 showed an altered expression pattern concerning genes that belong to the group of cell wall and membrane synthesis genes. This appeared quite straightforward, due to known microbial mechanisms which alter the membrane composition against acid stress (Warnecke and Gill 2005).

Table 5.9 Gene sets affected through the evolutionary adaptation of *B. succiniciproducens* DD3-Suc2 and DD3-Suc3 towards high succinate levels, as compared to the gene expression patterns of the parental DD3. Data show the normalized enrichment score (NES), the nominal p-value (NOM p-val) and the false discovery rate (FDR) (Subramanian et al. 2005). Data derive from three biological replicates in minimal glucose medium.

Gene sets	NES	NOM p-val	FDR
Enriched in DD3-Suc2 vs. DD3			
Translation	1.71	< 0.001	0.033
Nucleotide metabolism and transport	1.67	< 0.001	0.020
Enriched in DD3-Suc3 vs. DD3			
Cell wall, membrane, envelope biogenesis	1.63	< 0.001	0.046

A more detailed inspection of the expression data revealed 75 genes that were significantly changed in their expression in DD3-Suc2, as compared to the ancestor DD3. Among these, 30 genes were induced (Table 5.10), including five operons related to carbohydrate and energy conversion, stress tolerance and amino acid metabolism (Table 9.6). Additionally, genes encoding for components of proton dislocation i.e. NADH dehydrogenase and the cytochrome:quinol oxidase were induced 5- and 3-fold, respectively. This could support a decrease of intracellular proton concentration, known as a putative mechanism against organic acid stress (Warnecke and Gill 2005) to maintain constant internal pH (Booth 1999). In addition, the PDH complex was twofold induced. The corresponding carbon flux, however, remained unchanged (Figure 5.17). This could indicate the up-regulation of the PDH complex genes to maintain flux homeostasis or perturbing factors limiting flux through their reaction.

Table 5.10 Gene expression changes after evolutionary adaptation of *B. succiniciproducens* towards 10 g L^{-1} succinate. Data comprise genes up- and down-regulated in DD3-Suc2, as compared to the parental strain DD3 (corrected p-value < 0.05).

Systematic name[a]	Gene[a]	Fold change	Description[b]	Operon number[c]	Function[d]
MS0181	*ndh*	5.1	NADH dehydrogenase		
MS0716	*appB*	3.3	Cytochrome oxidase subunit 2		
MS0715	*cydA*	3.1	Cytochrome oxidase subunit 1		
MS1335	*aceF*	2.3	Pyruvate dehydrogenase complex, E2 component	4	Energy production and conversion
MS1336	*aceE*	2.3	Pyruvate dehydrogenase complex, E1 component	4	
MS1334	*lpd*	2.2	Pyruvate dehydrogenase complex, E3 component	4	
MS1251	*cysN*	5.3	Sulfate adenylyltransferase subunit 1	2	
MS0941	*metE*	4.6	Methionine synthase II		
MS0787	*metF*	4.6	5,10-methylenetetrahydrofolate reductase		
MS1252	*cysH*	4.6	Sulfate adenylyltransferase subunit 2	2	
MS1250	*cysJ*	4.5	Sulfite reductase alpha subunit (flavoprotein)	2	
MS1249	*cysI*	4.0	Sulfite reductase beta subunit (hemoprotein)	2	
MS1253	*cysH*	3.6	Phosphoadenosine phosphosulfate reductase		Amino acid metabolism and transport
MS1277	*artI*	3.1	ABC-type amino acid transport (substrate-binding protein)	3	
MS1684	*artI*	2.7	ABC-type amino acid transport (potential glutamine binding protein)		
MS1261	*cysA*	2.6	Sulfate transport system, ATP-binding protein		
MS1276	*artM*	2.3	ABC-type cystine transport system, permease	3	
MS1275	*glnQ*	2.3	ABC-type cystine transport system, ATP-binding protein	3	
MS0045	*ilvC*	2.2	Ketol acid reductoisomerase		
MS0372		2.5	Autonomous glycyl radical enzyme		Nucleotide metabolism and transport
MS0575	*uraA*	2.0	Purine permease		
MS0992	*nrdA*	2.0	Ribonucleotide reductase, alpha subunit		
MS1254	*cysG*	2.3	Uroporphyrinogen-III methyltransferase		
MS1683	*gshA*	2.1	Bifunctional glutamate-cysteine ligase/glutathione synthetase		Coenzyme metabolism
MS1015	*cirA*	2.1	Vitamin B_{12} transporter		
MS1856		2.0	6-pyruvoyl-tetrahydropterin synthase	5	
MS1857	*nrdG*	2.2	7-carboxy-7-deazaguanine synthase; queuosine biosynthesis (radical SAM superfamily)	5	Molecular chaperons and related functions
MS0458	*groS*	2.0	Co-chaperonin GroES	1	
MS0389	*sodA*	3.8	Superoxide dismutase (Mn)		Inorganic ion transport and metabolism
MS1205	*cirA*	2.4	Iron complex outermembrane recepter protein		
MS0040	*oadG*	- 3.5	Oxaloacetate decarboxylase, gamma subunit	6	
MS1653	*frdB*	- 3.4	Fumarate reductase, Fe-S protein subunit	12	
MS1654	*frdC*	- 3.3	Fumarate reductase subunit C	12	
MS0038	*oadB*	- 3.3	Oxaloacetate decarboxylase, beta subunit	6	
MS1655	*frdD*	- 3.3	Fumarate reductase subunit D	12	Energy production and conversion
MS1652	*sdhA*	- 3.2	Fumarate reductase, flavoprotein subunit	12	
MS2293	*pckA*	- 3.0	Phosphoenolpyruvate carboxykinase (ATP)		
MS0039	*oadA*	- 2.9	Oxaloacetate decarboxylase, alpha subunit	6	
MS1105	*leuA*	- 2.7	Tartrate dehydrogenase/decarboxylase		
MS0760	*fumC*	- 2.1	Fumarate hydratase		
MS0732		- 2.1	Formate dehydrogenase subunit alpha		
MS0550	*proW*	- 3.6	ABC-type proline/glycine betaine transport system, permease component	7	Amino acid metabolism and transport
MS0551	*proX*	- 3.5	ABC-type proline/glycine betaine transport systems, periplasmic components, substrate binding protein	7	
MS0549	*proV*	- 3.4	ABC-type proline/glycine betaine transport system, ATPase component	7	
MS0731	*gltD*	- 2.9	Putative NADPH-dependent glutamate synthase beta chain and related oxidoreductases	9	
MS0815	*pepD*	- 2.5	Aminotripeptidase		
MS0288/89		- 2.1	Putative transporter protein (Asp-Al_Ex superfamily)		

MS0633	*nrdD*	-	2.0	Anaerobic ribonucleoside-triphosphate reductase		Nucleotide metabolism and transport
MS2216	*dcuB*	-	3.6	Anaerobic C4-dicarboxylate transporter (DcuA DcuB superfamily)		Carbohydrate metabolism and transport
MS1612	*rbsB*	-	2.9	ABC-type sugar transport system, periplasmic component		
MS2066	*lamb*	-	2.5	Maltose-inducible porin	14	
MS2377		-	2.5	Phosphotransferase system, mannose/fructose/N-acetylgalactosamine-specific, component IID	15	
MS2378		-	2.4	Phosphotransferase system, mannose/fructose/N-acetylgalactosamine-specific, component IIC	15	
MS2379		-	2.3	Phosphotransferase system, mannose/fructose/N-acetylgalactosamine-specific, component EIIAB	15	
MS1121	*glgC*	-	2.3	Glucose-1-phosphate adenylyltransferase	10	
MS1877	*dcuB*	-	2.3	Anaerobic C4-dicarboxylate transporter (DcuA DcuB superfamily)		
MS2355	*mipB*	-	2.3	Transaldolase		
MS0616		-	2.1	Phosphotransferase system, mannose/fructose/N-acetylgalactosamine-specific, component IID	8	
MS0618		-	2.1	Phosphotransferase system, mannose/fructose/N-acetylgalactosamine-specific, component IIB	8	
MS0617		-	2.1	Phosphotransferase system, mannose/fructose/N-acetylgalactosamine-specific, component IIC	8	
MS2068	*malE*	-	2.0	ABC-type maltose transport system, maltose-binding periplasmic protein		
MS0639	*rbsB*	-	2.0	ABC-type sugar transport system, periplasmic component		
MS1124	*malQ*	-	2.0	4-alpha-glucanotransferase	10	
MS1006	*bioD*	-	3.4	Dethiobiotin synthetase		Coenzyme metabolism
MS0842	*cof*	-	3.2	Pyridoxyl phosphate phosphatase		
MS0352		-	2.9	Ribosome-associated protein Y		Translation
MS1504	*ompR*	-	2.0	Aerobic respiration control protein ArcA homolog		Transcription
MS1159		-	2.6	Ferrous iron transport protein A (FeoA superfamily)		Inorganic ion transport and metabolism
MS1583	*tbpA*	-	2.6	ABC-type Fe3+ transport system, periplasmic component		
MS1817	*hybA*	-	2.2	Formate-dependent nitrite reductase, 4Fe-4S subunit	13	
MS1158	*feoB*	-	2.2	Fe2+ transport system protein B	11	
MS1818	*nrfB*	-	2.1	Formate-dependent nitrite reductase, penta-heme cytochrome c	13	
MS1816	*nrfD*	-	2.1	Formate-dependent nitrite reductase, membrane component	13	
MS1819	*nrfA*	-	2.0	Formate-dependent nitrite reductase, periplasmic cytochrome c552 subunit	13	
MS0349	*uspA*	-	6.1	Universal stress protein UspA homolog		Signal transduction

[a] Gene entries and names are given in accordance with KEGG annotations for *M. succiniciproducens* MBELE55.
[b] Information are adopted from Hong et al. 2004 and/or NCBI database using BLASTP swissprot (sequence coverage of 50 % and amino acid sequence homologies above 30 %) in combination with annotations from KEGG.
[c] Operons and their corresponding genes were assigned according to the Database of prOkaryotic OpeRons (Dam et al. 2007; Mao et al. 2009) and the Prokaryotic Operon DataBase (Taboada et al. 2012) for *M. succiniciproducens* MBELE55 predictions (see Table 9.5).
[d] Functional grouping was taken from literature (Hong et al. 2004).

Regarding general stress response, several genes showed changes in their expression level. Ribonucleotide reductase (RNR), conserved among most microorganisms and essential for DNA synthesis, was over-expressed in combination with an acid-induced glycyl radical enzyme, which supports RNR function under anaerobic conditions (Buckel and Golding 2006). Moreover, genes encoding enzymes of the qeueosine pathway were found to be up-regulated (Table 5.10). Qeueosine increases the accuracy of translation processes (Urbonavicius et al. 2001). In addition, superoxide dismutase and a *Gro* chaperone were induced, as also observed for acid-stressed *L. lactic* (Sanders et al. 1995). The glutamate/cysteine ligase, involved in glutathione biosynthesis, was increased 2.1-fold, as compared to DD3. Expression of superoxide dismutase and synthesis of glutathione are part of the general stress response (Mager et al. 2000). The strongest transcriptional activation was found for genes contributing to the biosynthesis of cysteine. In addition, a cysteine related ABC amino acid transport system was induced. This could activate glutathione biosynthesis based on the fact that cysteine represents a building block for glutathione. Thus, it may support stress tolerance regarding optimized glutathione accessibility. Glutathione indeed improved succinate production with *M. succiniciproducens* MBELL55E (Hoon et al. 2010), certainly based on the fact that cysteine is known to be an essential compound during *M. succiniciproducens* MBEL55E and *A. succinogenes* cultivation, due to incomplete biosynthetic pathways (Song et al. 2008; McKinlay et al. 2010).

Among the 45 repressed genes in DD3-Suc2, as compared to DD3, were ten operons (Table 9.7), mainly related to transport and carbohydrate conversion. Two candidates (MS1877, MS2216), encoding for anaerobic C4-dicarboxylic acid transporters, were significantly reduced in expression. These genes, belonging to the *DcuA DcuB* superfamily, potentially prevent efflux of produced succinate to adjust to the extracellular stress and thus limit its production. The resulting intracellular accumulation of succinate may be the reason for the observed induction of genes related to proton-pumping to minimize internal pH perturbations. In contrast to *E. coli*, where the *dcu* genes share an operon with aspartase and fumarase, respectively (Six et al. 1994), and are thus physiologically controlled, such a genomic structure could not be found in *B. succiniciproducens*, proving non-proximal transcription of the transporters. A putative permease of the Asp-Al_Ex superfamily showed repression on the transcription level. Recently, a novel succinate transporter was predicted for *C. glutamicum*, exhibiting the same domains as the transporter here and it was characterized to be part of the succinate excretion system (Huhn et al. 2011). Regarding carbohydrate metabolism, PEPCK, the major anaplerotic enzyme towards succinate, was 3-fold repressed in the succinate tolerant mutant DD3-Suc2. The reaction from fumarate towards succinate was obviously repressed on the level of the complete fumarate reductase complex (Table 9.6). Altogether, the whole reductive TCA cycle branch and potential succinate efflux mechanisms were repressed in a concerted manner (Figure 5.21).

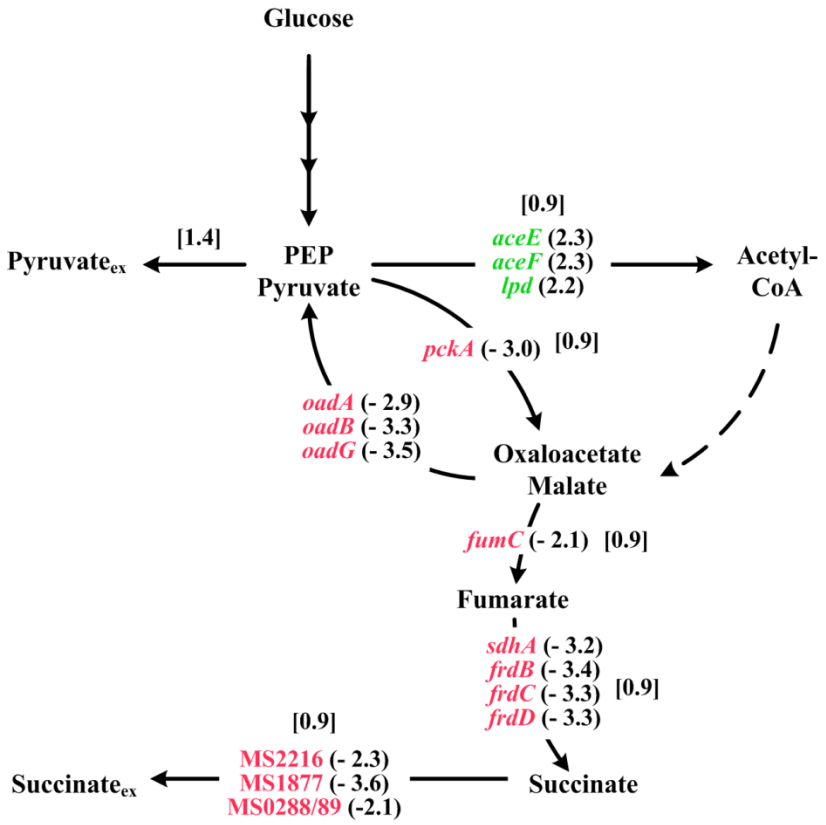

Figure 5.21 *In vivo* flux and gene expression response of *B. succiniciproducens* DD3-Suc2 linked to biosynthetic pathway of succinate as compared to the parental strain DD3. Flux ratios (Table 9.4) are shown in squared brackets. Transcriptional changes (Table 5.10) are shown in curly brackets. Systematic and gene names are allocated to their reactions and indicate up- (green) and down-regulation (red).

Obviously, cells actively down-regulate formation and export of succinate to counteract external succinate stress (Figure 5.21). Moreover, genes encoding for sugar transporters and components of glycogen metabolism were decreased in expression. In addition, the gene encoding for the response regulator *ArcA* was repressed in DD3-Suc2. The regulator *ArcA* is specifically responsible for regulating the intracellular redox system (Malpica et al. 2006). It controls the glucose specific PTS system in *E.coli* (Jeong et al. 2004) and is also responsible for several genes and operons involved in anaerobic metabolism, e.g. the *cydAB* genes coding for a cytochrome:quinol oxidase (Gunsalus and Park 1994). Additionally, this regulator plays an important role in the related succinate producer *M. succiniciproducens*, where it seems to control various genes, e.g. PDH and fumarate reductase (Yun et al. 2012). Interestingly, genes related to glycine betaine/proline transport were repressed in DD3-Suc2, despite their well-known function as osmoprotectants (Arakawa and Timasheff 1985; Bourot et al. 2000).

Table 5.11 Impact of succinate adaptation towards 25 g^{-1} L^{-1} on *B. succiniciproducens* gene expression profile. Data comprise genes up- and down-regulated in DD3-Suc3, as compared to the parental strain DD3 (corrected p-value < 0.05).

Systematic name[a]	Gene[a]	Fold change	Description[b]	Operon number[c]	Function[d]
MS1188		3.2	Phosphoglycerate dehydrogenase		Energy production and conversion
MS0883		2.7	NADH-dependent butanol dehydrogenase A		
MS0760	*fumC*	2.0	Fumarate hydratase		
MS1674	*ftsL*	2.4	Cell division protein FtsL	4	Cell division and chromosome partitioning
MS1676		2.4	Cell division protein MraZ		
MS1673	*ftsI*	2.3	Cell division protein FtsI (peptidoglycan synthesis)	4	
MS1703	*thrA*	4.6	Bifunctional aspartokinase I/homoserine dehydrogenase I	5	Amino acid metabolism and transport
MS1984	*aspA*	4.4	Aspartate ammonia-lyase		
MS1702	*thrB*	2.9	Homoserine kinase	5	
MS1701	*thrC*	2.9	Threonine synthetase	5	
MS1177	*dapD*	2.8	2,3,4,5-tetrahydropyridine-2,6-carboxylate N-succinyltransferase		
MS0924	*metX*	2.8	Homoserine O-acetyltransferase		
MS0045	*ilvC*	2.3	Ketol acid reductoisomerase		
MS0992	*nrdA*	3.0	Ribonucleotide reductase, alpha subunit		Nucleotide metabolism and transport
MS1197	*pykA*	2.6	Pyruvate kinase		Carbohydrate metabolism and transport
MS0967	*glmM*	2.4	Phosphoglucosamine mutase	1	
MS1965	*glpF*	2.3	Aquporin Z (MIP family)		
MS1615	*fbp*	2.1	Fructose 1,6-bisphosphatase		
MS1111	*chb*	2.0	N-acetyl beta hexosaminidase (GH family)		
MS0669	*metK*	5.0	S-adenosylmethionine synthetase		Coenzyme metabolism
MS0503	*hemB*	2.2	Delta-aminolevulinic acid dehydratase		
MS1446		3.1	Ribosome maturation protein RimP	3	Translation
MS1444	*infB*	3.1	Translation initiation factor IF-2	3	
MS1442	*rbfA*	2.7	Ribosome binding factor A	2	
MS2312	*cca*	2.5	tRNA nucleotidyltransferase	7	
MS1441	*truB*	2.4	tRNA pseudouridine synthase B	2	
MS1175	*truA*	2.0	tRNA pseudouridine synthase A		
MS1445	*nusA*	3.7	Transcription termination/antitermination protein		Transcription
MS2131	*araC*	3.2	HTH-type transcriptional activator		
MS1675	*mraW*	2.6	Ribosomal RNA small subunit methyltransferase H	4	
MS1331		2.1	DNA mismatch repair protein		Replication, recombination and repair
MS1565	*mltE*	3.4	Soluble lytic murein transglycosylase		Cell wall, membrane, envelope biogenesis
MS0387		3.2	Phosphoethanolamine transferase		
MS1697		2.8	Opacity family porin protein		
MS1189	*kdsA*	2.6	2-dehydro-3-deoxyphosphooctonate aldolase		
MS0242	*dgkA*	2.3	Diacylglycerol kinase		
MS1670	*mraY*	2.2	Phospho-N-acetylmuramoyl-pentapeptide-transferase	4	
MS0267	*nlpE*	2.1	Outer membrane protein assembly factor		
MS1672	*murE*	2.1	UDP-N-acetylmuramoylalanyl-D-glutamate--2,6-diaminopimelate ligase	4	
MS1671	*murF*	2.1	UDP-N-acetylmuramoyl-tripeptide--D-alanyl-D-alanine ligase	4	
MS1922	*lpxD*	2.1	UDP-3-O-[3-hydroxymyristoyl] glucosamine N-acyltransferase	5	
MS1161		2.0	Opacity family porin protein		
MS1829	*dacC*	2.0	D-alanyl-D-alanine carboxypeptidase		
MS0993	*degQ*	2.9	Periplasmic serine proteases		Molecular chaperons and related functions
MS1923	*hlpA*	2.5	Outer membrane protein, periplasmic chaperone	5	
MS1134	*htpX*	2.4	Protease HtpX		

MS1141	*sseA*		2.7	Sulfurtransferase		
MS1417	*pheA*		2.2	Glutathione-regulated potassium-efflux system, quinone oxidoreductase		Inorganic ion transport and metabolism
MS1959	*arsC*		2.1	Arsenate reductase		
MS1205	*cirA*		2.0	Iron complex outermembrane recepter protein		
MS1131	*tolC*		2.0	Cation efflux system		
MS2229	*rseA*		2.1	Sigma-E factor negative regulatory protein		Signal transduction
MS1823		-	2.7	Glycerol-3-phosphate acyltransferase		
MS1654	*frdC*	-	2.7	Fumarate reductase subunit C	10	
MS1028		-	2.6	Formate dehydrogenase, cytochrome b556 subunit		Energy production and conversion
MS1655	*frdD*	-	2.5	Fumarate reductase subunit D	10	
MS1653	*frdB*	-	2.4	Fumarate reductase, Fe-S protein subunit	10	
MS1105	*leuB*	-	2.2	Tartrate dehydrogenase/decarboxylase		
MS1029	*hybA*	-	2.2	Formate dehydrogenase iron-sulfur subunit		
MS0551	*proX*	-	12.7	ABC-type proline/glycine betaine transport system, substrate binding protein	8	
MS0550	*proW*	-	10.3	ABC-type proline/glycine betaine transport systems, periplasmic components, permease component	8	
MS0549	*proV*	-	8.8	ABC-type proline/glycine betaine transport system, ATPase component	8	
MS0353	*alsT*	-	4.3	Na^+/alanine or glycine symporter		
MS1687	*artM*	-	3.1	ABC-type amino acid transport system, permease	11	
MS0832	*sstT*	-	2.8	Na^+/serine-threonine symporter		Amino acid metabolism and transport
MS1686	*artM*	-	2.6	ABC-type amino acid transport system, permease	11	
MS0815	*pepD*	-	2.4	Aminotripeptidase		
MS1321	*nhaC*	-	2.3	Arginine/ornithine antiporter		
MS1790	*aroQ*	-	2.3	3-dehydroquinate dehydratase II		
MS1685	*glnQ*	-	2.2	ABC-type amino acid transport system, ATPase component	11	
MS0030	*gltS*	-	2.2	Na^+/glutamate symporter		
MS1770	*cysK*	-	2.1	Cysteine synthase		
MS1318	*ilvH*	-	2.1	Acetolactate synthase, small subunit		
MS1253	*cysH*	-	2.0	Phosphoadenosine phosphosulfate reductase		
MS2066		-	6.8	Maltose-inducible porin	17	
MS2068	*malE*	-	4.0	ABC-type maltose transport systems, Maltose-binding periplasmic protein	18	
MS2069	*malF*	-	3.6	ABC-type maltose transport systems, permease	18	
MS2070	*malG*	-	3.5	ABC-type maltose transport systems, permease	18	Carbohydrate metabolism and transport
MS2074	*malQ*	-	3.2	4-alpha-glucanotransferase	19	
MS2073	*glgP*	-	3.0	Glycogen phosphorylase	19	
MS2071	*malS*	-	2.9	Periplasmic alpha-amylase precursor		
MS2067	*malK*	-	2.8	ABC-type maltose transport systems, ATP-binding protein	17	
MS2065		-	2.1	Maltose regulon periplasmic protein		
MS1795	*menF*	-	3.7	Menaquinone specific isochorismate synthase	13	
MS1254	*cysG*	-	3.3	Uroporphyrinogen-III methyltransferase		
MS1794	*menD*	-	3.1	2-succinyl-5-enolpyruvyl-6-hydroxy-3-cyclohexene-1-carboxylate synthase	13	Coenzyme metabolism
MS1824	*folB*	-	2.3	Dihydroneopterin aldolase	16	
MS1793	*mhpC*	-	2.3	2-succinyl-6-hydroxy-2,4-cyclohexadiene-1-carboxylate synthase	13	
MS1821	*rluD*	-	2.4	Pseudouridylate synthases, 23S RNA-specific	15	Translation
MS1476	*rpsA*	-	2.2	small subunit ribosomal protein S1		
MS2116	*lysR*	-	2.7	HTH-type transcriptional activator		Transcription
MS0227	*betT*	-	7.9	Choline-glycine betaine transporter		
MS1333	*spr*	-	3.4	Cell wall-associated hydrolases (invasion-associated proteins)		
MS1808	*artI*	-	3.0	Membrane-bound lytic murein transgycosylase		Cell wall, membrane, envelope biogenesis
MS1220	*ompA*	-	2.6	Outer membrane protein P5		
MS1820	*nrfG*	-	2.1	Outer membrane protein assembly factor		
MS0911	*rfe*	-	2.0	UDP-GlcNAc:undecaprenyl-phosphate GlcNAc-1-phosphate transferase	9	

MS1255	*sbp*	-	5.2	ABC-type sulfate transport system, periplasmic component		
MS1816	*nrfD*	-	4.6	Formate-dependent nitrite reductase, membrane component	14	
MS1817	*hybA*	-	4.6	Formate-dependent nitrite reductase, 4Fe-4S subunit	14	Inorganic ion transport and metabolism
MS1819	*nrfA*	-	4.5	Formate-dependent nitrite reductase, periplasmic cytochrome c552 subunit	14	
MS1818	*nrfB*	-	4.4	Formate-dependent nitrite reductase, penta-heme cytochrome c	14	
MS1801	*nhaA*	-	4.0	Na^+/H^+ antiporter		
MS1805	*cha*	-	2.1	Carbonic anhydrase		
MS1259	*cysU*	-	2.0	ABC-type sulfate transport system, permease		

[a] Gene entries and names are given in accordance with KEGG annotations for *M. succiniciproducens* MBELE55.
[b] Information are adopted from Hong et al. 2004 and/or NCBI database using BLASTP swissprot (sequence coverage of 50 % and amino acid sequence homologies above 30 %) in combination with annotations from KEGG.
[c] Operons and their corresponding genes were assigned according to the Database of prOkaryotic OpeRons (Dam et al. 2007; Mao et al. 2009) and the Prokaryotic Operon DataBase (Taboada et al. 2012) for *M. succiniciproducens* MBELE55 predictions (see Table 9.5).
[d] Functional grouping was taken from literature (Hong et al. 2004).

Next, the gene expression profile of DD3-Suc3 was analyzed to identify transcriptomic changes that were kept throughout the further evolutionary adaptation of DD3-Suc2 and highlight additional changes linked to its superior tolerance. Taken together, 52 genes were induced in DD3-Suc3. Among them were genes related to peptidoglycan and lipid biosynthesis and cell division. Indeed, the adjustment of membrane properties by variation of the lipid composition is widely known to mediate organic acid tolerance in bacteria (Booth 1999; Warnecke and Gill 2005). Regarding the transcription and translation machinery, the gene *nusA* increased about 4-fold in expression. Twelve operons were repressed in DD3-Suc3 as compared to the control DD3. They mostly related to transport of carbohydrates and amino acids (Table 5.11). These expression changes were specific for DD3-Suc3. Obviously, a few genes were similarly expressed in both mutants. In this line, the glycine betaine/proline transporter system was strongly repressed in DD3-Suc3, even though both substances are very well known as osmoprotectants (Arakawa and Timasheff 1985; Bourot et al. 2000). Further conjointly repressed genes comprised the fumarate reductase and the nitrite reductase (Table 5.10 and Table 5.11). Taken together, gene expression analysis of succinate adapted *B. succiniciproducens* strains draw a rather complex picture of the adapted metabolism.

5.3.6 Identification of genomic mutations acquired in *B. succiniciproducens* DD1-Suc1, DD3-Suc2 and DD3-Suc3 during evolutionary adaptation

All strains were sequenced to unravel genomic modifications acquired during adaptation towards high succinate. Significance of occurring mutations was ensured by a sequence coverage > 50 and a variant frequency of 75 %. The sequence analysis of the first isolate revealed two mutations that resulted from evolutionary adaptation towards moderate succinate levels. Both mutations are also present in the

subsequent isolate DD3-Suc2. Interestingly the most tolerant strain DD3-Suc3 did not contain all mutations present in its ancestors. This fact implies that it had evolved independently from the others and at some point during evolution became fitter and outcompeted the other mutants from the population. One can conclude that the mutation in the *pta* gene (MS0998) was the first one accumulating in advance of the mutation in the *pykA* gene (MS1197).

Table 5.12 Single nucleotide polymorphisms (SNP) and deletion – insertion – polymorphisms (DIP) are listed with their respective position specific nucleotide (Nt ex) and amino acid (AA ex) exchange in the succinate adapted strains *B. succiniciproducens* DD3-Suc1, DD3-Suc2 and DD3-Suc3. The wild-type genome was annotated according to the published *M. succiniciproducens* MBEL55E genome (Hong et al. 2004) and served as reference for detection of mutations in the adapted phenotypes.

Strain	An	Nt ex	AA ex	Pm	Gene	Function
DD3-Suc1	MS0998	1996G>A	Val666Ile	SNP	*pta*	Phosphate acetyltransferase
	MS1197	1391G>A	Cys417Tyr	SNP	*pykA*	Pyruvate kinase
DD3-Suc2	MS0998	1996G>A	Val666Ile	SNP	*pta*	Phosphate acetyltransferase
	MS1197	1391G>A	Cys417Tyr	SNP	*pykA*	Pyruvate kinase
	MS1875	62A>G	Glu21Gly	SNP	*acpP*	Acyl-carrier protein
DD3-Suc3	MS0904	1134A>T	-	SNP	N.A.	N.A.
	MS0998	1996G>A	Val666Ile	SNP	*pta*	Phosphate acetyltransferase
	MS1445	432delA	Lys144fs	DIP	*nusA*	Transcription termination/antitermination factor
	MS1494	846A>T	-	SNP	*rfaG*	Lipopolysaccharide glucosyltransferase

Pm: type of occurring polymorphism, N.A.: not assigned.

The deriving evolutionary tree that can be de deduced from the obtained sequencing data, visualized the evolutionary process. The mutation affected genes contribute to energy production and conversion, carbohydrate metabolism and transport, lipid metabolism, transcription, and cell wall, membrane, and envelope biogenesis, respectively (Figure 5.22).

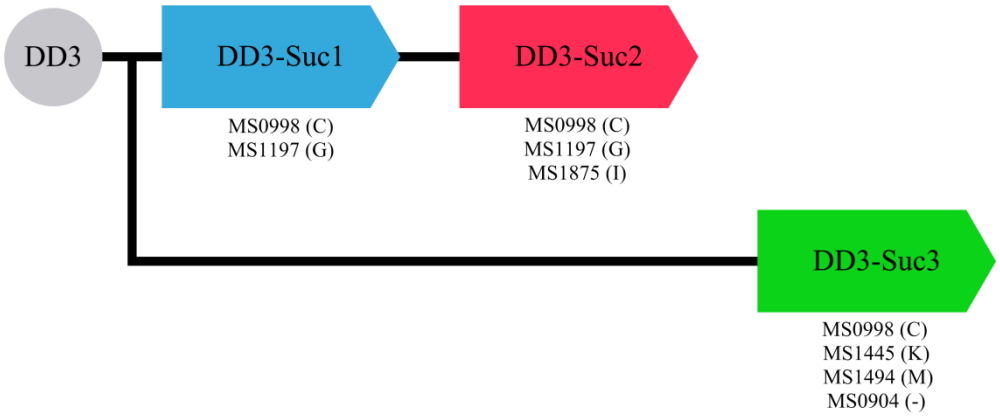

Figure 5.22 Genealogy tree for succinate adaptation of *B. succiniciproducens* DD3 towards 5, 10, and 25 g L^{-1} added succinate, yielding DD3-Suc1, DD3-Suc2 and DD3-Suc, respectively. Systematic name and COG identifier (in brackets) are taken from *M. succiniciproducens* MBEL55E annotation (Hong et al. 2004). For further information on the single modifications see Table 5.12.

Taken together, *B. succiniciproducens* could be successfully adapted to increased succinate levels. The adapted strains could be proven at high succinate levels, not feasible for the initially applied DD3. The characterization of the molecular mechanisms behind the acquired tolerance, by careful growth experiments and system biology approaches, revealed a complex picture. The increased tolerance obviously resulted from concerted reduction of succinate formation, together with beneficial changes in cellular constitutes such as osmoprotectants, and more robustness. With regard to rational improvement of *B. succiniciproducens*, it appeared most relevant to dissect the types of tolerance mechanisms, acquired during the adaptation process. Particularly, mutations that resulted in reduced product formation seemed detrimental regarding industrial performance. Other genetic targets however, promised the possibility to rationally achieve superior tolerant phenotypes.

5.4 Evolutionary adaptation of *B. succiniciproducens* towards lower pH-values

5.4.1 Adaptation of *B. succiniciproducens* towards pH 5.3

A desired low pH that would economize biotechnological succinate production represents a harsh condition for non-acidophilic microorganisms. From the industrial perspective, a low pH reduces the demand for costly acidification during downstream processing and for buffer agents, otherwise needed to maintain the pH at neutral. Overall, production costs for succinate decrease with decreasing cultivation pH (Jansen et al. 2012). *B. succiniciproducens* has its fermentative optimum within a pH range of 7.5 to 6.0 (Figure 5.4) (Scholten et al. 2011). As shown, *B. succiniciproducens* DD3 exhibited a reasonable fermentation performance at pH 6 (Figure 5.4) and produced about 40 g L^{-1} succinate within 55 hours, while completely consuming the supplied glucose. A further decrease of the pH to about 5.5, however, tremendously reduced the performance of DD3. Succinate was only produced up to a titer of 11 g L^{-1}. An initial cultivation of the double mutant DD3 at pH 5.3 did not yield any growth and succinate production so that pH 5.5 could be regarded as critical pH for growth and production performance of *B. succiniciproducens*. According to these findings, pH adaptation started at an initial pH-value of 5.5. In order to maintain and control the pH-value at desired levels, the adaptation was conducted in small scale bioreactors equipped with automatic control of the pH and operated as sequential batches.

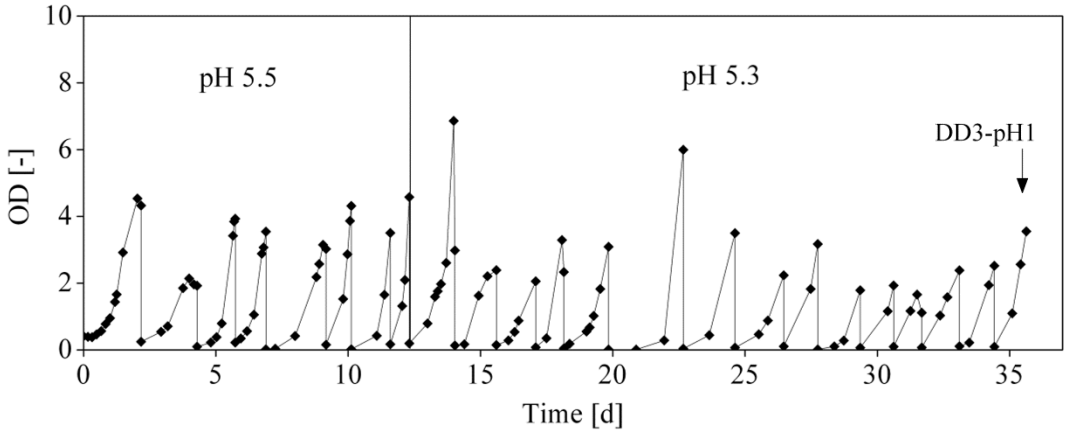

Figure 5.23 Bioreactor based sequential batch adaptation of *B. succiniciproducens* DD3 under non-physiological pH values. The vertical line indicates the switch from the primary critical pH 5.5 to pH 5.3. Once cells have reached sufficient cell concentration, a fraction was harvested and inoculated into the next batch.

The first adaptation rounds showed slow but consistent growth. After about five days and during the third iterative batch, cell density increased faster, indicating an adaptation of the population to the acidic environment. The cells were allowed to further adapt to pH 5.5 before the cultivation pH was decreased to 5.3. Interestingly, the cell growth was not significantly hampered, despite certain lag-

phases at the beginning of each batch. Through further adaptation, the lag-phases shortened and cells grew quickly at pH 5.3. Finally, the heterogenic population was used to isolate the pH-tolerant phenotype DD3-pH1.

5.4.2 Physiology of the pH-tolerant strain *B. succiniciproducens* DD3-pH1

Closer inspection of the growth performance of the isolated strain DD3-pH1 was carried out to describe its superior performance. Bioreactor cultivations were conducted at various pH-values at 37 °C in minimal glucose medium and growth as well as production performance were monitored in comparison to the parent strain DD3 (Table 5.13).

Table 5.13 Fermentation performance of pH-tolerant phenotype *B. succiniciproducens* DD3-pH1 at different pH-values in bioreactor cultivation, as compared to its ancestor DD3. Growth rate (μ) is given for the exponential growth phase. Succinate yield ($Y_{Suc/S}$) and maximal succinate productivity (P_{Suc}) are calculated for the complete 48 h period of cultivation. Product titers for succinate ($\Delta c_{Succinate}$), formate ($\Delta c_{Formate}$), acetate ($\Delta c_{Acetate}$), lactate ($\Delta c_{Lactate}$), ethanol ($\Delta c_{Ethanol}$) and pyruvate $\Delta c_{Pyruvate}$) represent final concentrations after 48 h.

	DD3			**DD3-pH1**			
	pH 6	pH 5.5	pH 5.3	pH 6	pH 5.5	pH 5.2	pH 5.0
μ [h^{-1}]	0.18	0.10	0.02	0.22	0.17	0.09	< 0.01
$Y_{Suc/S}$ [mol mol^{-1}]	0.93	0.86	-	0.99	1.01	0.95	< 0.1
$\Delta c_{Succinate}$ [g L^{-1}]	39.1	10.6	1.0	40.8	21.5	11.5	< 0.1
$\Delta c_{Formate}$ [g L^{-1}]	< 0.1	< 0.1	< 0.1	< 0.1	< 0.1	< 0.1	< 0.1
$\Delta c_{Acetate}$ [g L^{-1}]	2.6	2.1	0.4	1.1	3.8	1.5	< 0.1
$\Delta c_{Pyruvate}$ [g L^{-1}]	0.3	< 0.1	< 0.1	1.2	0.5	< 0.1	< 0.1
$\Delta c_{Ethanol}$ [g L^{-1}]	< 0.1	< 0.1	< 0.1	0.1	< 0.1	< 0.1	< 0.1
$\Delta c_{Lactate}$ [g L^{-1}]	< 0.1	0.2	< 0.1	0.1	0.1	0.1	< 0.1
P_{Suc} [g L^{-1} h^{-1}]	0.8	0.2	< 0.1	1.3	0.5	0.3	< 0.1

At pH 6.0, the evolved strain DD3-pH1 exceeded the performance of DD3 in maximal productivity by about 60 % and in growth rate by about 20 % (Table 5.13). A pH-value of 5.5 reduced growth and succinate production. However, the evolved mutant performed by far better than DD3. This fact indicated the successful adaptation of *B. succiniciproducens* to lower pH-values. At pH 5.2, which partially abolished DD3 proliferation, the adapted phenotype was still able to grow exponentially and produced 11 g L^{-1} succinate. Further decrease to a pH of 5.0, however, was not tolerated by DD3-pH1. The graphical presentation of the resulting growth rates at different pH values clearly reveals the superiority of the evolved strain (Figure 5.24). For all pH-values tested, DD3-pH1 data points were located closer to the area of fast growth and low pH, preferred as industrial settings.

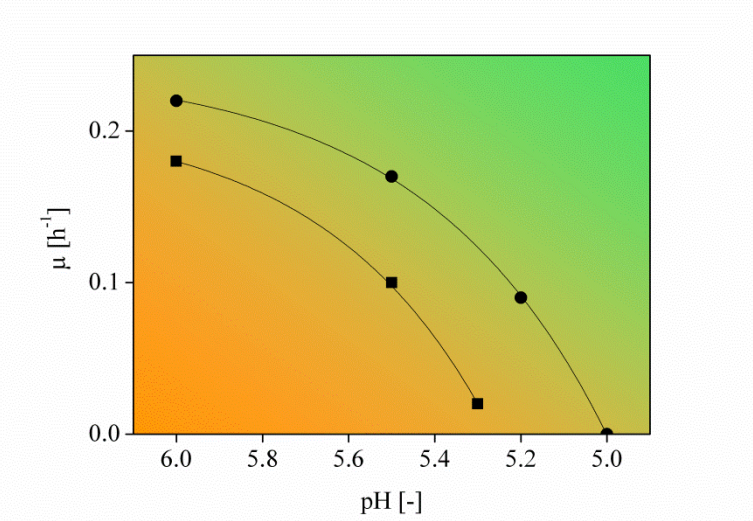

Figure 5.24 The specific growth rate is shown for (■) *B. succiniciproducens* DD3 and (●) DD3-pH1 at different pH-values. Data derive from pH-controlled bioreactor cultivations in minimal glucose medium. The color gradient represents industrially desired (green) and unfavored (orange) characteristics.

5.4.3 Adaptation derived genetic modifications in DD3-pH1

As verified by genome sequencing, *B. succiniciproducens* DD3-pH1 accumulated only two mutations. The affected genes belonged to the functional groups of carbohydrate metabolism and cell wall, membrane, envelope biogenesis. A closer view revealed that the first mutation was located in the pyruvate kinase gene, which had also evolved in the succinate adapted strains. In addition, a gene belonging to the cell wall synthesis apparatus harbored a frame-shift mutation, putatively leading to an incomplete protein.

Table 5.14 Single nucleotide polymorphisms (SNP) and deletion – insertion – polymorphisms (DIP) with their respective position specific nucleotide (Nt ex) and amino acid (AA ex) exchange in the pH adapted strains *B. succiniciproducens* DD3-pH1.

Strain	An	Nt ex	AA ex	Pm	Gene	Function
DD3-pH1	MS1197	640G>T	Gly167Cys	SNP	*pykA*	Pyruvate kinase
	MS1492	80_81insC	Tyr27fs	DIP	*wcaJ*	EpsL like protein

Pm: type of occurring polymorphism.

Overall, the successful pH adaptation of *B. succiniciproducens* yielded the promising new phenotype DD3-pH1. Its superior performance at low pH-values, as compared to its ancestor DD3 (Figure 5.24) showed high potential with regard to industrial applicability. In addition, the small number of evolutionary acquired mutations is a good starting point for rationally engineering towards this phenotype.

5.5 Metabolic engineering of *B. succiniciproducens* exploiting targets identified from evolutionary adaptation

As shown, *B. succiniciproducens* mutants established a narrow set of genetic mutations, which obviously contributed to their improved phenotypes. It now was highly interesting to test candidate genes individually in order to see to which extent they allow a rational improvement of the producing strains. According to obtained sequence data and the knowledge of the physiology and biochemistry of *B. succiniciproducens*, different second-generation mutants were created on basis of producing strains. Vector construction and subsequent transformation of *E. coli* and *B. succiniciproducens* as well as control of integration were applied according to 4.3.

5.5.1 Modification of the pyruvate node at the level of pyruvate kinase

The pyruvate kinase gene *pykA* was mutated independently during the evolutionary adaptation to high succinate levels and to low pH, respectively. This indicated a central role of the metabolic reaction of the encoded enzyme, i.e. the interconversion of PEP to pyruvate. Indeed, a re-direction of carbon fluxes was observed at the pyruvate node in the adapted strains (Figure 5.10, Figure 5.17 and Figure 5.18). The node is relevant for distributing cellular carbon flux between different pathways, i.e. TCA cycle, anaplerosis, gluconeogenesis, anabolism and overflow metabolism and to flexibly adapt the supply of energy and building block to cellular needs (Sauer and Eikmanns 2005). Particularly under anaerobic conditions, the pyruvate node is important for redox-balancing. Different approaches have been attempted to engineer the node by rational strain development (Becker et al. 2013). However, considering the complexity of the interlinked metabolic networks around the node, knockout-studies in *E. coli* showed important effects on glycolysis, PPP and by-product formation (Siddiquee et al. 2004). The genomic sequencing of the adapted strains revealed a nucleotide exchange in the *pykA* gene of DD3-Suc2, replacing cysteine at position 417 by tyrosine. The pH-adapted DD3-pH1 revealed a *pykA* mutation leading to substitution of Gly^{167} to Cys. In order to obtain second generation mutants, the first step of the engineering strategy, deletion of the gene, was attempted, but did not result in positive clones. Then, direct homologue recombination of mutated and native gene was pursued as second strategy, but permanently revealed the parental genotype.

As genetic engineering strategies could not be completed successfully, the study of the effect of the acquired mutations on enzyme kinetics seemed interesting. Regarding the enzyme structure, both modifications were located in proximity to the allosteric and the active site, respectively, when mapped against *G. stearothermophilus* (PDB ID: 2E28 (Suzuki et al. 2008)). This potentially indicated that both, enzyme control and activity were affected. To further study this, experiments were

conducted to investigate the kinetic properties of pyruvate kinase for the wild-type and the mutated variants. The comparative assays were carried out with cell extract from DD3, DD3-Suc2 and DD3-pH1 and with varied concentrations of PEP as substrate.

$$v = \frac{v_{max}[S]}{[S] \cdot \left(1 + \frac{[S]}{K_I}\right) + K_M} \qquad \text{(Equation 2)}$$

A substrate inhibition model described the data well (Equation 2), where [S] is the substrate concentration, K_I represents the dissociation constant for the binding of the inhibitor to the free enzyme, K_M represents the Michaelis constant and v and v_{max} are reaction rate and maximal reaction rate, respectively. Such a behavior seemed consistent with the metabolism of *B. succiniciproducens*, since the primary pathway for PEP runs via the PEPCK. Thus PEP-dependent inhibition of pyruvate kinase seems to be involved in the control of succinate production.

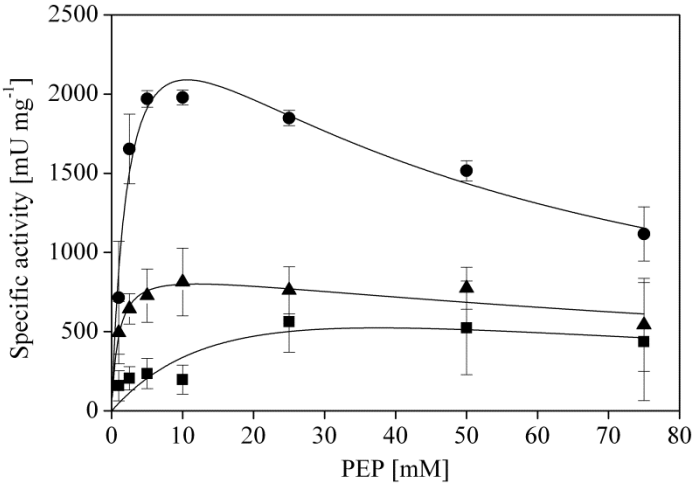

Figure 5.25 Enzyme kinetics of pyruvate kinase. The data points for (●) *B. succiniciproducens* DD3, (■) DD3-Suc2 and (▲) DD3-pH1 represent mean values of three replicates and their corresponding standard deviation. In all cases, higher levels of PEP inhibited the enzyme.

Regarding the obtained characteristics, all three enzyme variants strongly differed from each other in their kinetics (Figure 5.25 and Table 5.16). The wild-type enzyme revealed a theoretical maximum reaction rate of about 3000 mU mg^{-1}, combined with a high substrate affinity. The variant from DD3-Suc2, putatively affected at the allosteric site, exhibited a decrease of the maximal activity by about 60 %. In addition, the K_M-value increased about 8-fold, resulting in significantly less substrate affinity. The pyruvate kinase of DD3-pH1 exhibited a similar K_M-value, as compared to the wild-type enzyme, but its maximal enzyme activity was decreased by 70 %, with a substantially higher K_I-value. Taken together, the mutated enzymes appeared strongly reduced in their *in vivo* activity, which suggested a potential re-direction of flux towards the reductive TCA cycle. Generally, the attenuation and deletion of pyruvate kinase in bacteria resulted in a re-direction of flux at the pyruvate node by stimulating

anaplerotic reactions at the interconversion of PEP and OAA (Emmerling et al. 2002; Becker et al. 2008; Meza et al. 2012). In all cases, the substantially decreased enzyme activity of the mutated variants is assumed to match with the desired changes, so that a positive effect on succinate production can be expected.

Table 5.15 Enzyme kinetics of pyruvate kinase of *B. succiniciproducens* DD3, DD3-Suc2 and DD3-pH1. The values represent modeled data, assuming substrate inhibition kinetics. The underlying assays were conducted as three biological replicates.

Strain	v_{max} [mU mg^{-1}]	K_M [mM]	K_I [mM]
DD3	3041	2.4	46.8
DD3-Suc2	1158	22.7	62.1
DD3-pH1	931	1	147.5

5.5.2 Transcription machinery engineering of *B. succiniciproducens* through overexpression of a mutated *rpoC*

Genomic analysis of adapted *B. succiniciproducens* DD3-T2 revealed a modification in the beta'-subunit of the DNA-directed RNA polymerase, which may contribute to RNA synthesis and DNA interaction (Nedea et al. 1999). Hereby, a nucleotide exchange resulted in the change of Thr^{231} to Lys. This modification locus might affect the global transcription machinery, which has a high potential in strain improvement (Alper and Stephanopoulos 2007). Structural analysis of the identified mutation within the bacterial multisubunit RNA polymerase revealed no obvious contribution to conserved domains (Lane and Darst 2010).

Table 5.16 Growth and production characteristics of *B. succiniciproducens* DD3 pJFF224-XN and DD3 pSUC-1 showing the impact of overexpressing the mutated polymerase subunit encoded by *rpoC*^{T231K} at 37 °C. The data comprise specific growth rate (μ), biomass yield ($Y_{X/S}$), succinate yield ($Y_{Suc/S}$), formate yield ($Y_{For/S}$), acetate yield ($Y_{Ace/S}$), lactate yield ($Y_{Lac/S}$), ethanol yield ($Y_{EtOH/S}$), pyruvate yield ($Y_{Pyr/S}$) and maximal succinate productivity (P_{Suc}). Data represent values from three biological replicates with their corresponding standard deviations in minimal glucose medium, supplemented with 5 mg L^{-1} chlorampehnicol as selection marker.

	DD3 pJFF224-XN	DD3 pSUC-1
μ [h^{-1}]	0.06 ± 0.01	0. 11 ± 0.01
$Y_{X/S}$ [g mol^{-1}]	17.9 ± 1.5	26.3 ± 1.4
$Y_{Suc/S}$ [mol mol^{-1}]	1.19 ± 0.03	1.18 ± 0.07
$Y_{For/S}$ [mol mol^{-1}]	< 0.01	< 0.01
$Y_{Ace/S}$ [mol mol^{-1}]	0.34 ± 0.03	0.15 ± 0.01
$Y_{Lac/S}$ [mol mol^{-1}]	< 0.01	< 0.01
$Y_{EtOH/S}$ [mol mol^{-1}]	< 0.01	< 0.01
$Y_{Pyr/S}$ [mol mol^{-1}]	0.06 ± 0.01	0.18 ± 0.02
P_{Suc} [g L^{-1} h^{-1}]	0.33 ± 0.02	0.56 ± 0.04

Yields were determined during exponential phase by linear fitting of the concentration of biomass and product with that of the substrate.

In order to investigate the effect of this mutated polymerase, the gene was co-expressed in DD3 via a plasmid, yielding DD3 pSUC-1. The constructed plasmid contained the mutated gene under control of the native promoter. The point mutation was validated by sequencing and plasmid carriage was guaranteed by addition of 5 mg L^{-1} chloramphenicol to the medium.

Taken together, the engineered mutant revealed a remarkably improved production performance. In particular, the overexpression yielded a better growth performance with a twofold increased maximal growth rate and an increased succinate production, as compared to the control DD3 pJFF224-XN, carrying the empty vector (Table 5.16). The specific yield for succinate remained at the high level of the parent strain. It was now interesting to test the effect of overexpressing the mutated polymerase subunit for its contribution to temperature tolerance, considering its acquisition during the evolutionary adaptation towards higher temperature. The cultivation of DD3 pSUC-1 at 42 °C revealed improved growth and succinate production, as compared to DD3 pJFF224-XN. It even exceeded the performance of the basic strain DD3 by 30 %, regarding cell concentration and succinate titer, respectively (Figure 5.26). However, cell growth stopped at a maximal concentration equivalent to OD_{600} of about 3, indicating further temperature sensitive parts of the metabolism.

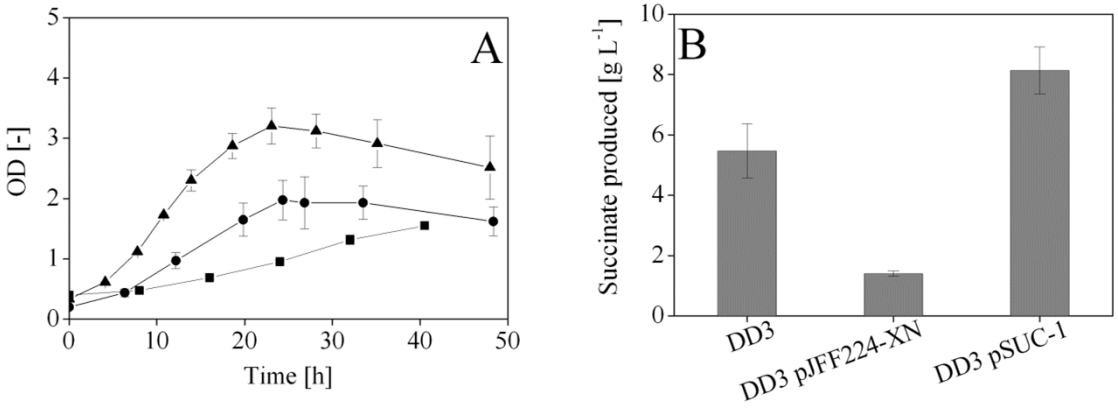

Figure 5.26 Growth physiology of the rationally engineered (▲) *B. succiniciproducens* DD3 pSUC-1 compared to the control strains (●) DD3 and (■) DD3 pJFF224-XN at 42 °C in minimal glucose medium, supplemented with 5 mg L^{-1} chloramphenicol, for retaining the plasmid. Data comprise growth (A) and succinate titer (B) from three biological replicates with corresponding standard deviations.

Obviously, the *rpoC* mutation affected the cellular propagation in a beneficial manner. Its plasmid based introduction into *B. succiniciproducens* DD3 improved growth and production performance at both temperatures, i.e. 37 and 42 °C, respectively, as compared to DD3 pJFF224-XN. First, these observations proved the temperature tolerant phenotype to be very complex, due to the multitude of genes that might be affected by an altered transcription machinery (Alper and Stephanopoulos 2007). Nevertheless, the identified *rpoC* modification could improve the competitiveness of succinate production with *B. succiniciproducens*.

5.5.3 Engineering of cell envelope metabolism through a mutation in a sugar transferase

During high temperature adaptation, *B. succiniciproducens* DD3 acquired a mutation in the *rfe* gene, encoding for the UDP-GlcNAc:undecaprenyl-phosphate GlcNAc-1-phosphate transferase. Rfe is an integral membrane protein with 11 predicted transmembrane helices. Known functions of this gene are associated to outer membrane glycolipid compounds in Gram-negative cells (Lehrer et al. 2007). Sequence analysis located the amino acid exchange Thr^{16} to Pro in the first transmembrane helix, belonging to the presumed functional N-terminal region (Amer and Valvano 2000). However, transmembrane helix prediction (http://www.cbs.dtu.dk/services/TMHMM/) revealed no changes in the structure. In a next step, both, the complete disruption of the *rfe* gene and the site-specific integration of the point mutation, were tested for phenotypic effects within *B. succiniciproducens* by constructing the strains DD3 *Δrfe* and DD3 rfe^{T16P}, respectively.

Table 5.17 Physiology of rationally engineered strains *B. succiniciproducens* DD3 *Δrfe* and DD3 rfe^{T16P} compared to DD3. Data comprise specific growth rate (μ), biomass yield ($Y_{X/S}$), succinate yield ($Y_{Suc/S}$), formate yield ($Y_{For/S}$), acetate yield ($Y_{Ace/S}$), lactate yield ($Y_{Lac/S}$), ethanol yield ($Y_{EtOH/S}$), pyruvate yield ($Y_{Pyr/S}$) and maximal succinate productivity (P_{Suc}). Data represent values from three biological replicates in minimal glucose medium with corresponding standard deviations.

	DD3	**DD3 *Δrfe***	**DD3 rfe^{T16P}**
μ [h^{-1}]	0.16 ± 0.01	0.06 ± 0.01	0. 20 ± 0.01
$Y_{X/S}$ [g mol^{-1}]	29.8 ± 2.5	12 ± 1.1	33.8 ± 2.5
$Y_{Suc/S}$ [mol mol^{-1}]	1.13 ± 0.04	1.1 ± 0.04	1.05 ± 0.07
$Y_{For/S}$ [mol mol^{-1}]	< 0.01	< 0.01	< 0.01
$Y_{Ace/S}$ [mol mol^{-1}]	0.21 ± 0.06	0.23 ± 0.06	0.44 ± 0.03
$Y_{Lac/S}$ [mol mol^{-1}]	< 0.01	< 0.01	< 0.01
$Y_{EtOH/S}$ [mol mol^{-1}]	< 0.01	< 0.01	< 0.01
$Y_{Pyr/S}$ [mol mol^{-1}]	0.16 ± 0.03	< 0.01	0.03 ± 0
P_{Suc} [g L^{-1} h^{-1}]	0.76 ± 0.01	0.31 ± 0.07	0.62 ± 0.02

Yields were determined by linear fitting of the concentration of biomass and product with that of the substrate.

First, deletion of the *rfe* gene in *B. succiniciproducens* DD3 clearly impaired growth and specific biomass formation (Table 5.17), besides it caused a flocculent biomass appearance. Additionally, only 15 g L^{-1} succinate were produced, as compared to 36 g L^{-1} with DD3 after 48 h. Introduction of the evolved gene variant now improved the specific growth rate by 20 %, as compared to the basic strain. However, succinate productivity slightly decreased (Table 5.17). In a next step, DD3 rfe^{T16P} was tested for its temperature tolerance at 42 °C (Figure 5.27). Interestingly, the strain steadily grew throughout a 48 h period to a final cell concentration corresponding to an OD_{600} of 4. Hereby, succinate was produced with a titer of about 9 g L^{-1}. Thus, the second generation mutant exceeded the performance of DD3 in both, growth and succinate production, respectively. This indicates the contribution of *rfe* in temperature adaptation by possibly affecting cell envelope composition as previously discussed for other bacteria (Yuk and Marshall 2003; Koga 2012).

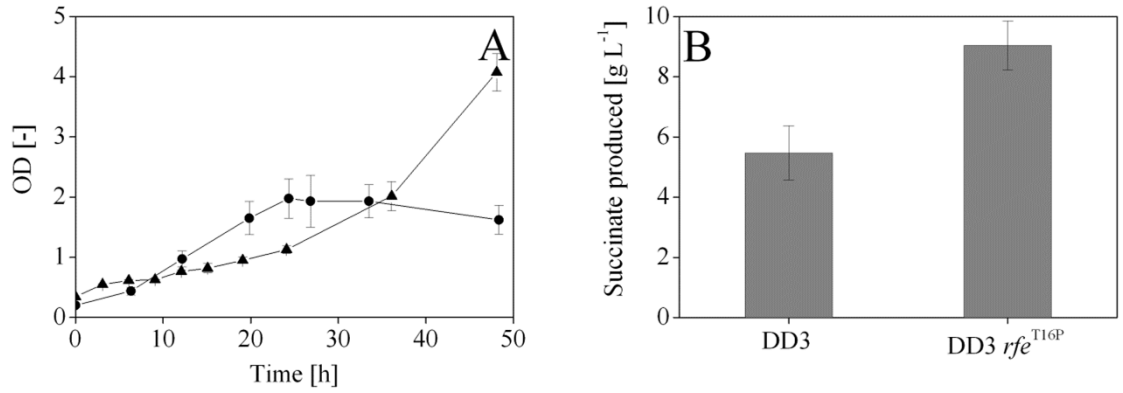

Figure 5.27 Physiologic characterization of second generation mutant (▲) *B. succiniciproducens* DD3 *rfe*^{T16P} compared to its ancestor (●) DD3 at 42 °C in minimal glucose medium. Data comprise growth (A) and succinate titer (B) of a 48 h cultivation period. Data derive from three biological replicates with corresponding standard deviations.

Overall, the introduction of the evolutionary acquired point mutation in *rfe* was proved highly advantageous for *B. succiniciproducens* performance. At both temperatures, 37 and 42 °C, respectively, DD3 *rfe*^{T16P} showed improved growth performance. At high temperature, succinate titer increased by about 65 % as compared to DD3, suggesting further consideration for industrial application.

5.5.4 Improving cellular sedimentation by engineering cell envelope metabolism

Low pH adaptation revealed a mutation in *B. succiniciproducens* DD3-pH1 in the gene *wcaJ* by nucleotide insertion in Tyr^{27}. This led to a frame shift mutation, introducing a stop codon at this very position, thus generating a truncated *wcaJ*-variant. Homology analysis revealed a conserved domain in *wcaJ*, dedicated to a bacterial sugar transferase function, that is supposed to be a part of the *B. subtilis*-like exopolysaccharide synthesis machinery (van Kranenburg et al. 1997; Nagorska et al. 2010). During cultivation of DD3-pH1, significantly faster cell sedimentation was observed with this strain, indicating changes in cellular composition. To verify the functional relationship between this improved and industrially attractive sedimentation performance and the frame shift mutation, DD3 *wcaJ*^{T27fs} was constructed, carrying the genome based modification.

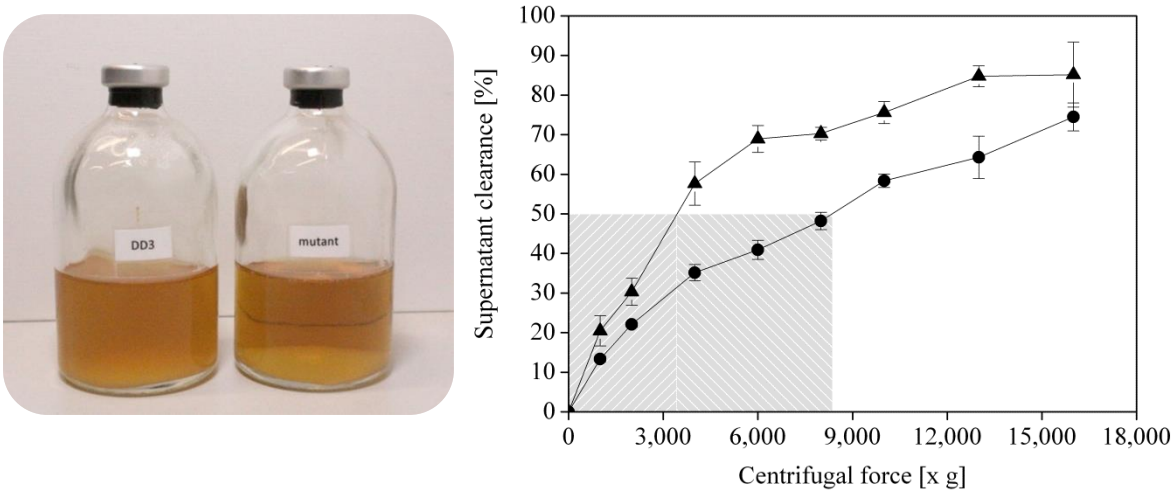

Figure 5.28 Sedimentation behavior of *B. succiniciproducens* DD3 and DD3 *wcaJ*^{T27fs} in complex medium. The picture shows sedimentation of DD3 (left) and DD3 *wcaJ*^{T27fs} (right) after 24 h (A). Data comprise sedimentation kinetics of (●) DD3 and (▲) DD3 *wcaJ*^{T27fs} in BHI medium according to defined centrifugal forces (B). Data points represent mean values of three replicates with standard deviations.

The industrial relevance of sedimentation behavior was then tested in terms of centrifugal cell separation. Therefore, a defined cell density was initially adjusted of cells grown in $MgCO_3$-free complex medium. For each centrifugation step, one milliliter of the cell suspension was pipetted into a 1.5 mL reaction tube. Subsequently, three samples were centrifuged for 30 seconds at defined centrifugal forces. Afterwards, cell concentration of the supernatant was measured photometrically and compared to the initial concentration. In doing so, 50 % supernatant clearance was achieved with DD3 *wcaJ*^{T27fs} at about 3,500 x g, whereas DD3 cell suspension was cleared to 50 % at approximately 8,000 x g (Figure 5.28). Considering energy costs in industrial downstream processing, a major factor in process competitiveness, this modification will decrease overall separation costs and therefore represents a promising target for process improvement.

5.5.5 Metabolic engineering of lysine biosynthesis through expression of modified diaminopimelate decarboxylase

The *lysA* encoded diaminopimelate decarboxylase is the last enzyme in lysine biosynthesis (Gokulan et al. 2003). The enzyme is conserved among all microorganisms and typically occurs as a dimer (Momany et al. 2002; Gokulan et al. 2003). The genome sequencing of *B. succiniciproducens* DD3-T2 revealed a nucleotide exchange in *lysA*. As consequence, the conserved amino acid Gly^{307} was replaced by Cys (Figure 5.29).

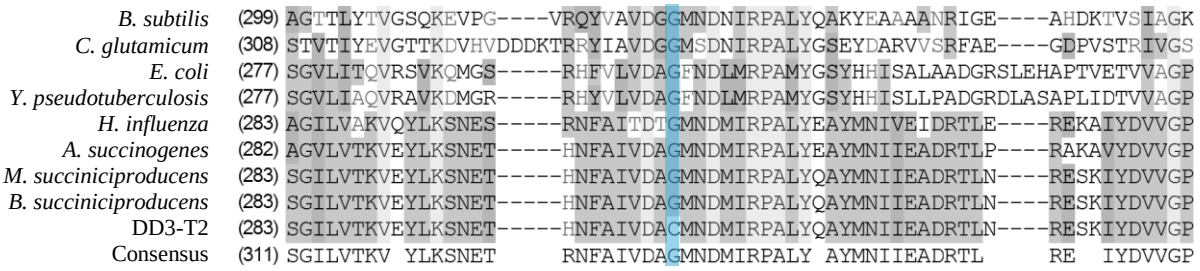

Figure 5.29 The alignment is shown for LysA proteins from different bacteria with the respective consensus sequence. The position of the evolutionary acquired amino acid exchange in *B. succiniciproducens* DD3-T2 is shown in blue, in respect to the aligned sequences.

Initially, the potential impact of lysine biosynthesis on temperature tolerance was analyzed by studying the growth effect of the wild-type by adding lysine to minimal medium. Compared to DD1, grown without external lysine, DD1 supplemented with 3 mM lysine grew to a cell concentration corresponding to OD_{600} of 6 and produced significantly more succinate, as compared to the control (Figure 5.30). Obviously, the lysine pathway is heat-sensitive and thus linked to growth of *B. succiniciproducens* at elevated temperatures.

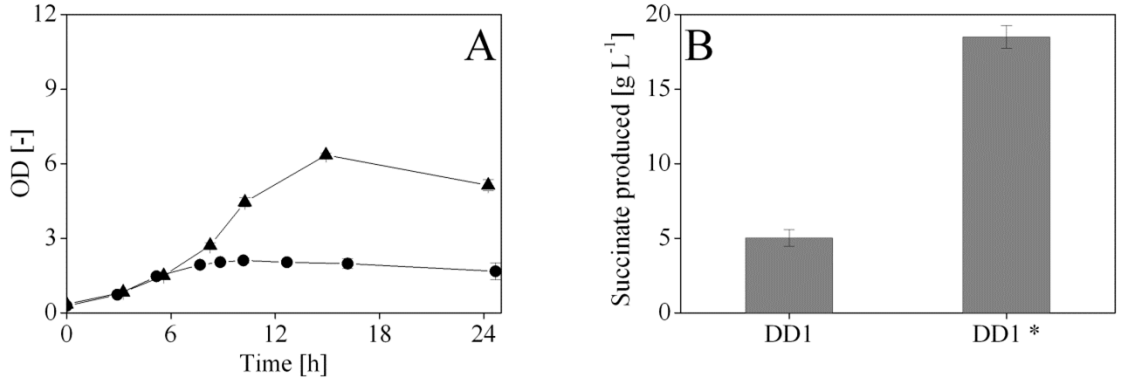

Figure 5.30 Growth and production performance of *B. succiniciproducens* DD1 in minimal glucose medium at 42 °C. Given data comprise the growth of (●) DD1 and (▲) DD1, supplemented with 3 mM lysine (A) and their respective succinate titer after 24 h cultivation period (B). Asterisk indicates lysine supplemented wild-type. Data derive from three biological replicates with corresponding standard deviations.

Regarding the consequence of the mutation on the enzyme, position specific analysis with the *E. coli* homologue revealed an introversive orientation of the modification locus, suggesting an enzyme stabilizing function while excluding dimer specific stabilization (PDB ID: 1KNW (Levdikov et al. 2003)) (Figure 5.31). This is supported by the beneficial growth effect of glycine betaine at high temperature (Table 5.2). In this line, the natural diaminopimelate decarboxylase seemed temperature instable.

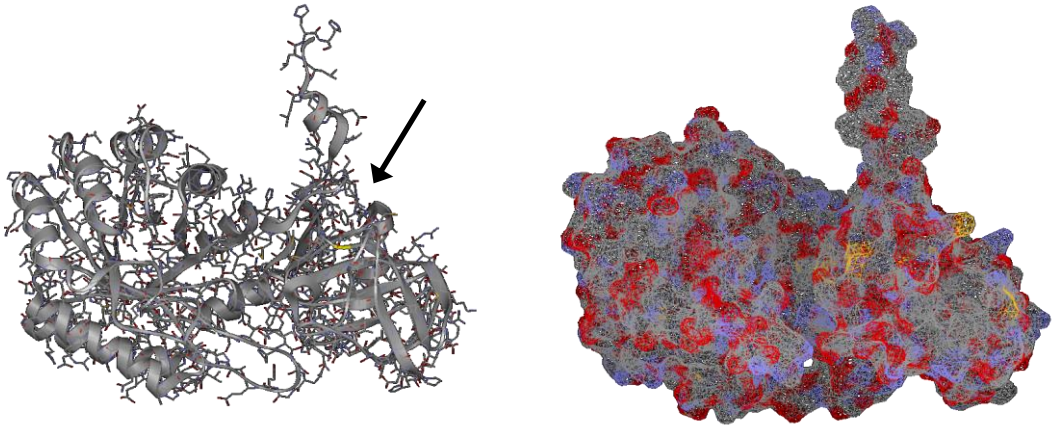

Figure 5.31 Overview of *E. coli* diaminopimelate decarboxylase (PDB ID: 1KNW (Levdikov et al. 2003)). Arrow indicates inward orientation of nucleotide exchange affected amino acid position (yellow) after homology study of *B. succiniciproducens lysA* sequence relative to *E. coli* sequence (left). This is supported by the calculated surface (Conolly method; probe radius 1.399) that reveals no outward orientation of the exchanged amino acid (right). Yellow domains are associated to other sulfur containing amino acids.

Introduction of the obtained modification into the priorly engineered production strain *B. succiniciproducens* DD5 yielded the second generation mutant DD5 *lysA*^{G307C}, which was verified by sequencing of the site-specific PCR product. Cultivation of DD5 *lysA*^{G307C}, in minimal glucose medium at 42 °C, showed stable growth and production performance. The succinate titer increased by nearly 400 % to about 27 g L^{-1} with a significantly improved maximal succinate productivity of 0.8 g L^{-1} h^{-1}, as compared to DD3 (Table 5.18). However, glucose was not completely consumed, in contrast to the temperature tolerant mutant DD3-T2. This indicated further temperature sensitive metabolic burdens. At 37 °C, the engineered strain DD5 *lysA*^{G307C} performed better than DD3 regarding growth and succinate productivity, which increased by about 60 % and 30 %, respectively.

Table 5.18 Growth and production characteristics of *B. succiniciproducens* DD5 *lysA*^{G307C} compared to DD3. Data comprise specific growth rate (μ), biomass yield ($Y_{X/S}$), succinate yield ($Y_{Suc/S}$), formate yield ($Y_{For/S}$), acetate yield ($Y_{Ace/S}$), lactate yield ($Y_{Lac/S}$), ethanol yield ($Y_{EtOH/S}$), pyruvate yield ($Y_{Pyr/S}$) and maximal succinate productivity (P_{Suc}). Data represent values from three biological replicates in minimal glucose medium with their corresponding standard deviations.

	DD3		**DD5 *lysA*^{G307C}**	
	37 °C	42 °C	37 °C	42 °C
μ [h^{-1}]	0.16 ± 0.01	-	0.26 ± 0	0. 25 ± 0
$Y_{X/S}$ [g mol^{-1}]	29.8 ± 2.5	19.2 ± 2.2	34.1 ± 1.9	30.3 ± 1.9
$Y_{Suc/S}$ [mol mol^{-1}]	1.13 ± 0.04	1.08 ± 0.12	1.08 ± 0.01	1.10 ± 0.04
$Y_{For/S}$ [mol mol^{-1}]	< 0.01	< 0.01	< 0.01	< 0.01
$Y_{Ace/S}$ [mol mol^{-1}]	0.21 ± 0.06	0.29 ± 0.02	0.33 ± 0.02	0.41 ± 0.04
$Y_{Lac/S}$ [mol mol^{-1}]	< 0.01	< 0.01	< 0.01	< 0.01
$Y_{EtOH/S}$ [mol mol^{-1}]	< 0.01	< 0.01	< 0.01	< 0.01
$Y_{Pyr/S}$ [mol mol^{-1}]	0.16 ± 0.03	0.11 ± 0.01	0.08 ± 0.01	0.03 ± 0.01
P_{Suc} [g L^{-1} h^{-1}]	0.76 ± 0.01	0.16 ± 0.02	0.97 ± 0.01	0.8 ± 0.05

Yields were determined during exponential phase by linear fitting of the concentration of biomass and product with that of the substrate.

Taken together, introduction of a modified diaminopimelate decarboxylase, carrying an evolutionary acquired point mutation, showed significantly advanced performance of *B. succiniciproducens* at standard and at high temperature, obviously improving industrial potential.

5.5.6 Metabolic engineering of by-product spectrum through expression of a modified phosphate acetyltransferase

During high succinate adaptation, *B. succiniciproducens* acquired a mutation in the *pta* gene, encoding for the phosphate acetyltransferase. Significance of this gene is related to the acetate biosynthetic pathway, which is directly coupled to energy production via ATP formation in *M. succiniciproducens* MBEL55E (Lee et al. 2006). Disruption of this pathway by deletion of the *ackA* gene led to decreased growth performance (Lee et al. 2006) and indicated cellular need for this reaction. To verify the phenotypic effect of the acquired mutation, strain DD1 *Δldh pta*^{V666I} was constructed. Introduction of the point mutation was validated by sequencing of the site-specific PCR product.

Table 5.19 Physiology of *B. succiniciproducens* DD1 and DD1 *Δldh pta*^{V666I}. The data comprise specific growth rate (μ), biomass yield ($Y_{X/S}$), succinate yield ($Y_{Suc/S}$), formate yield ($Y_{For/S}$), acetate yield ($Y_{Ace/S}$), lactate yield ($Y_{Lac/S}$), ethanol yield ($Y_{EtOH/S}$), pyruvate yield ($Y_{Pyr/S}$) and maximal succinate productivity (P_{Suc}). Data represent values from three biological replicates with standard deviation in minimal glucose medium.

	DD1	**DD1 *Δldh pta*^{V666I}**
μ [h^{-1}]	0.29 ± 0.01	0.43 ± 0.01
$Y_{X/S}$ [g mol^{-1}]	35.6 ± 0.2	34.5 ± 1.5
$Y_{Suc/S}$ [mol mol^{-1}]	0.76 ± 0.03	0.72 ± 0.07
$Y_{For/S}$ [mol mol^{-1}]	0.58 ± 0.02	0.15 ± 0.02
$Y_{Ace/S}$ [mol mol^{-1}]	0.57 ± 0.01	0.31 ± 0.02
$Y_{Lac/S}$ [mol mol^{-1}]	0.03 ± 0	< 0.01
$Y_{EtOH/S}$ [mol mol^{-1}]	0.03 ± 0	< 0.01
$Y_{Pyr/S}$ [mol mol^{-1}]	< 0.01	0.04 ± 0.01
P_{Suc} [g L^{-1} h^{-1}]	1.42 ± 0.04	0.78 ± 0.06

Yields were determined during exponential phase by linear fitting of the concentration of biomass and product with that of the substrate.

Obviously, cell growth was positively affected in DD1 *Δldh pta*^{V666I}, as compared to the wild-type DD1. Interestingly, despite similar yields for biomass and succinate, the by-product spectrum changed in DD1 *Δldh pta*^{V666I}. Formate and acetate were formed with about 75 and 50 % decreased yields, respectively, while pyruvate accumulated extracellular. This observation is supported by similar results for acetate and pyruvate yield in high succinate evolved strains DD3-Suc1, DD3-Suc2 and DD3-Suc3 (Table 5.8). This indicates a change in carbon distribution in *B. succiniciproducens* metabolism, since pyruvate was not observed as by-product in the wild-type and other wild-type succinate producing microorganisms (Lee et al. 2002; McKinlay et al. 2005; Becker et al. 2013). Moreover, this emphasizes the inevitability of future engineering rounds regarding further by-

products, especially pyruvate-based substances, as observed with the rationally engineered double mutant DD3 (Becker et al. 2013) and due to the high flexibility of the pyruvate node, observed with all adapted strains. Taken together, the mutation in the *pta* gene seemed to affect the carbon distribution regarding by-product formation in *B. succiniciproducens*, which is a highly relevant fact concerning industrial succinate production. Even though pyruvate filled in for formate and acetate, its higher tolerability, compared to formate and acetate (Lin et al. 2008), gives a promise for future performance and titer improvements.

5.6 Succinate production of evolved strains in industrial glycerol medium

In order to assess the production performance on raw materials, such as glycerol, the adapted strains *B. succiniciproducens* DD3-T2 and DD3-Suc2 were cultivated in a maltose/glycerol based complex medium and compared to their ancestor DD3.

Table 5.20 Production characteristics of *B. succiniciproducens* DD3 and the evolved phenotypes DD3-T2 and DD3-Suc2 in complex glycerol medium. Data comprise specific cell growth (μ), consumption of glycerol and maltose, formation of succinate, acetate, pyruvate, lactate and formate, maximal succinate productivity (P_{Suc}) and specific succinate yield ($Y_{Suc/S}$). Data represent mean values of three biological replicates with corresponding standard deviations.

	DD3	**DD3-T2**	**DD3-Suc2**
μ_{max}	0.22 ± 0.01	0. 29 ± 0.01	0.32 ± 0.01
$\Delta c_{Glycerol}$ [g L^{-1}]	15.0 ± 0.6	47.1 ± 0.8	27.0 ± 0.6
$\Delta c_{Maltose}$ [g L^{-1}]	16.0 ± 0	20 ± 0	17.2 ± 0.1
$\Delta c_{Succinatel}$ [g L^{-1}]	27.2 ± 1.1	74.3 ± 3.0	44.1 ± 2.1
$\Delta c_{Acetate}$ [g L^{-1}]	1.7 ± 0.2	1.6 ± 1.4	1.8 ± 0.2
$\Delta c_{Pyruvate}$ [g L^{-1}]	0.4 ± 0.1	0.2 ± 0	0.6 ± 0.1
$\Delta c_{Lactate}$ [g L^{-1}]	< 0.1	1.0 ± 0.2	0.1 ± 0
$\Delta c_{Formate}$ [g L^{-1}]	< 0.1	< 0.1	< 0.1
P_{Suc} [g L^{-1} h^{-1}]	1.07 ± 0.13	2.94 ± 0.26	1.82 ± 0.09
$Y_{Suc/S}$ [Cmol $Cmol^{-1}$]	0.92 ± 0.06	1.13 ± 0.04	0.99 ± 0.05

Cmol yield was determined during exponential phase by linear fitting of the C molar concentration of product with that of the substrates.

The two adapted strains showed improved growth rates (Table 5.20). During 24 h, DD3-T2 nearly completely consumed the provided glycerol, accompanied by complete maltose consumption and produced about 75 g L^{-1} succinate, three times more than DD3.

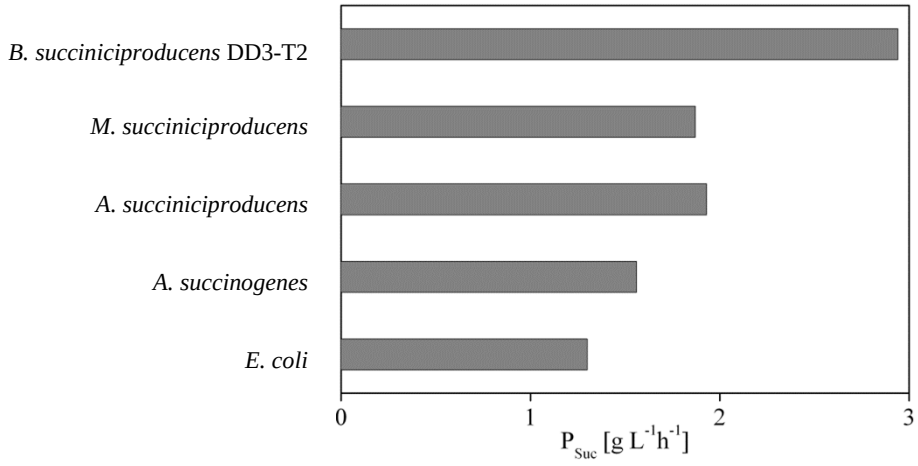

Figure 5.32 Maximal succinate productivity of *B. succiniciproducens* DD3-T2 (Table 5.20) as compared to other succinate producers. Reviewed data (Beauprez et al. 2010) comprise *M. succiniciproducens* (Lee et al. 2002), *A. succiniciproducens* (Glassner and Datta 1992), *A. succinogenes* (Guettler 1998) and *E. coli* (Andersson et al. 2007). Cultivations were conducted as anaerobic or dual-phase batches with complex medium.

The succinate productivity was increased about 2.5-fold, as compared to the ancestor strain DD3 (Table 5.20). Compared to other industrial succinate producers, the performance of DD3-T2 exceeds that of conventional batch fermentations (Figure 5.32). Furthermore, the observed productivity matches the industrial prerequisite of about 2.5 $g\,L^{-1}\,h^{-1}$ (Werpy and Peterson 2004). Thus, evolutionary adaptation and the derived mutant *B. succiniciproducens* DD3-T2 enabled superior bio-succinate production and displayed a mile-stone towards industrial production of this high-value chemical.

6 Conclusion and Outlook

The present work dealt with the systematic evolutionary adaptation of succinate producing *B. succiniciproducens* towards an improved industrial process for this top-value chemical. Initially, the approach comprised the establishment of a sequential batch culture, developed for serum bottles and small scale bioreactors, to specifically adapt the microorganism to industrial parameters, i.e. high temperature, high succinate levels and low pH. The analysis of successfully evolved phenotypes recruited comparative cultivation experiments and in-depth omics profiling to shed light on metabolic responses, underpinning the evolutionary adaptation. Hereby, only few acquired mutations seemed to be involved in the significant expansion of *B. succiniciproducens* tolerance, i.e. the derived mutants DD3-T2, DD3-Suc3 and DD3-pH1 could grow at 42 °C, 25 g L^{-1} succinate and a pH-value of 5.2, respectively, far beyond the values tolerated by the wild-type. Targets could be identified, suitable for eventual optimization strategies regarding tolerance and performance improvements. Finally, studying the effect of introducing identified targets into producing strains revealed faster growth, higher productivity, increased tolerance and simplified biomass separation. Hence, this work contributes to the realization of a bio-economical succinate process, enabling future opportunities towards competitive and sustainable succinate production.

In context with such industry scale succinate production, process requirements emerge, previously reviewed in different reports (Werpy and Peterson 2004; Patel et al. 2006; Bastidon 2012). Hereby, the industry has to contemplate on technological progress to accomplish several key challenges, i.e. (i) to achieve high productivities, ideally exceeding the benchmark of 2.5 g L^{-1} h^{-1}, (ii) to reduce unfavored by-products, (iii) to increase titers above 100 g L^{-1}, (iv) to develop low-cost media in combination with robust and unpretentious production strains, (v) to optimize directly affiliated recovery processes, and (vi) to overall reduce production costs to 0.55 $ kg^{-1} (Patel et al. 2006). In addition, broadening and improving the substrate conversion to the desired product displays one of the most attractive and crucial fields of work. There is a continuing quest for new, renewable and sustainable feedstocks, regarding procurement costs, applicability and efficiency. Non-food substrates, such as hemicellulose or glycerol are widely abundant in industry, mainly as waste products, and were recently studied in combination with succinate producing microorganisms for performance validation (Lee et al. 2003; Kim et al. 2004; Blankschien et al. 2010; Borges and Pereira Jr 2011; Liu et al. 2012). Taking this into account, future metabolic engineering approaches may also comprise further questions that emerged from systems biology studies in this work, i.e. validation of increased flux towards the pentose phosphate pathway as well as through the pyruvate dehydrogenase complex, functional verification of succinate secretion pathways or energy/redox balancing. Additional approaches may comprise an increase in succinate production efficiency by applying strategies, recently reported for lysine and diaminopentane production with *C. glutamicum* (Becker et al. 2011; Kind and Wittmann 2011). A carefully reflected combination of functional targets discovered in this work could be a promising task

for future work. Therefore, establishing a straight-forward genetic tool box, facilitating fast, simple and valid genetic engineering, would substantially improve rational engineering approaches with *B. succiniciproducens*.

The excellent production properties of *B. succiniciproducens*, the recent establishment of systems biological methods for in depth metabolic analysis and the successful demonstration of directed evolutionary adaptation, coupled with targeted strain improvements, make this organism an outstanding candidate for a future succinate bioprocess. Regarding the large variety of succinate application in the downstream market, rational engineering of *B. succiniciproducens* towards other promising non-natural reaction products that are chemically described, such as 1,4-butanediol or succinate esters (Cukalovic and Stevens 2008), seems rather promising. It might also be relevant to consider succinate precursors as valuable products, such as malate, fumarate, and pyruvate and in this line, directly derived amino acids. Taken together, *B. succiniciproducens* could thrive as a high-value cell factory. The understanding of its metabolic behavior, enabled by systems biology, combined with rational strategies of metabolic engineering will extend the production spectrum. This integrated approach may lead to a further mainstay in the new bioeconomy.

7 Abbreviations and Symbols

Abbreviations

aceEF	genes, encoding pyruvate dehydrogenase in *B. succiniciproducens*
ATP	adenosine triphosphate
AUC	area under curve
BHI	brain heart infusion
bp	base pair(s)
BSA	bovine serum albumin
C4	metabolite containing four carbon atoms
Cm	chloramphenicol
Cm^R	chloramphenicol resistence
COG	clusters of orthologous groups
Cys	cysteine
DD1	*B. succiniciproducens* wild-type
DD3	*B. succiniciproducens* Δ*ldh* Δ*pflD*
DD3-pH1	low pH evolved phenotype, isolated after 22 iterations
DD3-Suc1	high succinate evolved phenotype, isolated after 3 iterations
DD3-Suc2	high succinate evolved phenotype, isolated after 15 iterations
DD3-Suc3	high succinate evolved phenotype, isolated after 50 iterations
DD3-T1	high temperature evolved phenotype, isolated after 10 iterations
DD3-T2	high temperature evolved phenotype, isolated after 60 iterations
DD5	*B. succiniciproducens* Δ*ldh* Δ*pflA*
DIP	deletion – insertion – polymorphism
DNA	deoxyribonucleic acid
F6P	fructose 6-phosphate
FC	fold change
FDR	false discovery rate
fumC	gene, encoding fumarase in *B. succiniciproducens*
G6P	glucose 6-phosphate
GAP	glyceraldehyde 3-phosphate
GC	gas chromatography
GC-MS	gas chromatography-mass spectrometry
Glc	glucose
Gly	glycine
GSEA	gene set enrichment analysis
HPLC	high-performance liquid chromatography
Ile	isoleucine
int	integrative
KEGG	Kyoto Encyclopedia of Genes and Genomes
Kb	kilo base pairs
LB	Luria Bertani
ldhA	gene, encoding lactate dehydrogenase in *B. succiniciproducens*
Lys	lysine
lysA	gene, encoding diaminopimelate decarboxylase in *B. succiniciproducens*
MBDSTFA	N-methyl-N-tert-butyldimethylsilyl-trifluoroacetamide

MCS	multiple cloning site
MFA	metabolic flux analysis
MOPS	3-(N-morpholino)propanesulfonic acid
NAD(P)	nicotinamide adenine dinucleotide (phosphate), oxidized
NAD(P)H	nicotinamide adenine dinucleotide (phosphate), reduced
NES	normalized enrichment score
NOM p-val	normalized p-value
OAA	oxaloacetate
OD_{600}	optical density (λ = 600 nm)
OPA	ortho-phthaldialdehyde
ORI	origin of replication
P_{aceE}	promoter of pyruvate dehydrogenase subunit E1 in *B. succiniciproducens*
P_{ptsG}	promoter of trehalose (maltose)-specific transporter subunit IIBC of PTS in *B. succiniciproducens*
PA	polyamine
PBS	polybutylene succinate
PCR	polymerase chain reaction
PDB ID	protein database identifier
PDH	pyruvate dehydrogenase
PES	polyethylene succinate
PEP	phosphoenolpyruvate
PEP/Pyr	lumped pool of phosphoenolpyruvate and pyruvate
PEPCK	PEP-carboxykinase
pflA	gene, encoding formate C-acetyltransferase activator in *B. succiniciproducens*
pflD	gene, encoding formate C-acetyltransferase in *B. succiniciproducens*
PPP	pentose phosphate pathway
Pro	proline
pta	gene, encoding phosphate aetyltransferase in *B. succiniciproducens*
pykA	gene, encoding pyruvate kinase in *B. succiniciproducens*
Pyr	pyruvate
RIN	RNA integrity number
RNA	ribonucleic acid
rfe	gene, encoding UDP-GlcNAc:undecaprenyl-phosphate GlcNAc-1-phosphate transferase in *B. succiniciproducens*
rpm	rounds per minute
rpoC	gene, encoding beta'-subunit of the DNA-directed RNA polymerase in *B. succiniciproducens*
sacB	gene, encoding levansucrase in *B. subtilis*
SAP	shrimp alkaline phosphatase
SIM	selective ion monitoring
SNP	single nucleotide polymorphism
SOB	super optimal broth
SOC	super optimal broth with catabolite repression
TAE	buffer consisting of Tris, EDTA and acetic acid
TCA	tricarboxylic acid
Thr	threonine
TRIS	tris(hydroxymethyl)aminomethane)
Tyr	tyrosine
Val	valine

wcaJ	gene, encoding predicted colanic acid biosynthsis UDP-glucose lipid carrier transferase in *B. succiniciproducens*
wt	wild type

Symbols

μ	specific growth rate	[h^{-1}]
q_{Glc}	specific glucose uptake rate	[mmol g^{-1} h^{-1}]
t	time	[h] or [d]
T	temperature	[°C]
U	unit	[µmol min^{-1}]
P_{Suc}	maximal succinate productivity	[g L^{-1} h^{-1}]
$Y_{Ace/S}$	specific acetate yield	[mol mol^{-1}]
$Y_{EtOH/S}$	specific ethanol yield	[mol mol^{-1}]
$Y_{For/S}$	specific formate yield	[mol mol^{-1}]
$Y_{Lac/S}$	specific lactate yield	[mol mol^{-1}]
$Y_{Pyr/S}$	specific pyruvate yield	[mol mol^{-1}]
$Y_{Suc/S}$	specific succinate yield	[mol mol^{-1}]
$Y_{X/S}$	specific biomass yield	[g mol^{-1}]

8 References

Agricola, G. 1955. "De Natura Fossilium" (Textbook of Mineralogy). Translated. The Geological Society of America.

Ajinomoto. 2007. “Environmental Research and Technology Development”. Ajinomoto.

Alper, H., and G. Stephanopoulos. 2007. “Global Transcription Machinery Engineering: a New Approach for Improving Cellular Phenotype.” *Metabolic Engineering* 9 (3): 258–67.

Amber Artisans. 2013. “Baltic Amber – Alternative Medicine.”

Amer, A.O., and M.A. Valvano. 2000. “The N-Terminal Region of the *Escherichia Coli* WecA (Rfe) Protein, Containing Three Predicted Transmembrane Helices, Is Required for Function but Not for Membrane Insertion.” *Journal of Bacteriology* 182 (2): 498–503.

Andersson, C., J. Helmerius, D. Hodge, K.A. Berglund, and U. Rova. 2009. “Inhibition of Succinic Acid Production in Metabolically Engineered *Escherichia coli* by Neutralizing Agent, Organic Acids, and Osmolarity.” *Biotechnology Progress* 25 (1): 116–23.

Andersson, C., D. Hodge, K.A. Berglund, and U. Rova. 2007. “Effect of Different Carbon Sources on the Production of Succinic Acid Using Metabolically Engineered *Escherichia coli*.” *Biotechnology Progress* 23 (2): 381–88.

Arakawa, T., and S.N. Timasheff. 1985. “The Stabilization of Proteins by Osmolytes.” *Biophysical Journal* 47 (3): 411–14.

Barrick, J.E., D.S. Yu, S.H. Yoon, H. Jeong, T.K. Oh, D. Schneider, R.E. Lenski, and J.F. Kim. 2009. “Genome Evolution and Adaptation in a Long-Term Experiment with *Escherichia coli*.” *Nature* 461 (7268): 1243–47.

BASF SE, and CSM. 2012. “BASF and CSM Establish 50-50 Joint Venture for Biobased Succinic Acid.” BASF SE.

Bastidon, A.I. 2012. “Biosuccinic Acid.”

Beauprez, J.J., M. De Mey, and W.K. Soetaert. 2010. “Microbial Succinic Acid Production: Natural Versus Metabolic Engineered Producers.” *Process Biochemistry* 45 (7): 1103–14.

Bechthold, I., K. Bretz, S. Kabasci, R. Kopitzky, and A. Springer. 2008. “Succinic Acid: A New Platform Chemical for Biobased Polymers from Renewable Resources.” *Chemical Engineering & Technology* 31 (5): 647–54.

Becker, J., S. Kind, and C. Wittmann. 2012. “Systems Metabolic Engineering of *Corynebacterium glutamicum* for Biobased Production of Chemicals, Materials and Fuels.” In *Systems Metabolic Engineering*, edited by Christoph Wittmann and Sang Yup Lee, 152–92. Springer.

Becker, J., C. Klopprogge, A. Herold, O. Zelder, C.J. Bolten, and C. Wittmann. 2007. “Metabolic Flux Engineering of L-Lysine Production in *Corynebacterium glutamicum* - Overexpression and Modification of G6P Dehydrogenase.” *Journal of Biotechnology* 132 (2): 99–109.

Becker, J., C. Klopprogge, and C. Wittmann. 2008. “Metabolic Responses to Pyruvate Kinase Deletion in Lysine Producing *Corynebacterium glutamicum*.” *Microbial Cell Factories* 7 (8): 1–15.

Becker, J., J. Reinefeld, R. Stellmacher, R. Schäfer, A. Lange, H. Meyer, M. Lalk, et al. 2013. “Systems-Wide Analysis and Engineering of Metabolic Pathway Fluxes in Bio-Succinate Producing *Basfia succiniciproducens*.” *Biotechnology and Bioengineering* 110 (11): 3013–23.

Becker, J., O. Zelder, S. Häfner, H. Schröder, and C. Wittmann. 2011. “From Zero to Hero--Design-Based Systems Metabolic Engineering of *Corynebacterium glutamicum* for L-Lysine Production.” *Metabolic Engineering* 13 (2): 159–68.

BioAmber. 2011. “BioAmber Partners with Mitsubishi Chemical in Succinic Acid.” BioAmber.

Blaby, I.K., B.J. Lyons, E. Wroclawska-Hughes, G.C.F. Phillips, T.P. Pyle, S.G. Chamberlin, S.A. Benner, T.J. Lyons, V. de Crécy-Lagard, and E. de Crécy. 2012. “Experimental Evolution of a Facultative Thermophile from a Mesophilic Ancestor.” *Applied and Environmental Microbiology* 78 (1): 144–55.

Blankschien, M.D., J.M. Clomburg, and R. Gonzalez. 2010. “Metabolic Engineering of *Escherichia coli* for the Production of Succinate from Glycerol.” *Metabolic Engineering* 12 (5): 409–19.

Bochner, B.R. 2009. “Global Phenotypic Characterization of Bacteria.” *FEMS Microbiology Reviews* 33 (1): 191–205.

Bolten, C.J., P. Kiefer, F. Letisse, J.-C. Portais, and C. Wittmann. 2007. “Sampling for Metabolome Analysis of Microorganisms.” *Analytical Chemistry* 79 (10): 3843–49.

Booth, I.R. 1985. “Regulation of Cytoplasmic pH in Bacteria.” *Microbiological Reviews* 49 (4): 359–78.

Booth, I.R. 1999. “The Regulation of Intracellular pH in Bacteria.” In *Novartis Foundation Symposium 221 - Bacterial Responses to pH*, edited by Derek J. Chadwick and Gail Cardew, 19–37. Wiley Online Library.

Borges, E.R., and N. Pereira Jr. 2011. “Succinic Acid Production from Sugarcane Bagasse Hemicellulose Hydrolysate by *Actinobacillus succinogenes*.” *Journal of Industrial Microbiology & Biotechnology* 38 (8): 1001–11.

Bourot, S., O. Sire, A. Trautwetter, T. Touzé, L.F. Wu, C. Blanco, and T. Bernard. 2000. “Glycine Betaine-Assisted Protein Folding in a *lysA* Mutant of *Escherichia coli*.” *The Journal of Biological Chemistry* 275 (2): 1050–56.

Brill, J., T. Hoffmann, M. Bleisteiner, and E. Bremer. 2011. “Osmotically Controlled Synthesis of the Compatible Solute Proline Is Critical for Cellular Defense of *Bacillus subtilis* Against High Osmolarity.” *Journal of Bacteriology* 193 (19): 5335–46.

Buckel, W., and B.T. Golding. 2006. “Radical Enzymes in Anaerobes.” *Annual Review of Microbiology* 60: 27–49.

Bunch, P.K., F. Mat-Jan, N. Lee, and D.P. Clark. 1997. “The *ldhA* Gene Encoding the Fermentatove Lactate Dehydrogenase of *Escherichia coli*.” *Microbiology* 143: 187–95.

Buschke, N., R. Schäfer, J. Becker, and C. Wittmann. 2013. “Metabolic Engineering of Industrial Platform Microorganisms for Biorefinery Applications - Optimization of Substrate Spectrum and Process Robustness by Rational and Evolutive Strategies.” *Bioresource Technology* 135: 544–54.

Caldas, T., N. Demont-Caulet, A. Ghazi, and G. Richarme. 1999. “Thermoprotection by Glycine Betaine and Choline.” *Microbiology* 145: 2543–48.

Chan, S., S. Kanchanatawee, and K. Jantama. 2011. “Production of Succinic Acid from Sucrose and Sugarcane Molasses by Metabolically Engineered *Escherichia coli*.” *Bioresource Technology* 103 (1): 329-36.

Cheng, K.-K., X.-B. Zhao, J. Zeng, R.-C. Wu, Y.-Z. Xu, D.-H. Liu, and J.-A. Zhang. 2012. “Downstream Processing of Biotechnological Produced Succinic Acid.” *Applied Microbiology and Biotechnology* 95 (4): 841–50.

Cherubini, F. 2010. “The Biorefinery Concept: Using Biomass Instead of Oil for Producing Energy and Chemicals.” *Energy Conversion and Management* 51 (7): 1412–21.

Clarke, A. 2003. “Costs and Consequences of Evolutionary Temperature Adaptation.” *Trends in Ecology & Evolution* 18 (11): 573–81.

Cox, S.J., S. Shalel Levanon, A. Sanchez, H. Lin, B. Peercy, G.N. Bennett, and K.-Y. San. 2006. “Development of a Metabolic Network Design and Optimization Framework Incorporating Implementation Constraints: a Succinate Production Case Study.” *Metabolic Engineering* 8 (1): 46–57.

Cukalovic, A., and C. V Stevens. 2008. “Feasibility of Production Methods for Succinic Acid Derivatives: a Marriage of Renewable Resources and Chemical Technology.” *Biofuels, Bioproducts & Boprefining* 2: 505–29.

Dam, P., V. Olman, K. Harris, Z. Su, and Y. Xu. 2007. “Operon Prediction Using Both Genome-Specific and General Genomic Information.” *Nucleic Acids Research* 35 (1): 288–98.

Emmerling, M., M. Dauner, A. Ponti, J. Fiaux, M. Hochuli, T. Szyperski, K. Wüthrich, E.J. Bailey, and U. Sauer. 2002. “Metabolic Flux Responses to Pyruvate Kinase Knockout in *Escherichia coli*.” *Journal of Bacteriology* 184 (1): 152–64.

Fang, X., J. Li, X. Zheng, Y. Xi, K. Chen, P. Wei, P.-K. Ouyang, and M. Jiang. 2011. “Influence of Osmotic Stress on Fermentative Production of Succinic Acid by *Actinobacillus succinogenes*.” *Applied Biochemistry and Biotechnology* 165 (1): 138–47.

Feng, X., L. Page, J. Rubens, L. Chircus, P. Colletti, H.B. Pakrasi, and Y.J. Tang. 2010. “Bridging the Gap Between Fluxomics and Industrial Biotechnology.” *Journal of Biomedicine & Biotechnology:* 1-13.

Fong, S.S., A.R. Joyce, and B.Ø. Palsson. 2005. "Parallel Adaptive Evolution Cultures of *Escherichia coli* Lead to Convergent Growth Phenotypes with Different Gene Expression States." *Genome Research* 15 (858): 1365–72.

Frederick R. Blattner, G. Plunkett III, C.A. Bloch, N.T. Perna, V. Burland, M. Riley, J. Collade-Vides, et al. 1997. "The Complete Genome Sequence of *Escherichia coli* K-12." *Science* 277 (5331): 1453–62.

Frey, J. 1992. "Construction of a Broad Host Range Shuttle Vector for Gene Cloning and Expression in *Actinobacillus pleuropneumoniae* and Other *Pasteurellaceae*." *Research in Microbiology* 143: 263–69.

Frings, E., H.J. Kunte, and E.A. Galinski. 1993. "Compatible Solutes in Representatives of the Genera *Brevibacterium* and *Corynebacterium* : Occurrence of Tetrahydropyrimidines and Glutamine." *FEMS Microbiology Letters* 109: 25–32.

Fujimaki, T. 1998. "Processability and Properties of Aliphatic Polyesters , ' BIONOLLE ', Synthesized by Polycondensation Reaction." *Biodegradable Polymers and Macromolecules* 59 (1-3): 209–14.

Glassner, D.A., and R. Datta. 1992. "Process for the Production and Purfication of Succinic Acid." US 5143834.

Gokulan, K., B. Rupp, M.S. Pavelka, W.R. Jacobs, and J.C. Sacchettini. 2003. "Crystal Structure of *Mycobacterium tuberculosis* Diaminopimelate Decarboxylase, an Essential Enzyme in Bacterial Lysine Biosynthesis." *The Journal of Biological Chemistry* 278 (20): 18588–96.

Goude, R., S. Renaud, S. Bonnassie, T. Bernard, and C. Blanco. 2004. "Glutamine , Glutamate , and α-Glucosylglycerate Are the Major Osmotic Solutes Accumulated by *Erwinia chrysanthemi* Strain 3937." *Applied and Environmental Microbiology* 70 (11): 6535–41.

Guettler, M. V. 1998. "Process for Making Succinic Acid, Microorganisms for Use in the Process and Methods of Obtaining the Microorganism." US 5504004.

Guettler, M. V, D. Rumler, and M.K. Jain. 1999. "*Actinobacillus succinogens* Sp. Nov., a Novel Succinc-Acid-Producing Strain from the Bovine Rumen." *International Journal of Systematic Bacteriology* 49: 207–16.

Gunsalus, R.P., and S.-J. Park. 1994. "Aerobic-Anaerobic Gene Regulation in *Escherichia coli*: Control by the ArcAB and Fnr Regulons." *Research in Microbiology1* 145 (5-6): 437–50.

Hayes, D.J., S. Fitzpatrick, M.H.B. Hayes, and J.R.H. Ross. 2006. "The Biofine Process – Production of Levulinic Acid, Furfural, and Formic Acid from Lignocellulosic Feedstocks." In *Biorefineries – Industrial Processes and Products*, edited by Birgit Kamm, Patrick R. Gruber, and Michael Kamm, 1:139–64. Wiley-VCH.

Herendeen, S.L., R.A. VanBogelen, and F.C. Neidhardt. 1979. "Levels of Major Proteins of *Escherichia coli* During Growth at Different Temperatures." *Journal of Bacteriology* 139 (1): 185–94.

Hong, K.-K., and J. Nielsen. 2012. "Metabolic Engineering of *Saccharomyces cerevisiae*: a Key Cell Factory Platform for Future Biorefineries." *Cellular and Molecular Life Sciences* 69 (16): 2671–90.

Hong, S.H., J.S. Kim, S.Y. Lee, Y.H. In, S.S. Choi, J.-K. Rih, C.H. Kim, H. Jeong, C.G. Hur, and J.J. Kim. 2004. "The Genome Sequence of the Capnophilic Rumen Bacterium *Mannheimia succiniciproducens*." *Nature Biotechnology* 22 (10): 1275–81.

Hong, S.H., and S.Y. Lee. 2001. "Metabolic Flux Analysis for Succinic Acid Production by Recombinant *Escherichia coli* with Amplified Malic Enzyme Activity." *Biotechnology and Bioengineering* 74 (2): 89–95.

Hong, S.H., and S.Y. Lee. 2004. "Enhanced Production of Succinic Acid by Metabolically Engineered *Escherichia coli* with Amplified Activities of Malic Enzyme and Fumarase." *Biotechnology and Bioprocess Engineering* 9: 252–55.

Hoon, Y., I.J. Oh, C. Jung, S.Y. Lee, and J. Lee. 2010. "The Effect of Protectants and pH Changes on the Cellular Growth and Succinic Acid Yield of *Mannheimia succiniciproducens* LPK7." *Journal of Microbiology and Biotechnology* 20 (12): 1677–80.

Huhn, S., E. Jolkver, R. Krämer, and K. Marin. 2011. "Identification of the Membrane Protein SucE and Its Role in Succinate Transport in *Corynebacterium glutamicum*." *Applied Microbiology and Biotechnology* 89 (2): 327–35.

Inui, M., M. Suda, S. Okino, H. Nonaka, L.G. Puskás, A.A. Vertès, and H. Yukawa. 2007. "Transcriptional Profiling of *Corynebacterium glutamicum* Metabolism During Organic Acid Production Under Oxygen Deprivation Conditions." *Microbiology* 153 (8): 2491–2504.

Iwatani, S., Y. Yamada, and Y. Usuda. 2008. "Metabolic Flux Analysis in Biotechnology Processes." *Biotechnology Letters* 30: 791–99.

Jansen, M., R. Verwaal, L. Segueilha, M. Van De Graaf, and T. Geurts. 2012. "Low pH Fermentation to Succinic Acid , the Basis for Efficient Recovery." In *Biorefinery Conference Copenhagen*.

Jantama, K., M.J. Haupt, S. a Svoronos, X. Zhang, J.C. Moore, K.T. Shanmugam, and L.O. Ingram. 2008. "Combining Metabolic Engineering and Metabolic Evolution to Develop Nonrecombinant Strains of *Escherichia coli* C That Produce Succinate and Malate." *Biotechnology and Bioengineering* 99 (5): 1140–53.

Jeong, J.-Y., Y.-J. Kim, N. Cho, D. Shin, T.-W. Nam, S. Ryu, and Y.-J. Seok. 2004. "Expression of *ptsG* Encoding the Major Glucose Transporter Is Regulated by ArcA in *Escherichia coli*." *The Journal of Biological Chemistry* 279 (37): 38513–18.

Jiang, M., K. Chen, Z. Liu, P. Wei, H. Ying, and H. Chang. 2010. "Succinic Acid Production by *Actinobacillus succinogenes* Using Spent Brewer's Yeast Hydrolysate as a Nitrogen Source." *Applied Biochemistry and Biotechnology* 160: 244–54.

John, R.P., G.S. Anisha, A. Pandey, and K. Madhavan Nampoothri. 2010. "Genome Shuffling: A New Trend in Improved Bacterial Production of Lactic Acid." *Industrial Biotechnology* (June): 164–69.

Kalinowski, J., B. Bathe, D. Bartels, N. Bischoff, M. Bott, A. Burkovski, N. Dusch, et al. 2003. "The Complete *Corynebacterium glutamicum* ATCC 13032 Genome Sequence and Its Impact on the Production of l-Aspartate-Derived Amino Acids and Vitamins." *Journal of Biotechnology* 104 (1-3): 5–25.

Kamashev, D., and J. Rouviere-Yaniv. 2000. "The Histone-Like Protein HU Binds Specifically to DNA Recombination and Repair Intermediates." *The EMBO Journal* 19 (23): 6527–35.

Kim, D.Y., S.C. Yim, P.C. Lee, W.G. Lee, S.Y. Lee, and H.N. Chang. 2004. "Batch and Continuous Fermentation of Succinic Acid from Wood Hydrolysate by *Mannheimia succiniciproducens* MBEL55E." *Enzyme and Microbial Technology* 35 (6-7): 648–53.

Kim, P., M. Laivenieks, C. Vieille, and J.G. Zeikus. 2004. "Effect of Overexpression of *Actinobacillus succinogenes* Phosphoenolpyruvate Carboxykinase on Succinate Production in *Escherichia coli*." *Applied and Environmental Microbiology* 70 (2): 1238–41.

Kim, T.Y., H.U. Kim, J.M. Park, H. Song, and J.S. Kim. 2007. "Genome-Scale Analysis of *Mannheimia succiniciproducens* Metabolism." *Biotechnology and Bioengineering* 97 (4): 657–71.

Kim, T.Y., H.U. Kim, H. Song, and S.Y. Lee. 2009. "In Silico Analysis of the Effects of H_2 and CO_2 on the Metabolism of a Capnophilic Bacterium *Mannheimia succiniciproducens*." *Journal of Biotechnology* 144 (3): 184–89.

Kind, S., and C. Wittmann. 2011. "Bio-Based Production of the Platform Chemical 1,5-Diaminopentane." *Applied Microbiology and Biotechnology* 91 (5): 1287–96.

Koga, Y. 2012. "Thermal Adaptation of the Archaeal and Bacterial Lipid Membranes." *Archaea*:1-6.

Kohlstedt, M., J. Becker, and C. Wittmann. 2010. "Metabolic Fluxes and Beyond - Systems Biology Understanding and Engineering of Microbial Metabolism." *Applied Microbiology and Biotechnology* 88: 1065–75.

Krokan, H.E., R. Standal, and G. Slupphaug. 1997. "DNA Glycosylases in the Base Excision Repair of DNA." *Biochemical Journal* 325: 1–16.

Krömer, J.O., M. Fritz, E. Heinzle, and C. Wittmann. 2005. "*In Vivo* Quantification of Intracellular Amino Acids and Intermediates of the Methionine Pathway in *Corynebacterium glutamicum*." *Analytical Biochemistry* 340 (1): 171–73.

Kuhnert, P., E. Scholten, S. Haefner, D. Mayor, and J. Frey. 2010. "*Basfia succiniciproducens* Gen. Nov., Sp. Nov., a New Member of the Family *Pasteurellaceae* Isolated from Bovine Rumen." *International Journal of Systematic and Evolutionary Microbiology* 60: 44–50.

Kurzrock, T., and D. Weuster-Botz. 2010. "Recovery of Succinic Acid from Fermentation Broth." *Biotechnology Letters* 32 (3): 331–39.

Kwon, Y.-D., S. Kim, S.Y. Lee, and P. Kim. 2011. “Long-Term Continuous Adaptation of *Escherichia coli* to High Succinate Stress and Transcriptome Analysis of the Tolerant Strain.” *Journal of Bioscience and Bioengineering* 111 (1): 26–30.

Lane, W.J., and S. A. Darst. 2010. “Molecular Evolution of Multisubunit RNA Polymerases: Structural Analysis.” *Journal of Molecular Biology* 395 (4): 686–704.

Lee, J.W., S.Y. Lee, H. Song, and J.-S. Yoo. 2006. “The Proteome of *Mannheimia succiniciproducens*, a Capnophilic Rumen Bacterium.” *Proteomics* 6 (12): 3550–66.

Lee, P.C., S.Y. Lee, S.H. Hong, and H.N. Chang. 2002. “Isolation and Characterization of a New Succinic Acid-Producing Bacterium, *Mannheimia succiniciproducens* MBEL55E from Bovine Rumen.” *Applied Microbiology and Biotechnology* 58: 663–68.

Lee, P.C., S.Y. Lee, S.H. Hong, and H.N. Chang. 2003. “Batch and Continuous Cultures of *Mannheimia succiniciproducens* MBEL55E for the Production of Succinic Acid from Whey and Corn Steep Liquor.” *Bioprocess and Biosystems Engineering* 26: 63–67.

Lee, S.J., H. Song, and S.Y. Lee. 2006. “Genome-Based Metabolic Engineering of *Mannheimia succiniciproducens* for Succinic Acid Production.” *Applied and Environmental Microbiology* 72 (3): 1939–48.

Lee, S.Y. 2009. “Gene Encoding Fumaric Hydratase C and Use Thereof.” US 7588934.

Lee, S.Y., S.H. Park, S.H. Hong, Y. Lee, and S.H. Lee. 2005. “Fermentative Production of Building Blocks for Chemical Synthesis of Polyesters.” In *Bioplymers - Polyesters*, edited by Alexander Steinbüchel, 265–74. Wiley-VCH.

Lehrer, J., K. A. Vigeant, L.D. Tatar, and M. A. Valvano. 2007. “Functional Characterization and Membrane Topology of *Escherichia coli* WecA, a Sugar-Phosphate Transferase Initiating the Biosynthesis of Enterobacterial Common Antigen and O-Antigen Lipopolysaccharide.” *Journal of Bacteriology* 189 (7): 2618–28.

Levdikov, V., L. Blagova, N. Bose, and C. Momany. 2003. “Crystal Structure of Diaminopimelate Decarboxylase.” PDB ID 1KNW.

Li, Q., D. Wang, Y. Wu, M. Yang, W. Li, J. Xing, and Z. Su. 2010. “Kinetic Evaluation of Products Inhibition to Succinic Acid Producers *Escherichia coli* NZN111, AFP111, BL21, and *Actinobacillus succinogenes* 130Z T.” *Journal of Microbiology* 48 (3): 290–96.

Lim, B., and C.A. Gross. 2011. “Cellular Response to Heat Shock and Cold Shock.” In *Bacterial Stress Responses*, edited by Gisela Storz and Regina Hengge, 2nd ed., 93–114. ASM Press.

Lin, H., G.N. Bennett, and K.-Y. San. 2005. “Metabolic Engineering of Aerobic Succinate Production Systems in *Escherichia coli* to Improve Process Productivity and Achieve the Maximum Theoretical Succinate Yield.” *Metabolic Engineering* 7 (2): 116–27.

Lin, S.K.C., C. Du, A. Koutinas, R. Wang, and C. Webb. 2008. “Substrate and Product Inhibition Kinetics in Succinic Acid Production by *Actinobacillus succinogenes*.” *Biochemical Engineering Journal* 41: 128–35.

Lippert, K., and E. Galinski. 1992. “Enzyme Stabilization by Ectoine-Type Compatible Solutes: Protection Against Heating, Freezing and Drying.” *Applied Microbiology and Biotechnology* 37 (1): 61–65.

Litsanov, B., A. Kabus, M. Brocker, and M. Bott. 2012. “Efficient Aerobic Succinate Production from Glucose in Minimal Medium with *Corynebacterium glutamicum*.” *Microbial Biotechnology* 5 (1): 116–28.

Liu, R., L. Liang, K. Chen, J. Ma, M. Jiang, P. Wei, and P. Ouyang. 2012. “Fermentation of Xylose to Succinate by Enhancement of ATP Supply in Metabolically Engineered *Escherichia coli*.” *Applied Microbiology and Biotechnology*.

Liu, Y.-P., P. Zheng, Z.-H. Sun, Y. Ni, J.-J. Dong, and L.-L. Zhu. 2008. “Economical Succinic Acid Production from Cane Molasses by *Actinobacillus succinogenes*.” *Bioresource Technology* 99 (6): 1736–42.

Loubiere, P., M. Cocaign-Bousquet, J. Matos, G. Goma, and N.D. Lindley. 1997. “Influence of End-Products Inhibition and Nutrient Limitations on the Growth of *Lactococcus lactis* Subsp. Lactis.” *Journal of Applied Microbiology* 82 (1): 95–100.

Mager, W.H., a H. de Boer, M.H. Siderius, and H.P. Voss. 2000. “Cellular Responses to Oxidative and Osmotic Stress.” *Cell Stress & Chaperones* 5 (2): 73–75.

Mäkelä, P. 2004. “Agro-Industrial Uses of Glycinebetaine.” *Sugar Tech* 6 (4): 207–12.

Malpica, R., G.R.P. Sandoval, C. Rodríguez, B. Franco, and D. Georgellis. 2006. "Signaling by the Arc Two-Component System Provides a Link Between the Redox State of the Quinone Pool and Gene Expression." *Antioxidants & Redox Signaling* 8 (5-6): 781–95.

Mao, F., P. Dam, J. Chou, V. Olman, and Y. Xu. 2009. "DOOR: a Database for Prokaryotic Operons." *Nucleic Acids Research* 37 (Database issue): D459–63.

MarketsandMarkets. 2012. "Succinic Acid Market by Applications & Geography - Global Trends & Forecasts (2011-2016)."

Markman, L. 2009. "Teething: Facts and Fiction." *Pediatrics In Review / American Academy of Pediatrics* 30 (8): e59–64.

McKinlay, J.B., M. Laivenieks, B.D. Schindler, A. McKinlay, S. Siddaramappa, J.F. Challacombe, S.R. Lowry, et al. 2010. "A Genomic Perspective on the Potential of *Actinobacillus succinogenes* for Industrial Succinate Production." *BMC Genomics* 11: 680–95.

McKinlay, J.B., Y. Shachar-Hill, J.G. Zeikus, and C. Vieille. 2007. "Determining *Actinobacillus succinogenes* Metabolic Pathways and Fluxes by NMR and GC-MS Analyses of ^{13}C-Labeled Metabolic Product Isotopomers." *Metabolic Engineering* 9: 177–92.

McKinlay, J.B., and C. Vieille. 2008. "^{13}C-Metabolic Flux Analysis of *Actinobacillus succinogenes* Fermentative Metabolism at Different $NaHCO_3$ and H_2 Concentrations." *Metabolic Engineering* 10 (1): 55–68.

McKinlay, J.B., C. Vieille, and J.G. Zeikus. 2007. "Prospects for a Bio-Based Succinate Industry." *Applied Microbiology and Biotechnology* 76: 727–40.

McKinlay, J.B., J.G. Zeikus, and C. Vieille. 2005. "Insights into *Actinobacillus succinogenes* Fermentative Metabolism in a Chemically Defined Growth Medium." *Applied and Environmental Microbiology* 71 (11): 6651–56.

Melzer, G., M.E. Esfandabadi, E. Franco-Lara, and C. Wittmann. 2009. "Flux Design: In Silico Design of Cell Factories Based on Correlation of Pathway Fluxes to Desired Properties." *BMC Systems Biology* 3: 120.

Meza, E., J. Becker, F. Bolivar, G. Gosset, and C. Wittmann. 2012. "Consequences of Phosphoenolpyruvate:sugar Phosphotranferase System and Pyruvate Kinase Isozymes Inactivation in Central Carbon Metabolism Flux Distribution in *Escherichia coli*." *Microbial Cell Factories* 11 (127): 1–13.

Millard, C.S., Y.-P. Chao, J.C. Liao, and M.I. Donnelly. 1996. "Enhanced Production of Succinic Acid by Overexpression of Phosphoenolpyruvate Carboxylase in *Escherichia coli*." *Applied and Environmental Microbiology* 62 (5): 1808–10.

Momany, C., V. Levdikov, L. Blagova, and K. Crews. 2002. "Crystallization of Diaminopimelate Decarboxylase from *Escherichia coli*, a Stereospecific D -Amino-Acid Decarboxylase." *Acta Crystallographica Section D Biological Crystallography* 58: 549–52.

Mordukhova, E. A., H.-S. Lee, and J.-G. Pan. 2008. "Improved Thermostability and Acetic Acid Tolerance of *Escherichia coli* via Directed Evolution of Homoserine o-Succinyltransferase." *Applied and Environmental Microbiology* 74 (24): 7660–68.

Müller, H. 2005. "Tetrahydrofuran." In *Ullmann's Encyclopedia of Industrial Chemistry*, 5:1–6. Wiley-VCH.

Myriant. 2013a. "Myriant Produces Bio-Succinic Acid at Commercial Scale, ThyssenKrupp Uhde Readies to Provide Process and Performance Guaranty". Myriant.

Myriant. 2013b. "Showa Denko K.K. Selects Myriant as Its Supplier of High-Purity BioSuccinic Acid for the Production of Renewable-Based Poly(butylene Succinate) (PBS)". Myriant.

Nagorska, K., A. Ostrowski, K. Hinc, I.B. Holland, and M. Obuchowski. 2010. "Importance of Eps Genes from *Bacillus subtilis* in Biofilm Formation and Swarming." *Journal of Applied Genetics* 51 (3): 369–81.

Nedea, E.C., D. Markov, T. Naryshkina, and K. Severinov. 1999. "Localization of *Escherichia coli rpoC* Mutations That Affect RNA Polymerase Assembly and Activity at High Temperature." *Journal of Bacteriology* 181 (8): 2663–65.

Neidhardt, F.C., J.L. Ingraham, and M. Schaechter, ed. 1990. "Physiology of the Bacterial Cell - A Molecular Approach. " Vol. 20. Sinauer Associates.

Oishi, A., M. Zhang, K. Nakayama, T. Masuda, and Y. Taguchi. 2006. "Synthesis of Poly(butylene Succinate) and Poly(ethylene Succinate) Including Diglycollate Moiety." *Polymer Journal* 38 (7): 710–15.

Okino, S., M. Inui, and H. Yukawa. 2005. “Production of Organic Acids by *Corynebacterium glutamicum* Under Oxygen Deprivation.” *Applied Microbiology and Biotechnology* 68 (4): 475–80.

Okino, S., R. Noburyu, M. Suda, T. Jojima, M. Inui, and H. Yukawa. 2008. “An Efficient Succinic Acid Production Process in a Metabolically Engineered *Corynebacterium glutamicum* Strain.” *Applied Microbiology and Biotechnology* 81 (3): 459–64.

Otero, J.M., D. Cimini, K.R. Patil, S.G. Poulsen, L. Olsson, and J. Nielsen. 2013. “Industrial Systems Biology of *Saccharomyces cerevisiae* Enables Novel Succinic Acid Cell Factory.” *PloS One* 8 (1): e54144.

Paster, M., J.L. Pellegrino, and T.M. Carole. 2004. “Industrial Bioproducts : Today and Tomorrow.” Energetics.

Patel, M., M. Crank, V. Dornburg, B. Hermann, L. Roes, B. Hüsing, L. Overbeek, F. Terragni, and E. Recchia. 2006. “Medium and Long-Term Opportunities and Risks of the Biotechnological Production of Bulk Chemicals from Renewable Resources - The Potential of White Biotechnology.” funded by European Commission.

Patnaik, R. 2008. “Engineering Complex Phenotypes in Industrial Strains.” *Biotechnology Progress* 24 (1): 38–47.

Podkovyrov, S.M., and J.G. Zeikus. 1993. “Purification and Characterization of Phosphoenolpyruvate Carboxykinase, a Catabolic CO_2-Fixing Enzyme, from *Anaerobiospirillum succiniciproducens*.” *Journal of General Microbiology* 139: 223–28.

Quek, L.-E., C. Wittmann, L.K. Nielsen, and J.O. Krömer. 2009. “OpenFLUX: Efficient Modelling Software for ^{13}C-Based Metabolic Flux Analysis.” *Microbial Cell Factories* 8: 25.

Raab, A.M., G. Gebhardt, N. Bolotina, D. Weuster-Botz, and C. Lang. 2010. “Metabolic Engineering of *Saccharomyces cerevisiae* for the Biotechnological Production of Succinic Acid.” *Metabolic Engineering* 12 (6): 518–25.

Ron, E.Z., and B.D. Davis. 1971. “Growth Rate of *Escherichia coli* at Elevated Temperatures: Limitation by Methionine.” *Journal of Bacteriology* 107 (2): 391–96.

Roquette. 2013. “DSM and Roquette to Start Bio-Based Succinic Acid Joint Venture”. Roquette.

Samuelov, N.S., R. Lamed, S. Lowe, and J.G. Zeikus. 1991. “Influence of CO_2-HCO_3 - Levels and pH on Growth, Succinate Production, and Enzyme Activities of *Anaerobiospirillum succiniciproducens*.” *Applied and Environmental Microbiology* 57 (10): 3013–19.

Sánchez, A.M., G.N. Bennett, and K.-Y. San. 2005. “Efficient Succinic Acid Production from Glucose through Overexpression of Pyruvate Carboxylase in an *Escherichia coli* Alcohol Dehydrogenase and Lactate Dehydrogenase Mutant.” *Biotechnology Progress* 21 (2): 358–65.

Sanders, J.W., K.J. Leenhouts, A.J. Haandrikman, G. Venema, J.A.N.W. Sanders, K.J. Leenhouts, A.J. Haandrikman, G. Venema, and J.A.N. Kok. 1995. “Stress Response in *Lactococcus lactis*: Cloning, Expression Analysis and Mutation of the Lactococcal Superoxide Dismutase Gene.” *Jounral of Bacteriology* 177 (18): 5254–60.

Sauer, M., D. Porro, D. Mattanovich, and P. Branduardi. 2008. “Microbial Production of Organic Acids: Expanding the Markets.” *Trends in Biotechnology* 26 (2): 100–108.

Sauer, U., and B.J. Eikmanns. 2005. “The PEP-Pyruvate-Oxaloacetate Node as the Switch Point for Carbon Flux Distribution in Bacteria.” *FEMS Microbiology Reviews* 29 (4): 765–94.

Scholten, E., and D. Dägele. 2008. “Succinic Acid Production by a Newly Isolated Bacterium.” *Biotechnology Letters* 30: 2143–46.

Scholten, E., D. Dägele, S. Haefner, and H. Schröder. 2011. “Carboxylic Acid Producing Member of the *Pasteurellaceae*.” US 20110008851 A1.

Scholten, E., S. Haefner, and H. Schröder. 2010. “Bacterial Cells Having a Glyoxylte Shunt for the Manufacture of Succinic Acid.” US20100159543 A1.

Scholten, E., T. Renz, and J. Thomas. 2009. “Continuous Cultivation Approach for Fermentative Succinic Acid Production from Crude Glycerol by *Basfia succiniciproducens* DD1.” *Biotechnology Letters* 31: 1947–51.

Shanmugam, K.T., and L.O. Ingram. 2008. “Engineering Biocatalysts for Production of Commodity Chemicals.” *Journal of Molecular Mcrobiology and Biotechnology* 15: 8–15.

Siddiquee, K.A.Z., M.J. Arauzo-Bravo, and K. Shimizu. 2004. “Metabolic Flux Analysis of *pykF* Gene Knockout *Escherichia coli* Based on ^{13}C-Labeling Experiments Together with

Measurements of Enzyme Activities and Intracellular Metabolite Concentrations." *Applied Microbiology and Biotechnology* 63: 407–17.

Six, S., S.C. Andrews, G. Unden, and J.R. Guest. 1994. "*Escherichia coli* Possesses Two Homologous Anaerobic C4-Dicarboxylate Membrane Transporters (DcuA and DcuB) Distinct from the Aerobic Dicarboxylate Transport System (Dct)." *Journal of Bacteriology* 176 (21): 6470–78.

Skorokhodova, A.Y., A.Y. Gulevich, A.A. Morzhakova, R.S. Shakulov, and V.G. Debabov. 2013. "Comparison of Different Approaches to Activate the Glyoxylate Bypass in *Escherichia coli* K-12 for Succinate Biosynthesis During Dual-Phase Fermentation in Minimal Glucose Media." *Biotechnology Letters* 35 (4): 577–83.

Song, H., S.H. Jang, J.M. Park, and S.Y. Lee. 2008. "Modeling of Batch Fermentation Kinetics for Succinic Acid Production by *Mannheimia succiniciproducens*." *Biochemical Engineering Journal* 40 (1): 107–15.

Song, H., T.Y. Kim, B.-K. Choi, S.J. Choi, L.K. Nielsen, H.N. Chang, and S.Y. Lee. 2008. "Development of Chemically Defined Medium for *Mannheimia succiniciproducens* Based on Its Genome Sequence." *Applied Microbiology and Biotechnology* 79 (2): 263–72.

Song, H., and S.Y. Lee. 2006. "Production of Succinic Acid by Bacterial Fermentation." *Enzyme and Microbial Technology* 39: 352–61.

Stellmacher, R., J. Hangebrauk, E. Scholten, G. von Abendroth, and C. Wittmann. 2010. "Fermentative Herstellung von Bernsteinsäure Mit *Basfia succiniciproducens* DD1 in Serumflaschen." *Chemie Ingenieur Technik* 82 (8): 1223–29.

Stephanopoulos, G.N., A.A. Aristidou, and J. Nielsen. 1998. "Metabolic Engineering: Principles and Methodologies". Academic Press.

Stols, L., and M. Donelly. 1997. "Production of Succinic Acid through Overexpression of NAD(+)-Dependent Malic Enzyme in an *Escherichia coli* Mutant." *Applied and Environmental Microbiology* 63 (7): 2695–2701.

Subramanian, A., P. Tamayo, V.K. Mootha, S. Mukherjee, and B.L. Ebert. 2005. "Gene Set Enrichment Analysis: A Knowledge-Based Approach for Interpreting Genome-Wide Expression Profiles." *Proceedings of the National Academy of Sciences of the United States of America* 102 (43): 15545–50.

Suzuki, K., S. Ito, A. Shimizu-Ibuka, and H. Sakai. 2008. "Crystal Structure of Pyruvate Kinase from *Geobacillus stearothermophilus*." *Journal of Biochemistry* 144 (3): 305–12.

Taboada, B., R. Ciria, C.E. Martinez-Guerrero, and E. Merino. 2012. "ProOpDB: Prokaryotic Operon DataBase." *Nucleic Acids Research* 40 (Database issue): D627–31.

Tatusov, R.L., M.Y. Galperin, D. a Natale, and E. V Koonin. 2000. "The COG Database: a Tool for Genome-Scale Analysis of Protein Functions and Evolution." *Nucleic Acids Research* 28 (1): 33–36.

Transparency Market Research. 2013. "Succinic Acid Market - Global Industry Analysis, Size, Share, Growth, Trends and Forecast, 2012 - 2018."

Turnbull, A.L., and M.G. Surette. 2010. "Cysteine Biosynthesis, Oxidative Stress and Antibiotic Resistance in *Salmonella typhimurium*." *Research in Microbiology* 161 (8): 643–50.

Turner, P., G. Mamo, and E.N. Karlsson. 2007. "Potential and Utilization of Thermophiles and Thermostable Enzymes in Biorefining." *Microbial Cell Factories* 6:9.

Tweel, W. van den. 2010. "Sustainable Succinic Acid." DSM.

Urbance, S.E., A.L. Pometto, A. a Dispirito, and Y. Denli. 2004. "Evaluation of Succinic Acid Continuous and Repeat-Batch Biofilm Fermentation by *Actinobacillus succinogenes* Using Plastic Composite Support Bioreactors." *Applied Microbiology and Biotechnology* 65 (6): 664–70.

Urbonavicius, J., Q. Qian, J.M.B. Durand, T.G. Hagervall, and G.R. Björk. 2001. "Improvement of Reading Frame Maintenance Is a Common Function for Several tRNA Modifcations." *The EMBO Journal* 20 (17): 4863–73.

USDA. 2013. "Table 3b—World Raw Sugar Price, ICE Contract 11 Nearby Futures Price, Monthly Quarterly, and by Calendar and Fiscal Year." ICE Futures US.

USDA. 2009. "U.S. Biobased Products Market - Potential and Projections Through 2025." Edited by Meredith A. Williamson. *Energy Policy*. Nova Science Pub.

Vaas, L.A.I., J. Sikorski, V. Michael, M. Göker, and H.-P. Klenk. 2012. "Visualization and Curve-Parameter Estimation Strategies for Efficient Exploration of Phenotype Microarray Kinetics." *PLoS ONE* 7 (4): 1–18.

Van der Werf, M.J., M. V Guettler, M.K. Jain, and J.G. Zeikus. 1997. "Environmental and Physiological Factors Affecting the Succinate Product Ratio During Carbohydrate Fermentation by *Actinobacillus* Sp. 130Z." *Archives of Microbiology* 167: 332–42.

Van Hoek, P., A. Aristidou, J.J. Hahn, and A. Patist. 2003. "Fermentation Goes Large Scale." *CEP Magazine* (January): 37–42.

Van Kranenburg, R., J.D. Marugg, I.I. van Swam, N.J. Willem, and W.M. de Vos. 1997. "Molecular Characterization of the Plasmid-Encoded Eps Gene Cluster Essential for Exopolysaccharide Biosynthesis in *Lactococcus lactis*." *Molecular Microbiology* 24 (2): 387–97.

Vemuri, G.N., M.A. Eiteman, and E. Altman. 2002. "Effects of Growth Mode and Pyruvate Carboxylase on Succinic Acid Production by Metabolically Engineered Strains of *Escherichia coli*." *Applied and Environmental Microbiology* 68 (4): 1715–27.

Wang, X., C.S. Gong, and G.T. Tsao. 1998. "Bioconversion of Fumaric Acid to Succinic Acid by Recombinant *E. coli*." *Applied Biochemistry and Biotechnology* 70-72 (5): 919–28.

Wang, Y., K.-Y. San, and G.N. Bennett. 2013. "Cofactor Engineering for Advancing Chemical Biotechnology." *Current Opinion in Biotechnology*: 6–11.

Warnecke, T., and R.T. Gill. 2005. "Organic Acid Toxicity, Tolerance, and Production in *Escherichia coli* Biorefining Applications." *Microbial Cell Factories* 4: 25.

Werpy, T., and G. Peterson. 2004. "Top Value Added Chemicals from Biomass Volume I: Results of Screening for Potential Candidates from Sugars and Synthesis Gas." DOE.

Weston, L. A., and R.J. Kadner. 1988. "Role of Uhp Genes in Expression of the *Escherichia coli* Sugar-Phosphate Transport System." *Journal of Bacteriology* 170 (8): 3375–83.

Wisbiorefine. "Fermentation of 6-Carbon Sugars and Starches."

Wittmann, C. 2007. "Fluxome Analysis Using GC-MS." *Microbial Cell Factories* 6 (6): 1–17.

Wittmann, C., M. Hans, and E. Heinzle. 2002. "*In Vivo* Analysis of Intracellular Amino Acid Labelings by GC/MS." *Analytical Biochemistry* 307: 379–82.

Wittmann, C., and E. Heinzle. 2001a. "Modeling and Experimental Design for Metabolic Flux Analysis of Lysine-Producing *Corynebacteria* by Mass Spectrometry." *Metabolic Engineering* 3 (2): 173–91.

Wittmann, C., and E. Heinzle. 2001b. "Application of MALDI-TOF MS to Lysine-Producing *Corynebacterium glutamicum*: A Novel Approach for Metabolic Flux Analysis." *European Journal of Biochemistry* 268 (8): 2441–55.

Wittmann, C., and E. Heinzle. 2002. "Genealogy Profiling through Strain Improvement by Using Metabolic Network Analysis: Metabolic Flux Genealogy of Several Generations of Lysine-Producing *Corynebacteria*." *Applied and Environmental Microbiology* 68 (12): 5843–59.

Yang, Y., and A. Paquet. 2005. "Preprocessing Two-Color Spotted Arrays." In *Bioinformatics and Computational Biology Solutions Using R and Bioconductor*, edited by R Gentleman, V Carey, W Huber, R Irizarry, and S Dudoit, 49–69. Springer.

Yuk, H.-G., and D.L. Marshall. 2003. "Heat Adaptation Alters *Escherichia coli* O157:H7 Membrane Lipid Composition and Verotoxin Production." *Applied and Environmental Microbiology* 69 (9): 5115–19.

Yun, S., J.M. Shin, O.-C. Kim, Y.R. Jung, D.-B. Oh, S.Y. Lee, and O. Kwon. 2012. "Probing the ArcA Regulon in the Rumen Bacterium *Mannheimia succiniciproducens* by Genome-Wide Expression Profiling." *Journal of Microbiology* 50 (4): 665–72.

Zhang, X., K.T. Shanmugam, and L.O. Ingram. 2010. "Fermentation of Glycerol to Succinate by Metabolically Engineered Strains of *Escherichia coli*." *Applied and Environmental Microbiology* 76 (8): 2397–2401.

Zhang, Y., Z. Huang, C. Du, Y. Li, and Z. Cao. 2009. "Introduction of an NADH Regeneration System into *Klebsiella oxytoca* Leads to an Enhanced Oxidative and Reductive Metabolism of Glycerol." *Metabolic Engineering* 11 (2): 101–6.

Zhang, Y.-X., K. Perry, V.A. Vinci, K. Powell, W.P.C. Stemmer, and S.B. del Cardayré. 2002. "Genome Shuffling Leads to Rapid Phenotypic Improvement in Bacteria." *Nature* 415 (6872): 644–46.

9 Appendix

9.1 Data related to ^{13}C metabolic flux analysis

The precursor demand for biomass synthesis was taken from the literature (Becker et al. 2013). The excellent fit between simulated and experimentally obtained mass isotopomer fractions is shown for the evolutionary derived mutant *B. succiniciproducens* DD3-T2, DD3-Suc2 and DD3-Suc3. In addition, carbon fluxes towards biomass formation and redox balance are shown for all adapted strain, as compared to the parent strain DD3 (data taken from (Becker et al. 2013)). The fold change for carbon flux re-distribution is listed, as compared to DD3 (data taken from (Becker et al. 2013)).

Table 9.1 Precursor demand for biomass synthesis in *B. succiniciproducens*. Biomass composition was based on previous studies (Neidhardt et al. 1990; Kim et al. 2007).

Precursor	Demand	G6P	F6P	R5P	E4P	GAP	PGA	PEP	Pyr	AcCoA	OAA	AKG	CO_2	ATP	NADH	NADPH
Ala	600								1							1
Arg	188											1	1	7	-1	4
Asp	270										1					1
Asn	270										1			3		1
Cys	22						1							4	-1	5
Glu	270											1				1
Gln	270											1		1		1
Gly	471						1								-1	1
His	111			1										6	-3	1
Ile	261								1		1		-1	2		5
Leu	388								2	1			-2		-1	2
Lys	229								1		1		-1	2		4
Met	69										1			7		8
Phe	165				1			2					-1	1		2
Pro	371											1		1		3
Ser	209						1								-1	1
Thr	278										1			2		3
Trp	2			1	1			1					-1	5	-2	2
Tyr	56				1			2					-1	1	-1	2
Val	399								2				-1			2
Sum protein		0	0	113	223		702	444	2664	388	1297	1099	-1698	5651	-1672	9991
RNA				626			271				355		271	6126	-1169	1033
DNA				91			45				45		45	932	-181	253
Lipids						129	129			2116				1858		3612
LPS		51	16	24			24	24		329				470	-24	447
Peptidoglycan			55					28	83	55				248		193
Glycogen		154												154		
C1-units							49								-49	49
Polyamines														119		178
Tottal		**205**	**72**	**854**	**223**	**129**	**1220**	**496**	**2747**	**2888**	**1725**	**1186**	**-1382**	**15558**	**-3095**	**15756**

Table 9.2 Relative mass isotopomer fractions of amino acids from hydrolyzed cell protein and of secreted succinate from *B. succiniciproducens* cultivation with 99 % [1-^{13}C] glucose. Data denote experimental GC-MS data (exp) and values predicted by the solution of the mathematical model corresponding to optimized fluxes (calc). M+0 represents the amount of non-labeled mass isotopomers fractions, M+1 the amount of single labeled mass isotopomers fractions and corresponding terms refer to higher labeling.

Analyte fragment	**Mass isotopomer**	**Mass isotopomer distribution**							
		DD3-T2		**DD3-T2 42 °C**		**DD3-Suc2**		**DD3-Suc3**	
		exp	**calc**	**exp**	**calc**	**exp**	**calc**	**exp**	**Calc**
Alanine	M+0	0.434	0.431	0.415	0.414	0.418	0.414	0.413	0.408
M-57	M+1	0.419	0.419	0.434	0.432	0.434	0.436	0.438	0.441
	M+2	0.112	0.114	0.114	0.116	0.111	0.113	0.112	0.114
Alanine	M+0	0.453	0.454	0.434	0.436	0.436	0.434	0.432	0.428
M-85	M+1	0.435	0.436	0.451	0.451	0.452	0.453	0.456	0.458
	M+2	0.112	0.110	0.114	0.112	0.112	0.113	0.113	0.114
Glycine	M+0	0.741	0.737	0.733	0.731	0.755	0.755	0.738	0.738
M-57	M+1	0.185	0.189	0.192	0.194	0.173	0.174	0.188	0.188
	M+2	0.074	0.074	0.075	0.074	0.071	0.071	0.074	0.073
Glycine	M+0	0.811	0.813	0.803	0.805	0.820	0.821	0.804	0.804
M-85	M+1	0.189	0.187	0.197	0.195	0.180	0.179	0.196	0.196
Aspartate	M+0	0.363	0.362	0.350	0.350	0.351	0.349	0.344	0.343
M-57	M+1	0.402	0.402	0.412	0.411	0.415	0.414	0.420	0.418
	M+2	0.160	0.160	0.161	0.162	0.158	0.160	0.160	0.162
Aspartate	M+0	0.372	0.373	0.359	0.360	0.357	0.358	0.351	0.353
M-85	M+1	0.410	0.410	0.421	0.420	0.423	0.422	0.427	0.425
	M+2	0.159	0.158	0.160	0.159	0.159	0.159	0.160	0.160
Threonine	M+0	0.363	0.363	0.349	0.350	0.349	0.349	0.343	0.344
M-57	M+1	0.404	0.403	0.414	0.412	0.417	0.415	0.421	0.419
	M+2	0.159	0.160	0.161	0.162	0.159	0.160	0.161	0.161
Threonine	M+0	0.374	0.374	0.360	0.361	0.357	0.359	0.352	0.354
M-85	M+1	0.410	0.410	0.421	0.421	0.424	0.422	0.428	0.426
	M+2	0.157	0.157	0.159	0.158	0.159	0.159	0.160	0.160
Serine	M+0	0.379	0.375	0.363	0.360	0.361	0.360	0.354	0.355
M-57	M+1	0.407	0.405	0.418	0.416	0.423	0.422	0.426	0.425
	M+2	0.156	0.160	0.159	0.162	0.156	0.158	0.159	0.159
Serine	M+0	0.406	0.404	0.390	0.389	0.386	0.387	0.380	0.382
M-85	M+1	0.433	0.436	0.445	0.448	0.451	0.449	0.454	0.453
	M+2	0.162	0.160	0.165	0.163	0.163	0.164	0.166	0.165
Phenylalanine	M+0	0.190	0.188	0.165	0.165	0.175	0.173	0.155	0.154
M-57	M+1	0.373	0.375	0.362	0.363	0.374	0.376	0.359	0.360
	M+2	0.283	0.279	0.299	0.296	0.293	0.294	0.307	0.307
Tyrosine	M+0	0.167	0.162	0.145	0.142	0.152	0.149	0.135	0.133
M-57	M+1	0.342	0.342	0.329	0.330	0.339	0.341	0.324	0.326
	M+2	0.287	0.285	0.299	0.298	0.296	0.297	0.306	0.307
Succinate	M+0	0.430	0.420	0.416	0.405	0.406	0.404	0.399	0.398
M-57	M+1	0.410	0.415	0.423	0.428	0.431	0.432	0.435	0.436
	M+2	0.116	0.119	0.116	0.120	0.117	0.118	0.118	0.119

Table 9.3 Biomass specific *in vivo* carbon fluxes of *B. succiniciproducens* DD3-T2 at 37 and 42 °C, respectively, and DD3-Suc2 and DD3-Suc3 at 37 °C during growth on minimal glucose medium. Data also comprise specific biomass yield ($Y_{X/S}$), calculated by linear fitting of the concentration of biomass and product with that of the substrate.

Reaction	**DD3-T2**	**DD3-T2 (42 °C)**	**DD3-Suc2**	**DD3-Suc3**
$Y_{X/S}$ [g mol^{-1}]	29.2 ± 1.0	28.9 ± 0.5	30.1 ± 2.4	29.1 ± 1.5
GLC6P = GLC6P_B	0.6 ± 0	0.6 ± 0	0.6 ± 0	0.6 ± 0
F6P = F6P_B	0.2 ± 0	0.2 ± 0	0.2 ± 0	0.2 ± 0
P5P = P5P_B	2.5 ± 0	2.5 ± 0	2.6 ± 0.1	2.7 ± 0.1
E4P = E4P_B	0.7 ± 0	0.7 ± 0	0.7 ± 0	0.7 ± 0
GAP = GAP_B	0.4 ± 0	0.4 ± 0	0.4 ± 0	0.4 ± 0
3PG = 3PG_B	3.9 ± 0	3.8 ± 0	3.9 ± 0	4.0 ± 0.1
PYR_PEP = PYR_PEP_B	9.3 ± 0.1	9.3 ± 0.1	9.6 ± 0.1	9.9 ± 0.1
ACCOA = ACCOA_B	8.9 ± 0.1	8.8 ± 0.1	9.3 ± 0.2	10.4 ± 0.2
OAA_MAL = OAA_MAL_B	5.6 ± 0	5.6 ± 0	5.8 ± 0	5.9 ± 0.1
AKG = AKG_B	3.3 ± 0	3.2 ± 0	3.4 ± 0	3.5 ± 0.1

Table 9.4 Response of *in vivo* flux distribution of the evolutionary adapted stains *B. succiniciproducens* DD3-T2, at 37 and 42 °C, respectively, and DD3-Suc2 and DD3-Suc3 at 37 °C as compared to their ancestor DD3 (Becker et al. 2013) on minimal glucose medium. Flux fold change is calculated from specific glucose uptake rate corrected *in vivo* carbon fluxes.

Reaction	**DD3-T2**	**DD3-T2 (42 °C)**	**DD3-Suc2**	**DD3-Suc3**
Specific glucose uptake rate [mmol g^{-1} h^{-1}]	8.2 ± 0.5	9.1 ± 0.6	7.8 ± 0.8	7.6 ± 0.8
GLC_EX + ATP = GLC	1	1.1	1	0.9
GLC + ATP = GLC6P	1	1.1	1	0.9
GLC6P = F6P	0.9	1.1	0.9	0.9
F6P + ATP = F16BP	1	1.1	0.9	0.9
F16BP = DHAP + GAP	1	1.1	0.9	0.9
DHAP = GAP	1	1.1	0.9	0.9
GAP = 3PG + ATP + NADH	1	1.1	0.9	0.9
3PG = PYR_PEP	1	1.1	0.9	0.9
GLC6P = P5P + CO2 + NADPH + NADPH	2.3	1.4	2.1	1.6
P5P + P5P = S7P + GAP	2.8	1.4	2.5	1.8
GAP + S7P = E4P + F6P	2.8	1.4	2.5	1.8
P5P + E4P = GAP + F6P	3.9	1.6	3.4	2.3
PYR_PEP + CO2 = OAA_MAL + ATP	1.1	1.1	0.9	0.8
PYR_PEP = ACCOA + CO2 + NADH	1.5	2	0.9	1.5
DHAP = MethGlyox = LAC	0.3	0.4	0	0.7
OAA_MAL = 0.5 FUM + 0.5 FUM	1.1	1.1	0.9	0.8
FUM + NADH = SUC	1.1	1.1	0.9	0.8
ACCOA + OAA_MAL = CIT	0.6	0.7	0.6	0.6
CIT = AKG + CO2 + NADPH	0.6	0.7	0.6	0.6
$Acetate_{ex}$	2.1	3.2	1	2.0
$Ethanol_{ex}$	1.8	0.8	0	2.3
$Pyruvate_{ex}$	0.7	0.5	1.4	1.1
Pyruvate derived by-$products_{ex}$	0.1	0.1	0.9	0.4
$Lactate_{ex}$	0.3	0.4	0	0.7
$Succinate_{ex}$	1	1.1	0.9	0.8

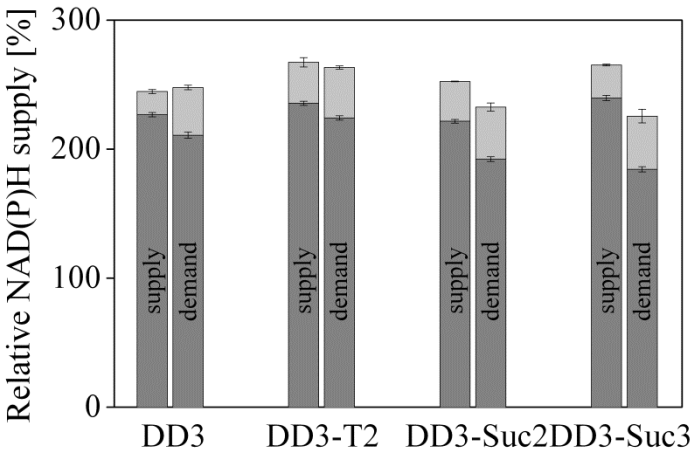

Figure 9.1 Redox balance of investigated *B. succiniciproducens* phenotypes DD3-T2, DD3-Suc2 and DD3-Suc3, as compared to their parent strains DD3 (Becker et al. 2013). NADH (dark grey) and NADPH (light grey) supply were calculated from metabolic flux distribution. Corresponding demands were estimated from production characteristics including biomass formation and specific yields for secreted products (Table 5.4 and Table 5.8). NADH supplying reactions were assumed for glyceraldehyde-3-phosphate dehydrogenase, pyruvate dehydrogenase, 2-oxo-glutarate dehydrogenase. Considered reactions for NADPH supply were glucose-6-phosphate dehydrogenase, 6-phosphogluconate dehydrogenase, and isocitrate dehydrogenase. NADH consuming reactions were assumed for alcohol dehydrogenase, malate dehydrogenase, and fumarate reductase. Under the assumption of an existing NADH dehydrogenase, transferring electrons from NADH to menaquinone, menaquinone consumption was regarded as NADH consumption (Kim et al. 2009). The NADPH demand for anabolism was obtained from cellular composition (Table 9.1). Data represent mean values with 90 % confidence intervals.

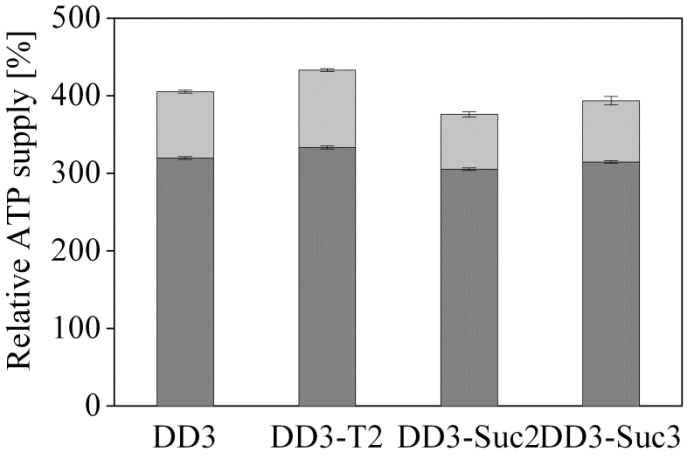

Figure 9.2 Energy balance for *B. succiniciproducens* phenotypes DD3-T2, DD3-Suc2 and DD3-Suc3, as compared to their parent strains DD3 (Becker et al. 2013). ATP demand (dark grey) and supply (light grey) were calculated from biomass formation, metabolic flux distribution and production characteristics. ATP supply was assumed for phosphoglycerate kinase, phosphoenolpyruvate carboxykinase, acetate kinase, and succinyl-CoA synthetase. The ATP demand was calculated from hexokinase and phosphofructokinase. The anabolic demand was obtained from cellular composition (Table 9.1). Data represent mean values with 90 % confidence intervals.

9.2 Gene expression analysis of evolved *B. succiniciproducens* phenotypes

The obtained gene expression profiles of *B. succiniciproducens* DD3-T2, DD3-Suc2 and DD3-Suc3 were used for database-aided operon search. Operons and their corresponding genes were listed according to the Database of prOkaryotic OpeRons (Dam et al. 2007; Mao et al. 2009) and the Prokaryotic Operon DataBase (Taboada et al. 2012) for *M. succiniciproducens* MBELE55 predictions.

Table 9.5 Operon linked gene expression of *B. succiniciproducens* DD3-T2. Data comprise operons, up- and down-regulated in response to temperature adaptation, as compared to the ancestor DD3.

Number	Systematic name[a]	Gene name[a]	Mean FC[b]	Specification[c]	Function[d]
1	MS616-18		2.0	Phosphotransferase system	G
2	MS1334-36	*lpd, aceF, aceE*	4.2	Pyruvate dehydrogenase complex	C
3	MS1606-08	*dAK*1, *dAK*2	2.2	Dihydroxyacetone kinase	G
4	MS2284-89	*uhpT, uhpA, uhpB, uhpC, baeS*	10.4	Hexose phosphate phosphorelay system	G, T, M
5	MS0549-51	*proV, proW, proX*	- 3.0	Glycine betain/proline transport	E
6	MS1791-95	*dgoA, menB, mhpC, mend, menF*	- 2.8	Menaquinone biosynthesis	H, R
7	MS1816-19	*nrfD, nrfC, nrfB, nrfA*	- 2.5	Formate dependent nitrite reductase	P, C
8	MS1821-22	*rluD*	- 2.0	Pseudouridine synthase and conserved protein	J, S
9	MS2073-74	*glgP, malQ*	- 2.0	Glycogen metabolism	G

[a] Gene entries and names are given by KEGG annotations for *M. succiniciproducens* MBELE55.
[b] Mean fold change represents the mean value of gene expression of all operon involved genes.
[c] The operon specifications were assigned using the databases of KEGG and BLAST.
[d] Functional grouping was taken from literature (Hong et al. 2004).

Table 9.6 Impact of succinate adaptation on *B. succiniciproducens* gene expression. Data comprise operons, up- and down-regulated in DD3-Suc2, as compared to the ancestor DD3.

Number	Systematic name[a]	Gene name[a]	Mean FC[b]	Specification[c]	Function[d]
1	MS0458-59	*groE, groEL*	2.0	Molecular chaperones	O
2	MS1249-52	*cysI, cysJ, cysN, cysH*	4.6	Cysteine biosynthesis	E
3	MS1275-77	*glnQ, artM, artI*	2.6	Cysteine related ABC transporter system	E
4	MS1334-35	*lpd, aceF, ace*	2.3	Pyruvate dehydrogenase complex	C
5	MS1855-57	*nrdG*	2.1	Queosine biosynthesis	R, H, O
6	MS0038-40	*oadB, oadA, oadG*	- 3.2	Oxaloacetate decarboxylase	C
7	MS0549-51	*proV, proW*	- 3.5	Glycine betain/proline transport	E
8	MS0616-18		- 2.1	Phosphotransferase system	G
9	MS0731-32	*gltD*	- 2.5	Putative glutamate synthase and formate dehydrogenase subunit alpha	E, R
10	MS1120-24	*glgA, glgC, glgX, glgB, malQ*	- 2.0	Glycogen metabolism	G
11	MS1156-58	*feoB, feoB*	- 2.2	Ferrous iron transport	P
12	MS1652-55	*sdhA, frdB, frdC, frdD*	- 3.3	Fumarate reductase	C

13	MS1816-19	*nrfD, nrfC, nrfB, nrfA*	-	2.2	Formate dependent nitrite reductase	P, C
14	MS2066-67	*lamB, malK*	-	2.2	Maltose, maltodextrins uptake	G
15	MS2377-79		-	2.4	Phosphotransferase system	G

[a] Gene entries and names are given by KEGG annotations for *M. succiniciproducens* MBELE55.
[b] Mean fold change represents the mean value of gene expression of all operon involved genes.
[c] The operon specifications were assigned using the databases of KEGG and BLAST.
[d] Functional grouping was taken from literature (Hong et al. 2004).

Table 9.7 Operon linked gene expression of *B. succiniciproducens* DD3-Suc3. Data comprise operons, up- and down-regulated in response to temperature adaptation, as compared to the ancestor DD3.

Number	Systematic name[a]	Gene name[a]		Mean FC[b]	Specification[c]	Function[d]
1	MS0966-67			2.2	Dihydropteroate synthase and phosphoglucosamine mutase	H, G
2	MS1441-42			2.5	Pseudouridine synthase and ribosome binding factor A	J
3	MS1444-46			3.3	Translation initiation factor IF2, transcription elongation factor and ribosome maturation protein	J, K
4	MS16(66)-75			2.0	Peptidoglycan biosynthesis	M, D
5	MS1(699)-703			3.1	Threonine synthesis	E, S
6	MS1922-23			2.3	Lipid biosynthesis	M
7	MS2311-12			2.2	Uncharacterized protein containing SH3 domain and tRNA nucleotidyl-transferase	T, J
8	MS0549-51		-	10.6	Glycine betain/proline transport	E
9	MS0911-12		-	2.0	Lipopolysaccharide biosynthesis	M
10	MS1652-55		-	2.4	Fumarate reductase	C
11	MS16(83)-87		-	2.4	ABC-type amino acid transport	E
12	MS1786-87		-	2.0	Na^+/solute symporter (pantothenate, proline) and uncharacterized protein	H, S
13	MS17(91)-95		-	2.6	Menaquinone biosynthesis	H, R
14	MS1816-(19)		-	4.6	Formate dependent nitrite reductase	P, C
15	MS1821-22		-	2.5	Pseudouridine synthase and uncharacterized protein	J, S
16	MS1824-25		-	2.2	Dihydroneopterin synthase and uncharacterized transporter protein	H, R
17	MS2066-67		-	4.8	Maltose, maltodextrins uptake	G
18	MS20(68)-70		-	3.7	Maltose, maltodextrins transport	G
19	MS2073-74		-	3.1	Glycogen metabolism	G

[a] Gene entries and names are given by KEGG annotations for *M. succiniciproducens* MBELE55.
[b] Mean fold change represents the mean value of gene expression of all operon involved genes.
[c] The operon specifications were assigned using the databases of KEGG and BLAST.
[d] Functional grouping was taken from literature (Hong et al. 2004).

9.3 Rational strain construction

The plasmid used for metabolic engineering of *B. succiniciproducens* is given in Table 9.8. Rationally engineered strains are given in Table 9.9. Strains, referred to BASF SE, were constructed by BASF SE in the laboratories of Dr. Joanna-Martyna Krawczyk. The applied site-specific primers for plasmid construction and nucleotide validation are given in Table 9.10.

Table 9.8 Plasmids used for genetic modifications of *B. succiniciproducens*.

Plasmid	Modification(s)	Reference
pSUC-1	pJFF224-XN + *rpoC* (MS0213) gene with nucleotide exchange 692C>A resulting in the amino acid exchange T231K under the native promoter	This work

Table 9.9 *Basfia succiniciproducens* strains genetically engineered for phenotype studies regarding succinate production improvement.

Strain	Modification(s)	Reference
DD3 pJFF224-XN	DD3 + empty expression vector pJFF224-XN	This work
DD3 pSUC-1	DD3 + expression of plasmid pSUC-1	This work
DD3 *Δrfe*	DD3 + deletion of the *rfe* (MS0911) gene	BASF SE
DD3 rfe^{T18P}	DD3 + nucleotide exchange 46A>C resulting in the amino acid exchange T18P in the *rfe* (MS0911) gene	BASF SE
DD3 $wcaJ^{Y27fs}$	DD3 + nucleotide insertion 80_81insC resulting in the frame shift mutation Y27fs in the *wcaJ* (MS1494) gene	BASF SE
DD5 $lysA^{G307C}$	DD5 + nucleotide exchange 919G>T resulting in the amino acid exchange G307C in the *lysA* (MS2084) gene	BASF SE
DD1*Δldh* pta^{V666I}	DD1 + deletion of the *ldh* gene encoding for lactate dehydrogenase + nucleotide exchange 1996G>A resulting in the amino acid exchange V666I in the *pta* (MS0998) gene	BASF SE

Table 9.10 Sequences of site-specific primers used for construction of transformation vector (Table 9.8) and validation of strain specific nucleotide exchanges (Table 9.9).

Name	Sequence (5' ⇨ 3')	Plasmid	Control
RSt01	AGGTCATTCAAAAGGTCATC	pJFF224-XN	
RSt02	AAGTGTCATAGCACCAACTG	pJFF224-XN	
RSt03	GACTAGTTGATAAAATGCACGCTCGTT	pJFF224-XN	
RSt04	CACTCGAGTTATTCCGCATCATCCGCCA	pJFF224-XN	
RSt05	TTATTATTGGATATGCCGTT		*rpoC* for
RSt06	GCCAAAGATTTTAACGGACG		*rpoC* rev
RSt07	TATCGTCGGTGTCCCAAATA		*rfe* for
RSt08	TCCAGTAAACCGATGACCAA		*rfe* rev
RSt09	AATTGGTCGGTCGTAGGAGA		*wcaJ* for
RSt10	TTCAACATACCAGGCATCCA		*wcaJ* rev
RSt11	GCCACCGATCGATTATTCT		*lysA* for
RSt11	GAAGACATGCTTGCTCCGTA		*lysA* rev
RSt11	TAATCGACGGTCCGTTACAA		*pta* for
RSt12	GCTTTCCGAGTAGTGCCTTT		*pta* rev